University of Zurich[UZH]

# Creating a Diffuse Bicycle Traffic Assignment Model for Switzerland

GEO 511 Master's Thesis

**Author**
Marc Morlang
19-749-126

**Supervised by**
Prof. Dr. Ross Purves

**Faculty representative**
Prof. Dr. Ross Purves

27.09.2024
Department of Geography, University of Zurich

## Abstract

Traffic assignment models show the amount of traffic on roads and are a commonly used tool in traffic planning for motorised and public transport. The Swiss national model for passenger traffic NPVM of 2017 also includes such a model for bicycles. The short distances and lack of a hierarchical road network of bicycle traffic make this model too sparse to be useful in traffic planning. This thesis presents a methodology to take the bicycle traffic distribution model of the NPVM and create a denser traffic pattern. The traffic distribution model provides the number of bicycle trips between each pair of traffic zones in Switzerland, which will be assigned to the road network of OpenStreetMap using the bicycle routing service Valhalla. To distribute the route start and end points within each traffic zone, the jittering and disaggregation approach introduced by Lovelace et al. (2022) was used. The distribution was weighted by population and full-time equivalents. The methodology was applied to the NPVM bicycle distribution model for 2017 and for the base scenario of 2050. To validate the results the 2017 bicycle traffic distribution model was compared to observations from automatic counting stations across Switzerland using GEH-values, SQV and linear regression. The results show bicycle traffic on roads across the country, creating a dense traffic pattern within settlements and connections between them. The validation indicates that the model performed better than the bicycle traffic distribution done for the NPVM. While the results in urban areas are acceptable, the performance of the model was poor in rural areas.

# Acknowledgments

I want to thank my supervisor Prof. Dr. Ross Purves for guiding me through the process of creating the model and writing this thesis. His advice on problem solving and what features to exclude was very valuable and improved the model a lot.

I want to thank everyone at the municipal and cantonal offices who helped me gather data on bicycle counting stations, which significantly increased the number of counters available for the validation of the model.

I want to thank Raphaël Ancel from traffic modelling at UVEK for giving me access to the 2050 scenario of the Swiss national model for passenger traffic.

I want to thank my family and friends for their support during my studies and the writing of the thesis.

# Table of Contents

# List of Figures

# List of Tables

# List of Abbreviations

| | |
|---|---|
| AADT | annual average daily traffic |
| AARE | average absolute relative error |
| AAWT | annual average weekday traffic |
| AUC | areas with urban character |
| BTAM | bicycle traffic assignment model |
| DFM | disaggregate factor method |
| GEH | value of traffic model quality named after Geoffrey E. Havers |
| MZMV | Mikrozensus Mobilität und Verkehr (micro census for mobility and traffic) |
| NPT | Network Planning Tool for Scotland |
| NPVM | Nationales Personenverkehrsmodell (national model for passenger traffic) |
| OD | origin-destination |
| OSM | OpenStreetMap |
| PCT | Propensity to Cycle Tool |
| SQV | Scalable Quality Value |
| SRTM | Shuttle Radar Topography Mission |
| ToM | typology of municipalities |
| URT | urban-rural typology |

# 1) Introduction

## 1.1) Motivation

### 1.1.1) Benefits of Cycling

Replacing short car trips with cycling has many benefits, both for individuals and the society in general. The biggest benefit to the person cycling is the physical activity it provides, leading to lower risks for cardiovascular disease and mortality, while increasing fitness. Many studies have shown that this benefit far outweighs the increased risk of injury and larger amount of inhaled air pollution associated with cycling (de Hartog, Boogaard, Nijland, & Hoek, 2010; Lindsay, Macmillan, & Woodward, 2011; Mueller, et al., 2015; Oja, et al., 2011; Rabl & de Nazelle, 2012). This health benefit is still present, even though smaller, when using e-bikes (Cairns, Behrendt, Raffo, Beaumont, & Kiefer, 2017). For society as a whole, the health benefits are even larger, due to a reduction in air pollution, traffic accidents, noise and stress. The reduction in air pollution, from carbon dioxide, black carbon, nitrogen oxide and others also provide a benefit to the environment and help in the fight against climate change (de Hartog, Boogaard, Nijland, & Hoek, 2010; Johansson, et al., 2017; Lindsay, Macmillan, & Woodward, 2011; Macmillan, et al., 2014; Mueller, et al., 2015).

Another benefit of cycling is the lower amount of space needed for travel and especially parking: the area needed to park one car, which have an average occupancy of 1.53 people (Bundesamt für Statistik BFS, 2023b), can provide storage for eight bicycles. Along with that goes a reduction in congestion, which in turn reduces the travel times for cars and their emissions (Gössling & Choi, 2015; Tordai, Munkácsy, Andrejszki, & Hauger, 2023). As transportation is important to access opportunities and activities, it should be available to everyone. Cycling and public transport have lower costs for their user than car ownership, helping to increase equity and aid the economic and social development of poorer people (Gössling & Choi, 2015; Lee, Sener, & Jones, 2017).

### 1.1.2) Cyclist Preferences and Safety

When cyclists choose a route, they mostly decide based on distance/time, terrain, and perceived safety. Shorter routes are preferred, with relative deviations from the shortest option influencing the decision (Broach, Dill, & Gliebe, 2012). The influence of terrain on route choice is stronger for riders of regular bikes than those of e-bikes due to the assistance provided by latter. Due to the reduced effort and resulting higher speed, they also travel larger distances (Rérat, 2021). Cyclists base their route choice based on their perceived safety, which may not be the same as actual safety. Significant detours are made to avoid unsafe infrastructure, such as high car traffic, car parking or tram tracks or to benefit from safe infrastructure such as separated bicycle paths (Broach, Dill, & Gliebe, 2012; Fyhri, Heinen, Fearnley, & Sundfør, 2017; Gössling & McRae, 2022). Municipalities can increase bicycle ridership by providing safe roads or discourage it by not doing so (Gössling & McRae, 2022). Cycling rates in Europe strongly decreased after the second world war due to increased car usage and car-centric infrastructure. This led to car-dependent lifestyles and larger distances between homes, workplaces and shops, further discouraging cycling as a mode of transport (Schepers, et al., 2021). Even though distances increased, more than 40% of car trips in Switzerland in 2021 were shorter than five kilometres, a distance easily done by bicycle (Bundesamt für Statistik BFS, 2023b).

### 1.1.3) Modelling Bicycle Traffic

Traffic models are commonly used to estimate where and how much cars and public transport are being used. These models are then used by municipalities, cantons or traffic and spatial planners to evaluate infrastructure projects. With the Swiss national model for passenger traffic NPVM of 2017 was created for cars, public transport, bicycles and pedestrians. The modelling for bicycles however, was performed in a way similar to car traffic (Bundesamt für Raumentwicklung ARE, 2020b), which does not serve the needs of cycle planning. Bicycle trips are much shorter than car trips (Bundesamt für Statistik BFS, 2017d), which requires a different modelling. The longer trip length allows car traffic models to only focus on main roads and use few locations where trips start and end (Bundesamt für Raumentwicklung ARE, 2020b). For bicycle traffic the shorter routes mean that the model needs to result in a denser network and more trip start and end locations are required (Lovelace, Félix, & Carlino, 2022).

## 1.2) Objectives and Research Questions

The objective of this thesis is to develop a bicycle traffic assignment model BTAM and apply it to the country of Switzerland. The intended result is a map showing the estimated number of cyclists on all roads in Switzerland. To achieve a good distribution of trips throughout traffic zones, the jittering method by Lovelace et al. (2022) will be applied.

**Research Questions:**

1. How can the jittering method developed by Lovelace et al. be applied to Switzerland?
2. How can a nationwide bicycle traffic distribution model be created, which is usable on a local level?

# 2) Background and State of the Art

## 2.1) Traffic Modelling and the Swiss National Model for Passenger Traffic

Traffic planning is about analysing the current state of traffic and travel behaviour, then predicting the expected situation in the future and finally finding solutions to adapt traffic network and infrastructure to those changes. Traffic models aim to show traffic patterns in the area of interest, based on the traffic analysis and forecast. They can be used to inform changes to traffic infrastructure and public transport networks (Schnabel & Lohse, 2011).

Traffic models for passenger travel work in the four stages of trip generation, trip distribution, mode choice and route choice. Freight traffic will not be discussed in this thesis. In the first step of trip generation, the number of trips originating and ending in each traffic zone is estimated. The steps of trip distribution and mode choice can be performed in either order or even simultaneously. In trip distribution the number of trips between each pair of traffic zones is determined and during mode choice the fraction of trips performed by each means of transport (usually foot, bicycle, car or public transport) is modelled. Finally, with route choice the path of trips along the transport network is calculated. Traffic models require multiple iterations until they reach equilibrium, because traffic supply and demand influence each other (i.e. high amounts of traffic on a road leads to fewer people taking that road) (Ortúzar & Willumsen, 2011; Schnabel & Lohse, 2011).

The Swiss national model for passenger traffic (Nationales Personenverkehrsmodell NPVM) for 2017 was developed by the federal office for spatial planning with support from other federal offices and external experts. It replaces the older national traffic model from 2000 which was less detailed and last updated in 2010. The NPVM is a traffic model for all of Switzerland created in the modelling software PTV VISUM, with the aim to analyse and predict the mobility of people on a national, cantonal and regional scale. The effects of changes in land use, timetables, infrastructure or other future scenarios can be modelled using it. The main result is the demand distribution on weekdays for the modes of pedestrian, bicycle, car and public transport, which contains the number of modelled trips between each pair of traffic zones. The demand distribution for the entire week was modelled by transforming these results. Other results include network utilisation for bicycle, car and public transport as well as travel times and distances for car and public transport (Bundesamt für Raumentwicklung ARE, 2017; Bundesamt für Raumentwicklung ARE, 2020c). The next chapters introduce how traffic models work in general and how the NPVM was created.

### 2.1.1) Foundations for Traffic Modelling

To mimic reality, the traffic model needs to reflect the structure of the area of interest. This includes the division of the area into smaller areas called traffic zones, the provision of road and public transport networks with the necessary attributes, the available modes of transport and an analysis of traffic (Schnabel & Lohse, 2011).

#### *2.1.1.1) Trips, Activities and Generalised Cost*

**Trips**

Trips refer to the movement of people between two different locations, which may be within the same traffic zone. Trips are always performed using one of the modes of transport withing the transport network of that mode. Routes refer to the path of a trip along the transport network (Schnabel & Lohse, 2011).

**Activities**

In traffic planning activities refer to the locations at the start and end of trips and what the person does there. For most trips one of the activities is the home location. Other activities include work, school, shopping or leisure (Schnabel & Lohse, 2011).

**Generalised Cost**

Trips have multiple expenses associated with them, with time and monetary cost often being most important. Different modes of transport have different categories of expense: While the expenses of a bicycle trip include physical exertion, with public transport the number of transfers needs to be accounted for. The size and importance of expenses also depends on the person, both in terms of the availability and accessibility of options or cost reductions (e.g. ownership of a car, distance to the closest bus stop) and the subjective perception and values of the person. To compare the total cost of different travel options the expenses need to be combined, which are then called generalised cost (Ortúzar & Willumsen, 2011; Schnabel & Lohse, 2011).

#### *2.1.1.2) Traffic Zones*

Traffic zones divide the area of interest into smaller zones, for which data (e.g. population, work places, shops,…) are aggregated. The generation and distribution of trips in the model is performed for traffic zones. To include traffic entering and exiting the area of interest, a region around this area should also be split into traffic zones. This region should include all places with a significant impact on the traffic within the area of interest, but the traffic zones can increase in size the further away they are (Schnabel & Lohse, 2011). The NPVM includes 7'965 traffic zones in Switzerland. An additional 13 traffic zones, from the municipalities of Liechtenstein and the German and Italian enclaves of Büsingen and Campione d'Italia, are treated like the Swiss zones during modelling (see Figure 1). Apart from these there are 807 traffic zones outside of Switzerland, with increasing size as they get further away (see Figure 2) (Bundesamt für Raumentwicklung ARE, 2020b).

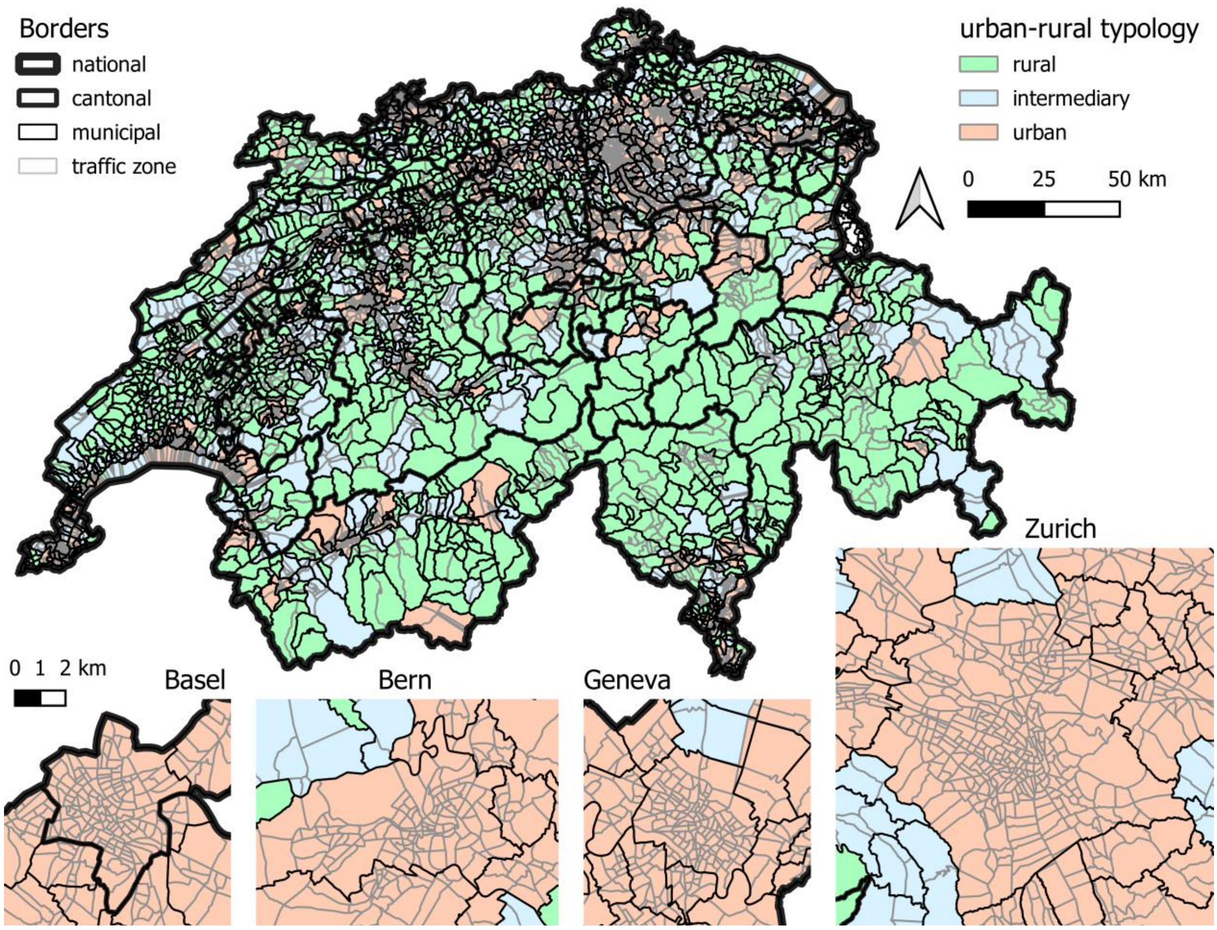


*Figure 1: Traffic zones of the NPVM in Switzerland, coloured by urban-rural typology.*

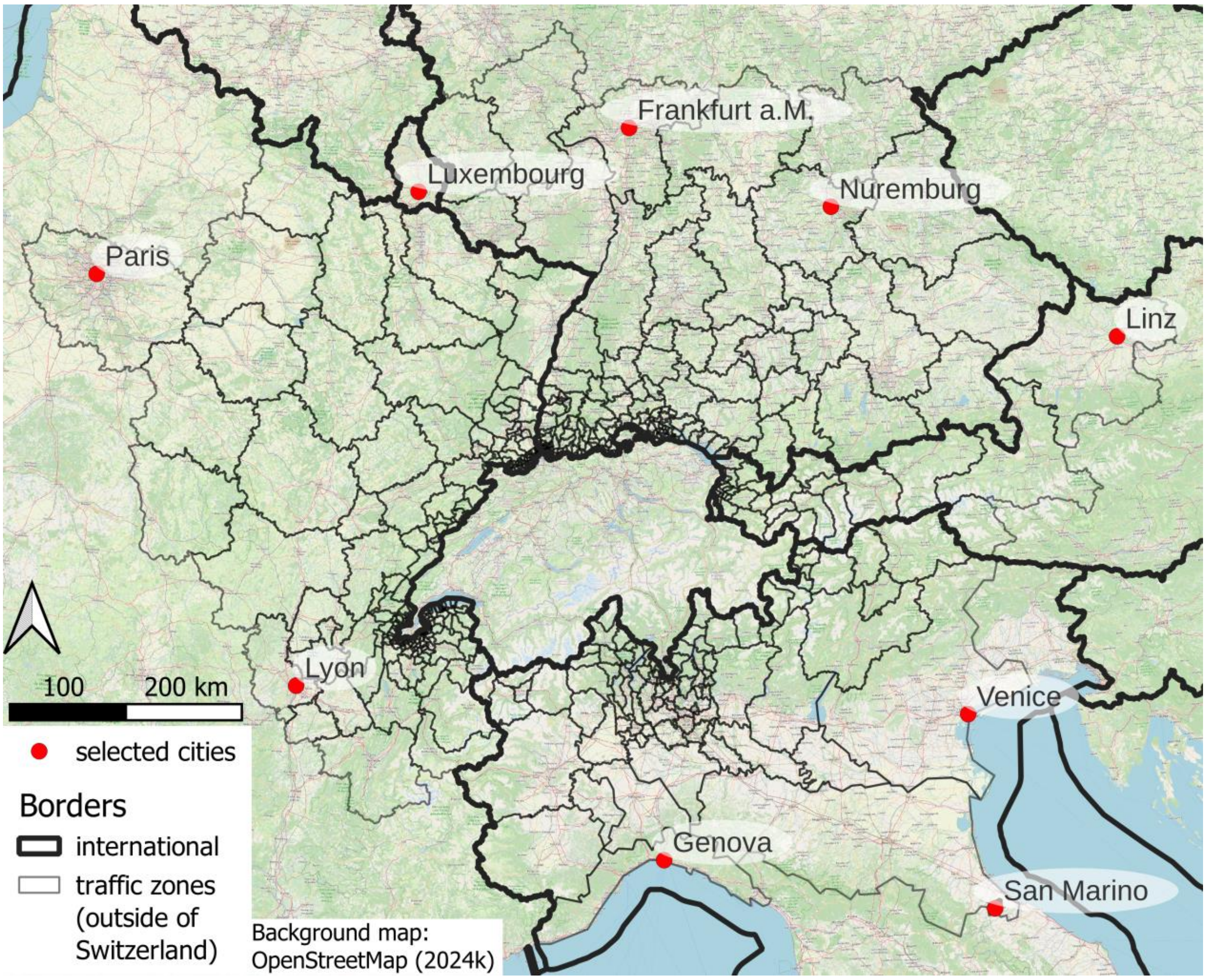


*Figure 2: Traffic zones of the NPVM outside of Switzerland with the locations of selected cities.*

The borders of traffic zones usually follow natural and artificial breaks in the settlement, such as rivers, railway tracks and main roads. Spatial characteristics such as municipal zoning (e.g. industrial and residential zones) and catchment areas of transit stops can be used to inform the border placements. Administrative boundaries are also useful to consider, as data is often available aggregated according to them. The size (in terms of area, population or other relevant measures) of traffic zones depends on the task and the area, including factors such as the density of the traffic network and the included modes of transport (Schnabel & Lohse, 2011). When creating the traffic zones for the NPVM, the aim was to make them as homogenous as possible regarding the sum of population and full-time equivalents (called population statistics in this thesis). The average is 1552 people and full-time equivalents. As visible in Figure 1, the area of the traffic zones varies strongly, with an average of 5.2 km². Traffic zones are always within a single municipality, even if this results in zones with low population statistics. Some facilities which generate a lot of traffic were given their own traffic zone. These 58 zones include airports, shopping centres and leisure facilities (Bundesamt für Raumentwicklung ARE, 2017).

#### *2.1.1.3) Origin-Destination Groups*

Origin-destination (OD) groups are disaggregated population classes which are homogeneous in their behaviour and belong to a pair of origin and destination activities. They are an important basis for traffic modelling, as they connect land use characteristics (e.g. home, workplace, school,…) with people (e.g. residents, workers, students,…) and their participation in traffic. They consist of activities (e.g. home, work, shopping) and include characteristics of the traffic zone (e.g. number of residents in an age group, number of workplaces) at the origin and destination. The OD-groups are generated based on representative traffic surveys (Schnabel & Lohse, 2011). The homogeneous population groups are created based on employment status, age group, availability of mobility tools (e.g. ownership of car or public transport subscription). The NPVM includes 26 OD-groups, some examples are shown in Table 1: The first line is an OD-group for trips from home to work. It is disaggregated by age groups and the availability of mobility tools to form several population groups with homogeneous behaviour. The number of employed people in the origin traffic zone and the number of workplaces in the destination traffic zone are used to determine the number of trips between these traffic zones for each of the groups (Bundesamt für Raumentwicklung ARE, 2020b).

*Table 1: Examples of OD-Groups, adapted from NPVM (Bundesamt für Raumentwicklung ARE, 2020b).*

| **Activity at Origin** | **Activity at Destination** | **Statistics at Origin** | **Statistics at Destination** |
|---|---|---|---|
| Home | Work | Number of workers 1) | Number of workplaces |
| Home | Shopping | Population 1) | Sales area |
| Education | Home | Number of student places | Number of students 2) |
| Work | Shopping/Leisure | Number of workplaces | Sales area, leisure visitors, population 1) |
| 1) Disaggregated by age group and mobility tools (e.g.: number of people with these characteristics: age 25-44, without a car, with a public transport subscription) | | | |
| 2) Disaggregated by mobility tools | | | |

#### *2.1.1.4) Travel Data*

Different types of data collection methods are required to gain the information needed for traffic analysis and modelling. Traffic surveys can be used for different purposes in traffic planning. They can be used to analyse the current transport system and identify problems within it or to create strategic transport models which are used in forecasting. The methods used and data collected in the survey depend on what it is going to be used for. Household surveys provide information on all trips done by a household within a time period and socio-economic data, such as family size and car ownership. They are useful for modelling trip generation and modal split, additionally they provide information on average trip lengths. Traffic counts (counting the number of vehicles passing a location) are needed for calibration and validation of the model. As travel choices change over time, surveys need to be repeated to capture this change (Ortúzar & Willumsen, 2011).

Surveys on peoples' actual choices or observations of their actual behaviour are called revealed preference. This is in contrast to stated preference methods, which collect data on the participants actions in a hypothetical scenario. This has the advantage of allowing questions regarding new or future developments in transport and infrastructure. Stated preference methods do however have the disadvantage of requiring the participant to imagine themselves in a fictional situation, which can change how they choose (Ortúzar & Willumsen, 2011; Schnabel & Lohse, 2011).

The NPVM relies on many different data sources. Official data sets on population STATPOP and companies STATENT (see chapter 3.5.3) were used throughout modelling together with the micro census for mobility and traffic (Mikrozensus Mobilität und Verkehr MZMV), the largest revealed preference survey on transport in Switzerland. With the SP-survey, a stated preference survey, was used during trip distribution and mode choice. Count data of cars, public transport and bicycles was used during calibration and validation (Bundesamt für Raumentwicklung ARE, 2020b).

#### *2.1.1.5) Traffic Networks*

A traffic network is required for each mode for which routing is being performed. While the network is a simplification of reality, it needs to include all elements relevant for the mode and use case. While the network for car traffic may not always need local roads, bicycle traffic is less hierarchical and more influenced by small roads, therefore always requiring a detailed road network. Segments should also get attributes regarding their characteristics, such as capacity, slope and surface type. While the network for private transport is based on the roads, for public transport the lines with their stops and timetables need to be modelled (Schnabel & Lohse, 2011).

To calculate the routes the traffic zones need to be connected to the traffic network. This is often done using connector points at the centroid of the traffic zone. These connector points act as start and end points of all routes originating or ending in the traffic zone (Schnabel & Lohse, 2011). Other methods do also exist (Lovelace, Félix, & Carlino, 2022) and will be presented in chapter 2.5. The use of few connector points per zone results in unrealistic traffic patterns in the local network (Schnabel & Lohse, 2011).

**Traffic Networks used in the NPVM**

Routing in the NPVM was done using three networks. A road network for cars and busses, another road network for bicycles and pedestrians and a rail network. Public transport lines and stops were included based on the 2017 timetable. Connections to the traffic zones were done using network nodes, with some restrictions for road types, or stops in case of public transport. Each traffic zone can have up to three connector nodes per mode/network, however only around 600 and 400 of almost 8000 zones have multiple connections for car and public transport, respectively. In these cases, subzones were created and assigned a portion of the trip demand. The closest node to the zones centre, weighted by population and workplace density, was chosen as connector for the road networks. For public transport stops with more services and those closer to the weighted zone centre were selected. Around 2500 of the almost 8000 traffic zones do not have a public transport connection (Bundesamt für Raumentwicklung ARE, 2020b).

The road network for cars and busses was based on the navigational network of the company TomTom. It includes information on the number of lanes, signalised and actual speeds, road types, capacities and possible turns at intersections (Bundesamt für Raumentwicklung ARE, 2017). While the network within Switzerland includes almost all roads, the network outside Switzerland gets less detailed with increasing distance (Bundesamt für Raumentwicklung ARE, 2020b).

The road network for bicycle and pedestrians was based on the network created for cars and busses, but only within Switzerland. To fill in additional segments only usable by cyclists the network was combined with the SwitzerlandMobility bicycle routes. Additionally, randomly sampled routes on the network were compared to those from Google Maps bicycle routing. Differences between the routes on both networks were reduced by adding missing segments. Both comparisons added around 1800 segments each to the 122’000 segments in the original network. Routing for bicycles was based on the routing engine from the city of Zurich. It considers motor vehicle speed and volume as well as slope. The gradient of segments was calculated based on elevation data from Copernicus with a resolution of 25m. This was done by interpolating the elevation of each node using the four nearest raster cells and calculating the slope over the entire length of the segment (Bundesamt für Raumentwicklung ARE, 2020b).

The network for railways, including trams, was a combination of the rail network of the federal office for transportation (within Switzerland) and the Swiss federal railways (outside of Switzerland). To allow for routing with transfers between local transport and rail, foot paths were added to connect stations to stops (Bundesamt für Raumentwicklung ARE, 2017).

### 2.1.2) Four Stage Traffic Models

#### *2.1.2.1) Trip Generation*

During trip generation the number of trips starting and ending in each traffic zone is modelled. The calculation is based on the location and characteristics of the traffic zone. The location is important as it can promote or impede mobility or certain modes of transport. Characteristics include amongst others the number of residents and employees, the number of workplaces and the sales area. Most important however are land use and the location of the traffic zone within the study area and transport network. This approach assumes that all trips are done with the aim of performing an activity in a different location. While this assumption holds true in most cases, some trips are made with the sole purpose of making a trip. This is especially the case with pedestrian and bicycle traffic, where trips are often made for sports or leisure (Schnabel & Lohse, 2011).

In the NPVM trips were generated based on the population characteristics of the traffic zone and mobility rates of the OD-groups. Trip attraction was modelled using data on employees, area for shopping, leisure facilities and airport passengers (Bundesamt für Raumentwicklung ARE, 2020b).

#### *2.1.2.2) Trip Distribution*

With trip distribution the trips starting in a given traffic zone are distributed to traffic zones in which they end. This assignment of traffic from origin traffic zones to its destination traffic zone creates the OD-matrix. It stores the number of trips from each starting zone to each destination zone, including intrazonal trips. The methods to determine trip distribution are in analogy to the law of gravity, as zones with more possible activities and zones with a lower travel cost between them have more trips. Additionally, the characteristics of the zones and their travellers needs to be accounted for and the number of trips starting and ending in each zone needs to be the same as determined in trip generation (Ortúzar & Willumsen, 2011; Schnabel & Lohse, 2011).

#### *2.1.2.3) Mode Choice*

Each trip has to be performed by a mode of transport, models usually include foot, bicycle, car and public transport. Which mode is chosen depends on characteristics of the travel modes (e.g. availability, travel time, comfort), the traveller (e.g. income, age, ownership of mobility tools) and the trip itself (e.g. trip purpose, mode options). The result of mode choice is the fraction of trips between each pair of zones is made by a particular mode (Schnabel & Lohse, 2011).

Trip distribution and mode choice largely depend on the same factors, with travel time being the most important. Many of the factors in the utility function are dependent on the zones, traveller and trip purpose, therefore both distribution and mode choice must be performed separately for each OD-group (Schnabel & Lohse, 2011).

Trip distribution and mode choice were performed together in the NPVM. Travel time is the only contributor to the generalised cost included for pedestrians and cyclists. Car and public transport have additional factors, for example travel cost and availability of mobility tools. The relative importance of these factors was determined based on the SP-Befragung, a stated preference survey conducted together with the MZMV (Bundesamt für Raumentwicklung ARE, 2020b).

#### *2.1.2.4) Route Choice*

In the final step of the traffic model the paths taken on the traffic networks are modelled. Result is the amount of traffic on each segment of the traffic networks. It is important for assessing the quality of the network and helps with decision making in traffic planning. Route choice can be done either statically or dynamically, in both cases the trip start times are spread across the day by assigning them to a time slice. Time slices are subdivisions of a day with equal length. In static route choice routing is performed separately for each time slice. Traffic volume, an important factor in route choice, is only based on trips started in the same time slice. Most trips should therefore be of shorter duration than the length of a time slice. Traffic variables are constant throughout a time slice and represent the mean over the time period. Dynamic route choice is more complex: Traffic flows are distributed while accounting for the changing position of travellers over time. Trips taking longer than one time slice are carried over into the calculation of the next time slice, which better estimates the traffic volume on sections of the network and therefore the associated cost. Different methods for static and dynamic route choice exist, with the general functioning of static route choice being explained next (Schnabel & Lohse, 2011).

Route choice is influenced by both objective and subjective factors, especially travel time (including waiting time). A routing algorithm is used to find the best routes between the starting point in the origin traffic zone and the end point in the destination traffic zone, while considering these different factors. For private transport travel time increases when traffic demand approaches or exceeds the capacity of the road. Capacity restraint functions are used to calculate variable travel times based on traffic volume, capacity and road characteristics. Multiple iterations of routing and travel time calculation are performed until the differences between iterations are below a predefined threshold (Schnabel & Lohse, 2011).

**Route Choice in the NPVM**
Route choice for the NPVM was performed using a static approach. It was done separately for bicycles, cars and public transport, it was not modelled for pedestrians. For car traffic a multi-step process was used, where freight traffic from a different model was first assigned to the road network. Afterwards passenger traffic was added, using variable travel times as the only cost factor. Public transport was assigned using a timetable-specific approach (Bundesamt für Raumentwicklung ARE, 2020b).

Route choice for bicycle traffic requires different approaches than for car traffic. First, bicycle traffic does not require an iterative approach to determine travel times, because increased traffic volumes do not lead to a decrease in travel time at current cycling volumes. Second, route choice depends on many different factors (e.g. car traffic or slope), not just travel time. These change the attractiveness of routes and are difficult to quantify consistently. For the NPVM travel time, slope, volume and speed of car traffic were used to select routes. The weighting of these factors was based on the bicycle routing model from the city of Zurich. Instead of using the route with the lowest generalised cost, multiple routes were calculated and one of them selected. This ensures that different alternative paths were being used in the final model (Bundesamt für Raumentwicklung ARE, 2020b).

### 2.1.3) Calibration and Validation of the NPVM

#### *2.1.3.1) Calibration*

After running the entire NPVM traffic model using uncalibrated parameter values, two stages of calibration were performed. In the first stage, the results were calibrated to better fit the MZMV indicator values, for example modal split, average trip distance or fraction of traffic within traffic zones. In a second stage the model was calibrated based on traffic counts for cars and public transport. This stage was mainly used on a local level and resulted only in minor changes to indicator values. A sensitivity analysis for car traffic and public transport was performed after calibration, with all results being found plausible and as expected (Bundesamt für Raumentwicklung ARE, 2020b).

#### *2.1.3.2) Validation*

The modal split across all trips in Switzerland was captured well by the NPVM (see Figure 3, left most columns), compared to the MZMV survey. However, bicycle traffic was strongly underestimated for distances between five and fifteen kilometres (see Figure 3). The strong discrepancies for distances above 75 km are due to differences between the MZMV and data from the Swiss national railways. The average trip distances were generally as in the MZMV, except for short trips on foot or by bicycle in municipalities with intermediate or rural typology. These had to be adjusted to better match the modal split. All in all, the model was found to sufficiently match the MZMV survey (Bundesamt für Raumentwicklung ARE, 2020b; Bundesamt für Raumentwicklung ARE, 2020c).

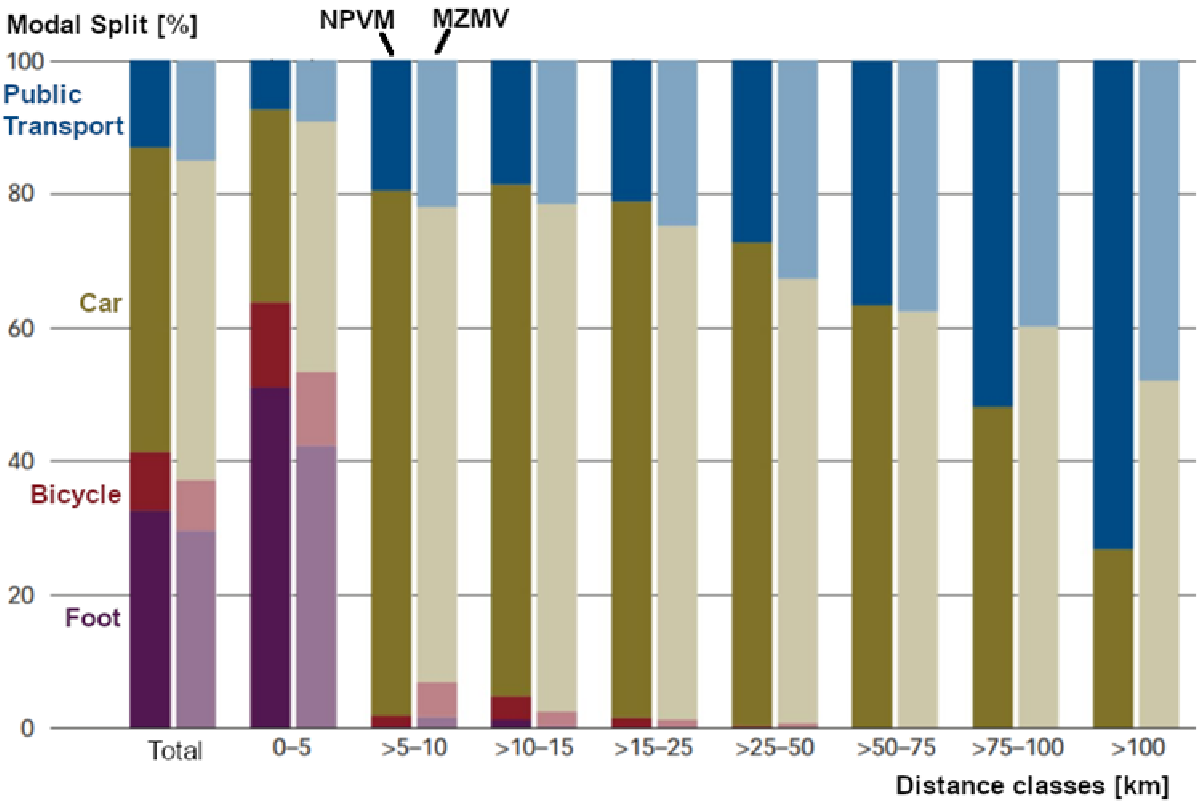


*Figure 3: Comparison of modal split between NPVM and MZMV for different distance classes (adapted from: (Bundesamt für Raumentwicklung ARE, 2020c)).*

A comparison of car and public transport traffic between the modelled values and those observed by traffic counters and transport agencies found they were matching well. For bicycle traffic 85 counting stations were used, with data from the year 2016. To generate direction-specific count data, the counts were halved for all but one station, resulting in 169 direction-specific count values. Unlike those for car traffic, these were only used for validation and not during calibration (Bundesamt für Raumentwicklung ARE, 2020b).

Figure 4 shows a plot of the observed against the modelled annual average weekday traffic AAWT of bicycles (left) and cars (right). For bicycles the points are spread out and do not follow the black line which shows the 1:1-relationship, with only 19% of the variation being explained. Furthermore, a lot of points are on the y-axis, which means that cyclists were observed in these locations, but none were modelled. The slope of the regression (0.5413) indicates an underestimation of bicycle counts. This is confirmed by comparing the sum of traffic across all stations, which also shows a slightly lower value for modelled than for observed counts. For car traffic however, the points follow the optimal line very well with the slope of the regression line and R-squared both being a perfect 1.00 (Bundesamt für Raumentwicklung ARE, 2020b).

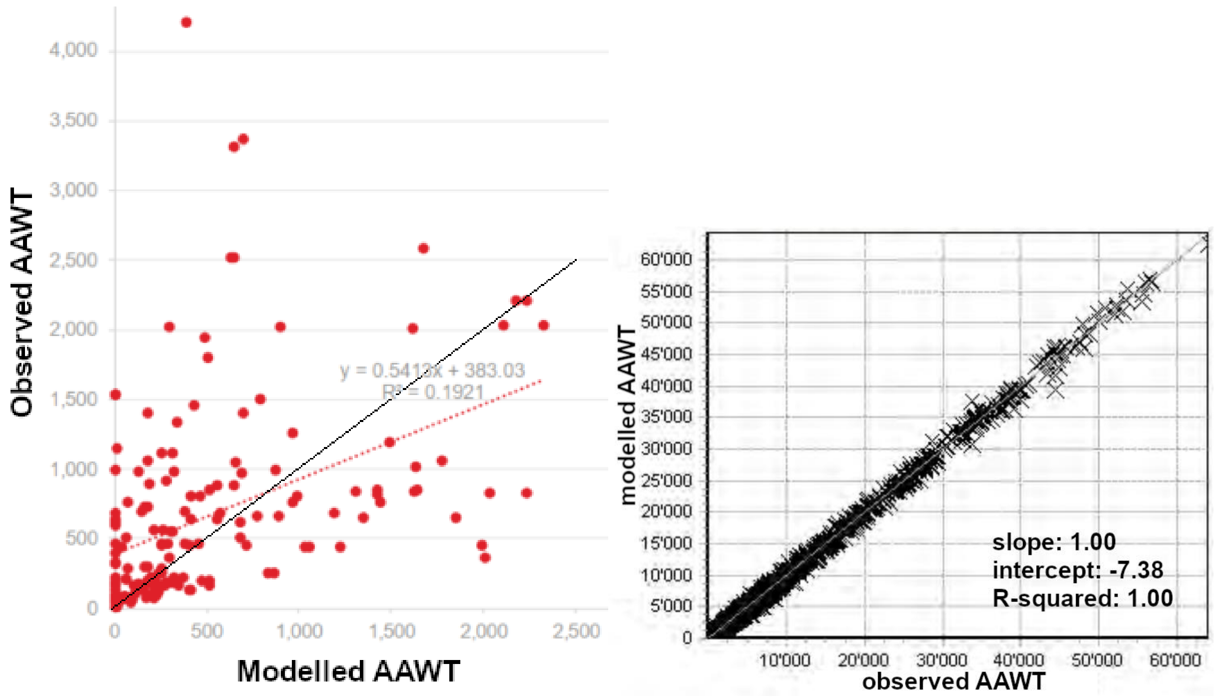


*Figure 4: Plot of observed AAWT against modelled AAWT at counting stations (left: bicycle, right: cars). The dotted line is a linear regression and the solid line shows the ideal 1:1-relationship. From NPVM, adapted from (Bundesamt für Raumentwicklung ARE, 2020b)).*

To quantitatively compare the modelled and observed bicycle counts the GEH-value was calculated, which is a quality measure commonly used in transport modelling. The measure is explained in more detail in chapter 2.9. The results are shown in Table 2, 43% of stations have a GEH-value below 10 and can therefore be considered as good, while 26% of stations have a GEH of above 25, which indicates a bad fit. Counting stations outside of settlement areas and with lower traffic volumes generally have better GEH-values than those within settlements. This might be due the measure being more generous for counts below the working range of 2'000 to 50'000 (Bundesamt für Raumentwicklung ARE, 2020b).

*Table 2: Distribution of GEH-values for bicycle traffic in the NPVM (Bundesamt für Raumentwicklung ARE, 2020b).*

| GEH | Number of Stations | Cumulative fraction [%] |
|---|---|---|
| <= 5 | 41 | 24 |
| 5-10 | 32 | 43 |
| 10-15 | 25 | 58 |
| 15-20 | 17 | 68 |
| 20-25 | 10 | 74 |
| >25 | 44 | 100 |

### 2.1.4) Transport Outlook 2050

The transport outlook for the year 2050 was developed by multiple Swiss federal offices. It used the NPVM for passenger traffic, the Swiss model for freight traffic (Aggregierte Methode Güterverkehr AMG) and the Swiss land use model (Flächennutzungsmodell FLNM). The outlook was developed to explore transport under different scenarios and is not a prediction of the future. It is the strategic basis for national planning of infrastructures and used to inform political decisions in spatial and traffic planning. Like the NPVM it covers all of Switzerland and considers border-crossing traffic. The base year for the outlook is 2017. Four different scenarios were implemented using the three models AGM, FLNM and NPVM by running them with modified input data. For the NPVM this includes for example the homogeneous population groups and public transport supply. These data sets were created by analysing past developments and using them to apply to the different scenarios (Bundesamt für Raumentwicklung ARE, 2022b).

The transport outlook presents four different possible states of traffic for the year 2050, based on currently foreseeable developments (Bundesamt für Raumentwicklung ARE, 2022b; Bundesamt für Raumentwicklung ARE, n.d.):

**Business-as-usual scenario**
In the business-as-usual scenario current trends are continued. Foreseeable demographic, technical and economic developments are taken into account as well as planned infrastructure projects. While technology does develop, its impact on mobility is slow. The volume of traffic and the settlement structure remain the same, as urban sprawl continues and sustainability is not a societal focus (Bundesamt für Raumentwicklung ARE, 2022b; Bundesamt für Raumentwicklung ARE, n.d.).

**Base scenario**
This scenario is building on top of the business-as-usual scenario and additionally includes different developments and measures which improve sustainability and resource efficient mobility. The development of bicycle infrastructure increases the number of cyclists. Using a car becomes comparatively more expensive than taking public transport. While commute traffic decreases, traffic to leisure activities increases. The population growth is strongest in urban municipalities, with many rural areas even experiencing a reduction in population. This is the scenario mainly used for planning and will be used in this thesis (Bundesamt für Raumentwicklung ARE, 2022b; Bundesamt für Raumentwicklung ARE, n.d.).

**Sustainable society scenario**
Builds on the base scenario and includes technological developments to improve sustainability. A strong sense of responsibility exists towards the environment and society. Using a private car becomes more expensive and the use of public transport cheaper, resulting in less traffic than in other scenarios (Bundesamt für Raumentwicklung ARE, 2022b; Bundesamt für Raumentwicklung ARE, n.d.).

**Individualised society scenario**
Also builds on the base scenario. Technological developments are mainly used for personal benefit, with most people owning a private car. Sustainability is only considered if it does not impede one's activities and is not expensive. Public transport becomes more expensive, while private cars do not (Bundesamt für Raumentwicklung ARE, 2022b; Bundesamt für Raumentwicklung ARE, n.d.).

## 2.2) Propensity to Cycle Tool

Inspiration for this thesis are the "Propensity to Cycle Tool" (PCT) and "Network Planning Tool for Scotland" (NPT). These tools model the dispersion of bicycle traffic on the road network in England and Wales (PCT) as well as in Scotland (NPT) under different scenarios (Lovelace & Morgan, 2023b).

The PCT for England was commissioned in 2015 by the English Department for Transport, with the extension to Wales being funded in 2018 by the Welsh government (Woodcock, et al., Propensity to Cycle Tool, n.d. a) and its results are accessible on the website www.pct.bike. It used different scenarios of cycling amounts to show traffic volumes of people travelling to work or school and analyse possible health and carbon emission benefits. The aim was to enable and direct investments in cycling both nationally and locally. The PCT therefore included estimates of cycling amounts at the levels of areas, desire-lines and on the road network as well as health economic and carbon emission impacts. Separate, but similar, models were calculated for commuter traffic and travel to school, with other trip purposes not included (Goodman, et al., 2019; Lovelace, et al., 2017).

### 2.2.1) Travel to Work

For travel to work, the OD-data was generated from the 2011 UK census, combining the locations of work and residence. It was aggregated to Middle Super Output Area zones, which are statistical regions with an average population of 3300. The baseline propensity to cycle was modelled as a function of route distance and hilliness, based on the interzonal OD data and estimates accounting for traffic not included in this dataset. This function represents the likelihood that a person is going to choose cycling for commute, given the distance and hilliness of the route. Four different scenarios of increased cycling propensity were generated, which can be thought of as representing changes in cycling culture, infrastructure and technology. The first scenario doubles the number of people cycling to work nationally. This was based on the UK governments target to double cycling by 2025. The OD data for this scenario was based on the sum of observed cyclists from the census, and modelled cyclists based on the propensity to cycle equation. The second scenario, called gender equality, increased women's propensity to cycle to be as high as that of men for each OD-pair. This was based on the observation that women cycle the same or more than men in regions where cycling is very common. The third scenario, Go Dutch, used the propensity to cycle from the Netherlands. This scenario can be thought of as England and Wales having the Dutch infrastructure and bicycle culture, but keeping its trip distances and hilliness. Unlike the first two scenarios, this one only depends on trip distances and hilliness, not the 2011 propensity to cycle. To create this scenario, the British and Dutch national travel surveys were analysed and used to create scaling factors converting the UK propensity to cycle into the Dutch propensity to cycle. The fourth and final scenario was an extension to the Go Dutch scenario, which additionally increased cycling to model the adoption of e-bikes (Lovelace, et al., 2017).

The results of the different scenarios, including the baseline case, were visualised separately for each region. Travel between regions and within a statistical zone was not displayed. The centroids of statistical zones were used as start and end point for desire lines and routes on the OpenStreetMap (OSM) road network. The routes were calculated using the bicycle routing engine CycleStreets, which offers both direct and cycle-friendly routes. Additionally, the sum of all bicycle commuters on a road segment can be viewed (Lovelace, et al., 2017). Examples of the visualisation are shown in Figure 5 and Figure 6.

The health impact of increased cycling levels was modelled using an approach based on the Health Economic Assessment Tool from the World Health Organisation. The increased physical activity from cycling was used to estimate the number of premature deaths avoided. The reduction in carbon emissions was modelled by assuming all modes being equally likely to be replaced by cycling and applying the average $CO^2$-equivalent emissions per kilometre of car driving (Lovelace, et al., 2017).

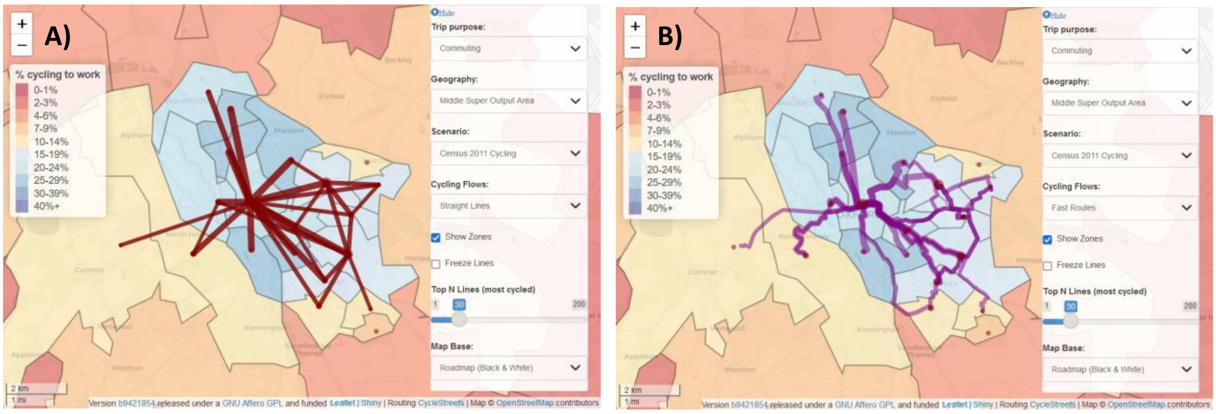


*Figure 5: Visualisation of the Propensity to Cycle Tool commuting model around Oxford. A) desire lines under the baseline scenario. B) visualisation of the fastest routes under the baseline scenario (screenshots from: (Woodcock, et al., Propensity to Cycle Tool, n.d. b)).*

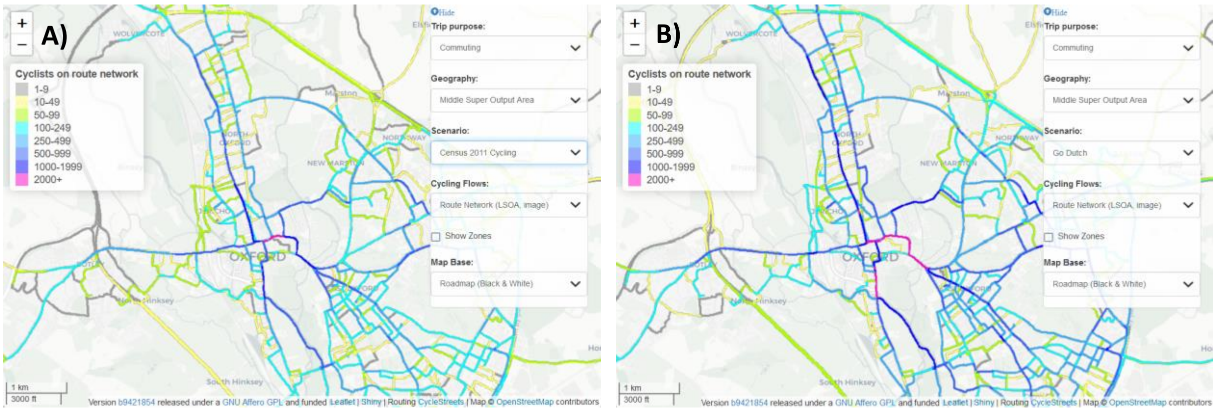


*Figure 6: Visualisation of the Propensity to Cycle Tool commuting model in Oxford. A) estimated number of commuter cyclists on road segments under the baseline scenario. B) estimated number of commuter cyclists on road segments under the Go Dutch scenario (screenshots from: (Woodcock, et al., Propensity to Cycle Tool, n.d. b)).*

### 2.2.2) Travel to School

The travel for school model was based on the National School Census for 2011, which only covers public schools in England, excluding private schools and Wales from the model. The OD data connects the pupils place of living, aggregated to Lower Super Output Areas (statistical zones with a population of around 1560 people), to their school. Separate models were calculated for primary and secondary school children. Next to the baseline scenario, the Government target (double cycling) and Go Dutch scenarios from Travel to Work were implemented (Goodman, et al., 2019). With Go Cambridge an additional scenario was added in 2019, applying the method of Go Dutch with reference data from the authority of Cambridge instead of the Netherlands (Goodman, 2019). The health impact from increased cycling levels was estimated using the additional physical activity energy expenditure from cycling compared to the pupil’s previous mode of travel to school. The carbon impact from reduced emissions from car traffic was calculated similarly to the travel to work method, but accounting for the increased number of trips due to drive home of the accompanying person. The visualisation of the results was the same as explained in the travel to work chapter (Goodman, et al., 2019).

## 2.3) Network Planning Tool for Scotland

The NPT was built for Scotland, based on the PCT. It was funded by Transport Scotland and is currently being developed at the University of Leeds, UK. The aim is to create a map of cycling potential on the street-level for the entirety of Scotland, which will enable strategic network planning. The main result is an interactive map with the estimated number of cyclists on each road segment for different trip purposes, scenarios and network types (Lovelace & Morgan, NPT Scotland, 2023b).

Four trip purposes are already implemented, as well as the option of displaying the sum of them. The first trip purpose is travel to work, which was estimated using the 2011 Census data, like in the PCT. The second and third types are travel by pupils to primary school and secondary school. The fourth purpose was not included in the PCT and includes other everyday trips: shopping, access to leisure facilities (e.g. parks or recreational destinations) and personal trips to visit family and friends. Not currently implemented are recreational cycling, where cycling itself is the main aim of travel, and mixed-mode trips. The scenarios implemented for these trip purposes are baseline, Go Dutch and e-bike. They work the same as in the PCT (Lovelace & Morgan, NPT Scotland, 2023b).

The OD-matrices created for the different purposes and scenarios are mapped onto the OSM road network using the routing engine CycleStreets, which was also used for PCT. The display can again be selected to show cyclist numbers per street segment based on direct routing or with detours to avoid roads with much traffic and use cycle-friendly roads instead. Other layers allow to show cyclist counts on a simplified road network where parallel ways of the same road are added together, the cycle friendliness and the gradient of roads (Lovelace & Morgan, NPT Scotland, 2023b). An example of the cyclist traffic dispersion map is shown in Figure 7.

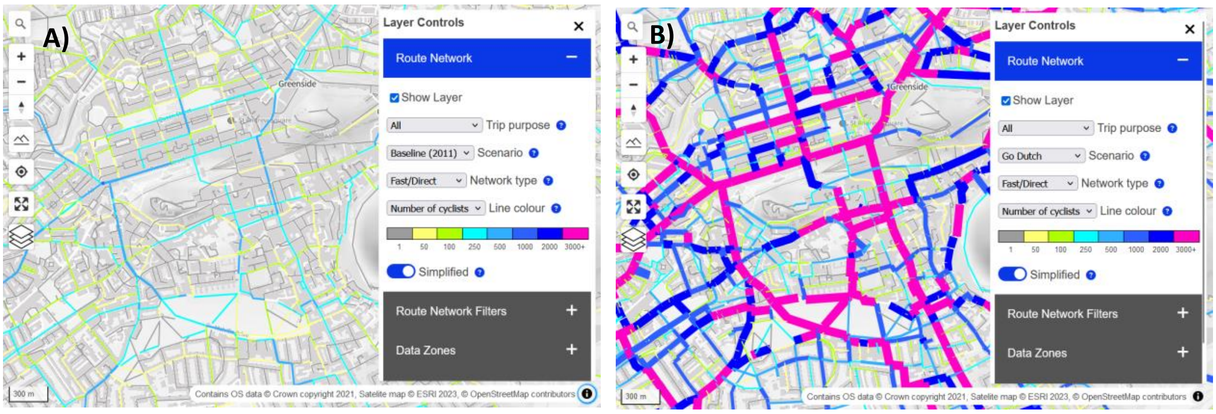


*Figure 7: Visualisation of the National Planning Tool for Scotland model in the centre of Edinburgh for all trip purposes using the simplified road network. A) estimated number of cyclists on road segments under the baseline scenario. B) estimated number of cyclists on road segments under the Go Dutch scenario (screenshots from: (Lovelace & Morgan, 2023a)).*

## 2.4) Routing Engines

Many different routing engines exist, with different properties. To reflect cyclist's route choices the routing service should have a routing profile for bicycles, which considers trip length or distance, hilliness and cycle friendliness in routing. Being able to host the service locally for free and all required data being available are the other requirements for their use in this thesis.

Many routing services use the OpenStreetMap (OSM) road network and provide routing APIs for bicycles (OpenStreetMap, 2023). A popular routing engine not using OSM is Google Maps. While it does offer a routing profile for cyclists and returns multiple route options, the methods used to generate the routes are not clear (Google, n.d.). The city of Zurich has a routing service for within the city, which uses the city's own road network. It has both an option for direct routes and for using more cycle friendly routes which avoid busy roads (Stadt Zürich, n.d.).

The service used for the Propensity to Cycle Tool and the Network Planning Tool for Scotland is CycleStreets (Lovelace, et al., 2017; Lovelace & Morgan, NPT Scotland, 2023b). This routing service is only for cyclists and covers the United Kingdom as well as some other countries, including Switzerland. Four different routing profiles are available, which are fastest, balanced, quietest and ebike. With the exception of ebike, all profiles include hilliness in their evaluation. Quietest and balanced additionally include the busyness of roads. Unfortunately, this service does not provide the ability to locally host the service (Nuttall & Lucas-Smith, n.d.). Openrouteservice does allow downloading and running the service locally. However, the avoidance of busy roads is only available for pedestrian traffic (gGmbH, 2023). The routing engine Valhalla can be hosted locally and allows the adjustment of a wide range of routing parameters, including hilliness and road types. As it is the only routing engine found that fits all the criteria and has the added advantage of customisation, it was chosen for this thesis and will be introduced in the next chapter (Valhalla, 2023).

### 2.4.1) Routing Engine Valhalla

Valhalla is an open-source routing service using open source data by Mapzen, which is a Linux Foundation Project since 2019 (Mapzen, 2019; Valhalla, 2023). It uses the OSM road network and Shuttle Radar Topography Mission SRTM elevation tiles as data input. Together they are converted into a graph network in a hierarchical data structure and split into tiles. Routing is performed using an A* algorithm, with the cost of edges and nodes in the network being computed during routing (Valhalla, 2023).

#### 2.4.1.1) Using Valhalla

A demonstration of the Valhalla Routing Engine is provided by FOSSGIS e.V. on the website https://valhalla.openstreetmap.de. It allows routing on the global OSM-network, as well as the adjustment of routing parameters. However, the rate at which routes can be requested is limited (FOSSGIS e.V., 2024; Valhalla, 2023). To calculate a large number of routes, such as for this thesis, Valhalla can be hosted locally on a computer or on a server and then accessed by API. This is possible using a Docker image by Valhalla or by GIS-OPS, a small company focussing on geographic information science. For this thesis the version provided by GIS-OPS on Github was chosen, due to its easier installation process (GIS-OPS, 2021; GIS-OPS, 2024; Valhalla, 2023). Docker images are software packages which include all information needed to run an application. When running an image using Docker, it becomes a container which is isolated from its environment, ensuring that it works regardless of the hardware and software infrastructure. Docker-Desktop is a free program allowing to run Docker images. For this thesis Docker Desktop version 4.30.0 is used (docker, n.d. a; docker, n.d. b).

#### 2.4.1.2) Description

Valhalla can provide different routing related services: Routing can be performed with and without a predefined order between multiple points. Time-distance matrices can be created between multiple points, but without returning the routes themselves. Other services are the creation of isochrone and isodistance maps. Finally, Valhalla can match coordinates onto the road network and provide information on nodes and edges near a location (Valhalla, 2023). For this thesis only the routing between points with a predefined order will be used.

As mentioned before, Valhalla stores the graph created from the road network and enriched with elevation data in tiles with a hierarchical structure (see Figure 8). The highest level contains only long-distance roads (OSM-tags motorway, trunk and primary) and is split into 4° tiles (light blue in Figure 8). The second level is in 1° tiles and additionally contains secondary and tertiary roads (green in Figure 8). The lowest level is stored in 0.25° tiles and contains all roads (orange in Figure 8). These tiles are subdivided again into bins of 0.05° size, which are used for finding edges near input coordinates. Tiling the data allows the routing engine to only load the parts of the road network which are necessary for routing, reducing memory requirements. This allows the engine to work on a wider range of devices, including mobile phones, where offline routing is most useful. The hierarchy increases this advantage, by not all loading local roads between origin and destination, when routing over a long distance. For bicycle and pedestrian routing however, only the lowest level is used (Valhalla, 2023).

Instead of storing the network segments with their cost, Valhalla stores them with their attributes. This approach is called dynamic run-time costing and only calculates the cost when the route is being computed. As discussed before, the generalized cost of edges consists of more factors than just its length or the time of traversing it. Road and surface type, elevation change and other parameters are used to improve routing. Additionally, different modes of traffic have access to different roads and need different routing parameters. This approach allows Valhalla to use different parameters for each route, without recalculating the entire network (Valhalla, 2023).

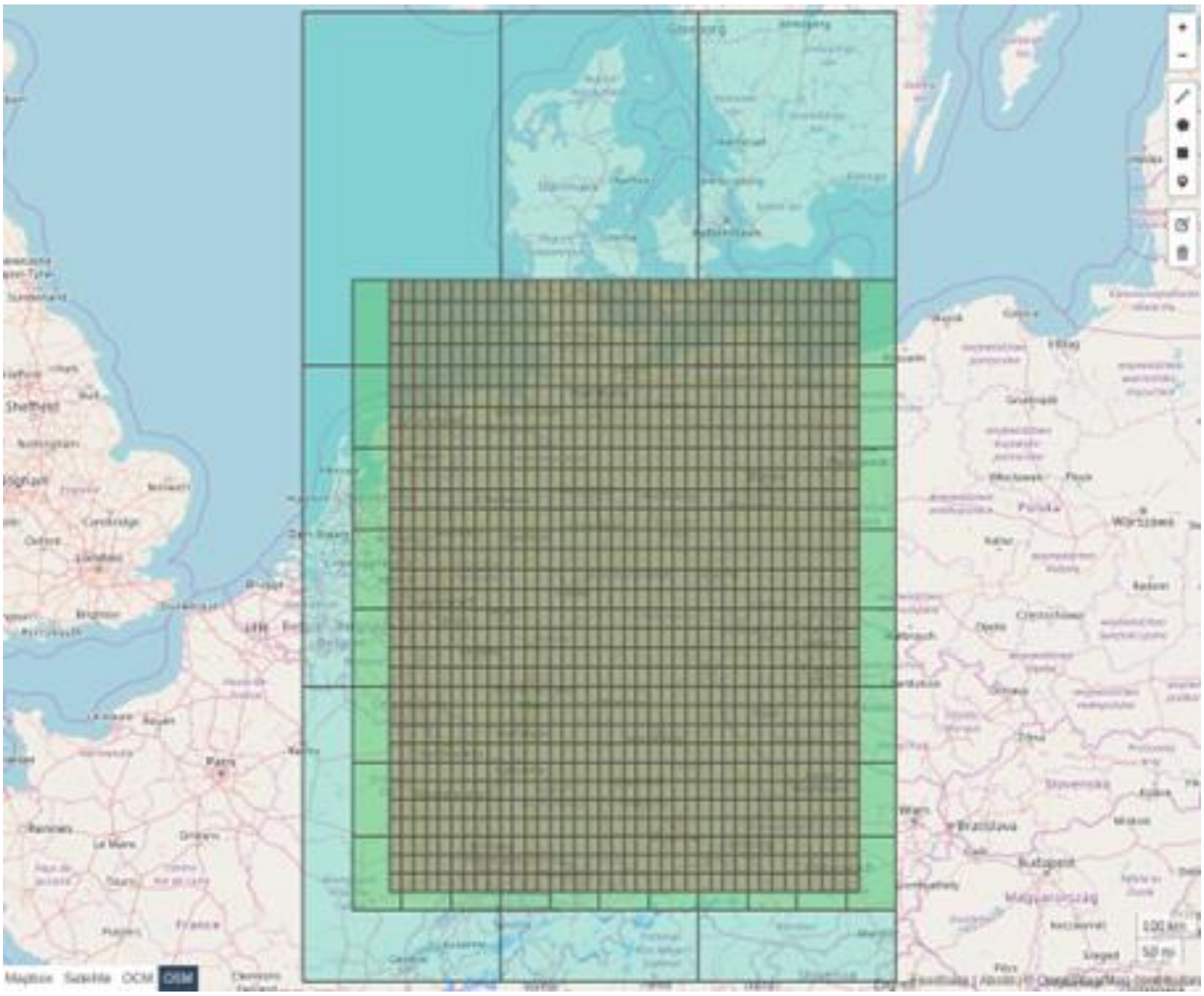

*Figure 8: Example of the hierarchical tile structure used, over the Germany (blue: highest level, green: medium level, orange: lowest level) (image from Valhalla, 2024).*

In Valhalla, the computation of routes starts with identifying the closest edge to each location included in the request. Only the edges in the bins closest to each location and usable by the selected mode are considered. No more bins are analysed, when the next bin is further away from the location than the closest found edge or the distance has become too great. In a second step the path is being computed using a bidirectional A* algorithm with dynamic, run-time costing, a variation of Dijkstra's algorithm. The algorithm and costing will be explained in the next section. Unidirectional A* algorithms are used when the routing has a fixed start or end time, when it involves public transport or is between adjacent edges. Next, the sequence of edges and nodes is formed into the path and enriched with attributes. The attributes are then used to create navigation maneuvers. Finally, the route shape is encoded and returned with the response in a JSON object (Valhalla, 2023).

Valhalla has to be accessed via its API, even if it is hosted locally using Docker Images. A route is requested by including JSON-formatted information regarding the locations, routing model and output. The output also takes the form of a JSON object. It includes summary information on the entire trip as well as the legs between the requested locations. Each leg has its own summary as well as a shape in the form of an encoded polyline and a list of maneuvers for navigation. If requested it also includes elevation information at regular intervals along the route (Valhalla, 2023). The encoded polyline format compresses a series of coordinates into a single string, reducing the file size. To do so, each latitude and longitude is converted into an ASCII character and stored. As the coordinates are rounded it is a lossy compression algorithm, Valhalla uses six instead of the usual five decimal places (Google, 2024; Valhalla, 2023).

**A* routing algorithm**

The A* routing algorithm is a variation on Dijkstra's algorithm and looks for the path with the lowest cost between a starting node and a goal node in a network. It works in the following steps, repeating steps two to six until the goal node is reached (Hart, Nilsson, & Raphael, 1968):

1. Visit the starting node.
2. Mark the node currently visited as "closed". Store the previously visited node and the cost of the path to the starting node.
3. Calculate the heuristic for all neighbouring nodes. The heuristic for the A* algorithm is the sum of the cost to the starting node and the cost to the goal node. The cost to the starting node is the cost of the shortest discovered path. The cost to the goal node is unknown and has to be approximated using additional information about the routing problem. For the algorithm to work, this cost must be lower or equal to the cost along the network, if it is set to zero the algorithm is identical to Dijkstra's algorithm. For example, when calculating the shortest path by distance along a road network, the airline distance to the goal (or any shorter distance value) could be used.
4. All neighbouring nodes which are not marked as "closed" are marked as "open" and their heuristic is stored.
5. Neighbouring nodes marked as "closed" and with a lower cost to the starting node than previously determined are marked as "open" and their heuristic is stored.
6. If the current node is the goal node, the algorithm is finished. Otherwise, visit the "open" node with the lowest heuristic value and go to step 2.

Valhalla uses a bidirectional A* algorithm, which starts simultaneously from the starting node towards the goal node and from the goal node towards the starting node. It ends when the paths meet in the centre and is more efficient, as it visits fewer nodes. The heuristic used is the sum of the known shortest cost to the starting node and the distance on the earth's surface multiplied by a cost factor based on the cost model (Valhalla, 2023).

## 2.5) Distribution of Route Start and End points

Where the routes between pairs of traffic zones enter and exit the road network has a strong influence on the final trip distribution: A smaller number of these connector points results in a concentration of traffic near them. The traffic pattern only appears realistic and diffuse, when multiple connector points are used for each traffic zone (Friedrich & Galster, 2009; Jafari, Gemar, Ruiz Juri, & Duthie, 2015; Schnabel & Lohse, 2011).

The connector points are usually based around the traffic zones centroid, with different methods to both determine the centroid and to assign connector points. In homogeneous traffic zones, the geometrical centre can be used as centroid, otherwise the centre of gravity of the zones origins and destinations might be used. This distribution can alternatively be approximated using the density of weighted network nodes. Another approach to determine a zones centroid is to perform an accessibility analysis and choose the network node with the highest accessibility as centroid (Friedrich & Galster, 2009).

The simplest method to determine connector points is to choose the node in the network which is closest to the centroid (Lovelace, Félix, & Carlino, 2022). Many more complex approaches exist in the literature, some of which will be quickly introduced: One method by Friedrich and Galster (2009) weights nodes according to the total length of the segments linking to it and chooses nodes with a high weight as connector. A second method from the same paper tries to choose nodes with equal travel times towards the centroid. There are also methods that assign separate connector nodes for different directions of travel (Friedrich & Galster, 2009; Jafari, Gemar, Ruiz Juri, & Duthie, 2015). One way of further spreading out the route start and end points is to subdivide traffic zones into subzones and apply the described methods to these smaller zones. The method used in this thesis is called jittering, it distributes multiple route start and end points throughout the traffic zone based on a geographical variable and will be explained in the next section (Lovelace, Félix, & Carlino, 2022).

### 2.5.1) Origin-Destination Data Jittering

Jittering means to add random noise to data for visualisation. In this case it is used to represent the spread of route start and end points within a traffic zone, which is especially important to consider for pedestrian and bicycle traffic. The method makes it possible to distribute connector nodes based on a variety of variables and to use multiple routes between each OD-pair (Lovelace, Félix, & Carlino, 2022).

The method works by choosing random coordinates within the appropriate traffic zones as start and end points for each route. This way routes have different connector points which are distributed across the traffic zone, avoiding a high concentration of trips in a small area. To avoid route start and end points in unrealistic locations (e.g. inside a forest or lake) additional geographic data can be used to constrain the coordinates being selected. These additional data can simply be the settlement area within the traffic zone, but more complex data with weighting by population density or other relevant factors might also be used (Lovelace, Félix, & Carlino, 2022).

To further distribute the connector nodes across the traffic zone, especially when the number of trips between zones has a large variability or is very high, multiple routes can be used between each OD-pair. With this process of disaggregation, the total number of trips between two traffic zones is spread across multiple routes, which have different start and end points. Using an upper threshold of trips per route, OD-pairs can be automatically disaggregated into multiple routes (Lovelace, Félix, & Carlino, 2022).

This method has the advantage of creating a more diffuse route network than other approaches, especially compared to simple centroid to centroid connections. Furthermore, it allows for customisation to fit the available data and requirements of the project, while being simple to implement. However, the use of randomness reduces reproducibility of the results. As the method was only published in 2022, further research on the quality of the method and optimal configuration needs to be done (Lovelace, Félix, & Carlino, 2022).

## 2.6) Aggregation of Trip Data

To visualise the number of trips on the road network, the trips need to be aggregated from the different routes passing through the same road segment. The routing engine used in this thesis only returns a linestring (an ordered list of coordinates) of the route and not the identifiers of the segments used. Identifying the road segment from the original network therefore becomes computationally expensive. Instead, the network can be rebuilt using the linestrings returned by the routing engine, using a method described by Morgan and Lovelace (2021).

First, the linestrings are broken down into their individual segments, by extracting each neighbouring pair of coordinates. The coordinate pairs are then stored so that the southernmost of the two point is first (if the latitude is the same, the westernmost coordinate is first). This way segments traversed in opposing directions are stored in the same way and duplicates can easily be removed. Next, the number of trips can be aggregated for each segment and additional attributes returned by the routing engine can be stored. Finally, touching segments with the same attributes can be merged back into linestrings. Large datasets can also be split into multiple regions, to improve performance (Morgan & Lovelace, 2021).

The resulting network only includes the road segments used for at least one route and the attributes returned by the routing engine. If the entire network or additional attributes are needed, another approach, such as identifying the segments in the original network by their coordinates, should be chosen. Another limitation occurs, when the start- and end points of routes can be in the middle of a segment as opposed to their ends. In these cases, the method will return colinear segments of different lengths. As these errors are short, they only have a small impact on the resulting network (Morgan & Lovelace, 2021).

## 2.7) Classification into Urban and Rural

### 2.7.1) Municipalities

Classifying municipalities into different groups with similar characteristics is useful for statistical data analysis and often allows to identify more connections in the data (Bundesamt für Statistik BFS, 2017c). The federal office for statistics in Switzerland publishes different spatial typologies of municipalities. “Areas with urban character” (AUC) focuses on urban areas and is based on morphological and functional criteria. “Typology of municipalities” (ToM) provides a differentiation into 9 or 25 different categories, based on AUC as well as population statistics and accessibility. “Urban-rural typology” (URT) is in turn based on ToM and only consists of the classes urban, intermediate and rural (Bundesamt für Statistik BFS, 2024). With regards to cycling, a differentiation of urban and rural regions is helpful, as the amount of traffic and the traffic patterns differ (Stiftung SchweizMobil, 2018), therefore the urban-rural typology will be used in this thesis, which is also used for the NPVM (Bundesamt für Raumentwicklung ARE, 2020b).

As mentioned, the URT is based on the ToM which in turn is based on the areas with AUC, a flowchart of the different categories is shown in Figure 9. The classification of areas with urban character is based on data from 2012 and is consistent over all of Switzerland. Both morphological (e.g. population and workplace density) and functional (e.g. commuter flow) aspects of urbanity are included. Municipalities are classed into five categories which can be combined into three groups. Only the three groups are used for the typology of municipalities: core agglomeration, agglomeration belt & multiply oriented municipalities and finally rural municipalities without urban character (Bundesamt für Statistik BFS, 2014).

To form the ToM, the three categories of AUC are each split into three subcategories based on density, size and accessibility. For URT the subcategories are merged to form the urban, intermediate and rural categories. Periurban municipalities with low density are assigned to the rural category, while rural core municipalities are assigned to the intermediate category, otherwise the categories are the same as with the AUC (Bundesamt für Statistik BFS, 2017c).

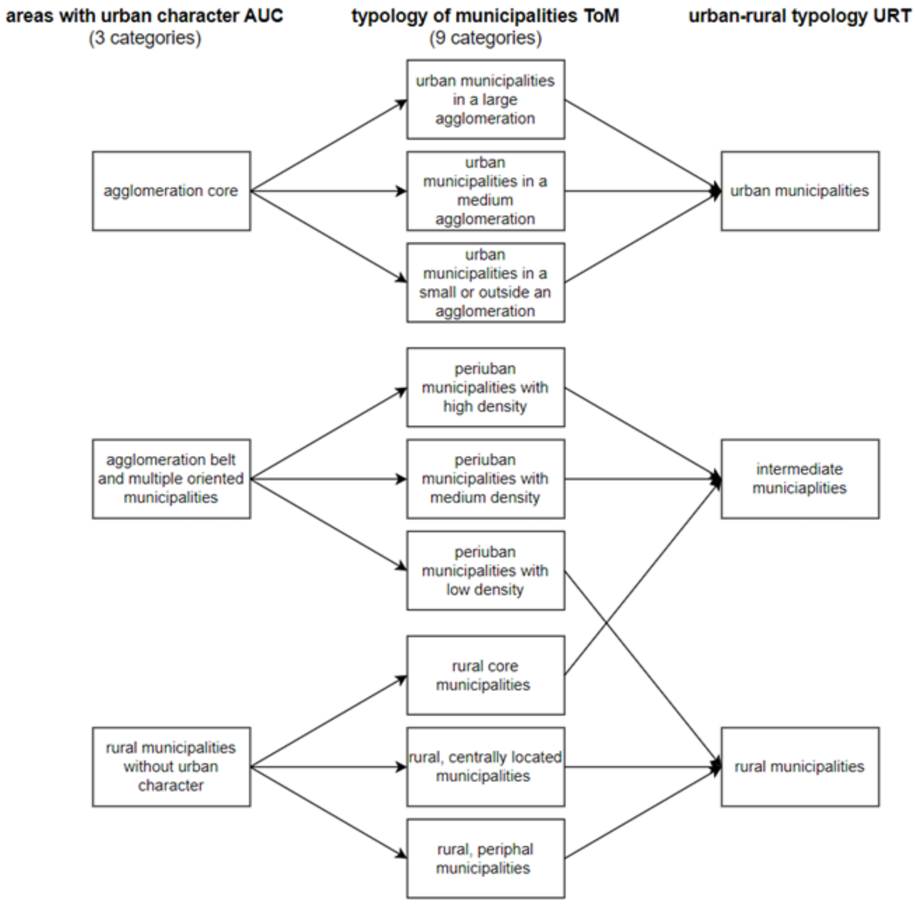


*Figure 9: Flowchart showing the relationship between the different municipality typologies (Bundesamt für Statistik BFS, 2014; Bundesamt für Statistik BFS, 2017c).*

### 2.7.2) Bicycle Counting Stations

The characteristics of bicycle traffic in Switzerland are very different for urban and rural areas. A classification of the counting stations is therefore very useful for the data analysis. Applying the urban-rural typology of the municipalities onto the counting stations assumes homogeneity of the municipalities. Municipalities however often include both urban and rural areas, such as agricultural land and forests next to settlements. For this reason, SwitzerlandMobility use a different classification scheme: All counters are classified as urban, if there is more urban than rural area within a radius of 500m around the counting station. Urban areas are defined as settlement area within municipalities classified as urban centres by the municipality classification from the year 2000 of the federal office of spatial planning. Rural areas are defined as agricultural land, forest, and tourism zones. Urban counting stations clearly separated from the settlement area by a river or train line are manually reclassified as rural (Stiftung SchweizMobil, 2018).

## 2.8) Imputation of Bicycle Traffic at Long Term Counters

Due to the high temporal variability in cycling, missing data can significantly impact the accuracy of the calculated AAWT (El Esawey, 2017). This is especially the case if data is continuously missing for a longer period, while randomly distributed short gaps have less of an impact (El Esawey, 2018b). To address this issue different imputation methods exist, for example expansion factor models, regression models and models using neural networks (Beitel & Miranda-Moreno, 2016; El Esawey, 2018a). The data required by different models can include historical counts at the same station, counts at other stations with similar temporal patterns and relationships with other variables such as weather and land use (El Esawey, 2017).

Expansion factor models are mainly used to calculate the annual average daily traffic AADT from short-term counting stations (with counts for a few days or weeks) using expansion factors of long-term counting stations (with counts for the whole year) and are based on methods from motorised traffic counts developed by the US Federal Highway Administration. An expansion factor relates the bicycle count on a day or collection of days to the average bicycle count over a longer period. For example a factor for all weekdays in January, one for all weekends in January, one for all weekdays in February, etc. This allows them to account for temporal variation in bicycle traffic. While traditional methods use monthly and day-of-week expansion factors, the disaggregate factor method DFM uses a factor for each individual day, which additionally accounts for day-to-day variation in weather (Nosal, 2014). The DFM was introduced in 2014 by Nosal and has since been improved and expanded by multiple authors. These additions include different ways to identify outliers in the long term counts and methods to match short and long term counts (Beitel & Miranda-Moreno, 2016; Beitel, McNee, McLaughlin, & Miranda-Moreno, 2018; El Esawey, 2023; Nosal, 2014; Nosal, Miranda-Moreno, & Krstulic, 2014). As the imputation of missing data used in this thesis is based on DFM, it will be explained in more detail in the next chapter.

### 2.8.1) Disaggregate Factor Method

The core of the DFM has remained unchanged from Nosal (2014). The daily factors of the long-term counter (equation ( 2 )) act as expansion factors and relate the daily counts to the annual average traffic. Equation ( 3 ) allows to estimate the annual average traffic for the short-term counter using the daily factors from the long-term counter. It gives an estimate of annual average weekday traffic AAWT for each day with short term measurements. The average of those values can be used to estimate AAWT for the year (Nosal, 2014). Nosal et al. (2014) made a comparison between this base DFM and the traditional expansion factor method (with monthly and day of the week expansion factors), a day by month method (with day of the week expansion factors for each month) and a weather model method. The less short-term count data is available, the larger is the difference between the methods, with DFM performing the best. With more than about two weeks of contiguous data however, the differences in performance become small. For the largest amount of short-term data tested (30 days), the average absolute relative error AARE of all models is between 8 % and 10 %, with the weather model being slightly better than DFM (Nosal, Miranda-Moreno, & Krstulic, 2014).

$$AAWT_i = \frac{1}{n_i} * \sum c_{id} \qquad (1)$$

$$df_{id} = \frac{c_{id}}{AAWT_i} \qquad (2)$$

$$\widehat{AAWT}_{id} = \sum_d \frac{c_{id}}{df_{jd}} \qquad (3)$$

| | |
|---|---|
| $AAWT_i$ | annual average weekday traffic for station i |
| $n_i$ | number of days with data for station i |
| $c_{id}$ | bicycle count for station i on day d |
| $df_{id}$, $df_{jd}$ | daily factor for station i on day d, daily factor for reference station j on day d |
| $\widehat{AAWT}_{id}$ | AAWT for station i, estimated using day d |

To match the short-term counters with long term counters of similar temporal behaviour, Nosal (2014) uses k-means clustering to create factor groups of the long-term counters. The indices used for clustering represent the daily and hourly variation of the counts. Beitel and Miranda-Moreno (2016) expanded on this method by introducing a third index representing weekly and monthly count variation. The short-term counters are then matched to one of the clusters of long-term counters (Beitel & Miranda-Moreno, 2016).

They also introduced two different modifications to the DFM method. While Nosal (2014) had only used weekdays for the DFM and manually removed holidays and missing counts, one of the modifications treats weekdays separately to weekends and holidays. The reason being the different cycling demand on weekdays opposed to weekends and holidays, which can introduce error into the estimate. Their second modification introduces an iterative algorithm to remove outliers from the daily AADT estimates. Erroneous data is removed if the daily AADT estimate is outside a certain interval of the mean of the AADT estimates. This accounts for errors in both the short-term counts and the long-term reference counts. The separation of weekdays and weekends/holidays results in a decreased AARE of 18%, the filtering approach reduces AARE by 25 % (Beitel & Miranda-Moreno, 2016).

Beitel et al. (2018) introduced methods to automatically validate and interpolate long term bicycle counts. Daily factors are used to calculate the correlation between all pairs of counting stations using equation ( 4 ). For each counting station i, the two counting stations with the highest correlation in their daily factors is chosen as reference stations j, if the correlation is at least 0.75. To identify days with anomalous data the ratio $\frac{df_i}{df_j}$ is calculated for each day. All days for which the ratio to both reference stations is outside the interval [1/2, 2] are removed. The daily factors of days with removed data are calculated as the average of the daily factors of the reference stations. As the correlation decreases with more days of anomalous data, this method is only suitable for counting station where not many days need interpolation. This method was able to identify over 90% of days with 12 or more hours of anomalous data. However, this method is vulnerable to multiple stations having anomalies on the same day (Beitel, McNee, McLaughlin, & Miranda-Moreno, 2018).

$$Correl\left(DF_i, DF_j\right) = \frac{\sum_d((df_{id} - 1) * (df_{jd} - 1))}{\sqrt{\sum_d(df_{id} - 1)^2 * \sum_d(df_{jd} - 1)^2}} \qquad (4)$$

$Correl(DF_i,DF_j)$ correlation between the vector of daily factors $DF_i$ of station i and the vector of daily factors $DF_j$ of reference station j

El Esawey (2023) has developed a method to identify anomalous data in long term bicycle counts with at least 300 days of data. As the method by Beitel et al. (2018), this method is also based on daily factors. The mean, standard deviation and coefficient of variation are calculated for each day over all stations. If the coefficient of variation is below a certain threshold (e.g. 20 %) for a day, all data of this day is considered to be good. Otherwise, outliers are identified in an iterative process for each day, until the number of newly identified outliers becomes small. In the first step of this process, the lowest and highest daily factors are removed if data is available for more than three counting stations. Next an upper and lower limit are defined as the mean of the daily factors plus/minus two standard deviations. All daily factors falling outside this range are then removed. Two refinements to this method were also proposed. The first refinement calls for a recalculation of the AADT and daily factors after each iteration. The second refinement expands upon the first refinement by additionally removing all data of counting stations with fewer than 300 valid days of data. Of the three variations, the first refinement showed the best results. Over 95% of the outliers that were smaller than 50% or larger than 250% of the correct value were identified (El Esawey, 2023).

## 2.9) GEH and SQV Measures

The GEH-value (named after its originator Geoffrey E. Havers, see equation ( 5 )) and Scalable Quality Value SQV (equation ( 6 )) are measures used in traffic planning. Their purpose is to compare pairs of modelled values and observed values, for example traffic counts at a counting station, and to assess the quality of the match (Friedrich, Pestel, Schiller, & Simon, 2019). While the GEH-value was used to validate the NPVM model, the Swiss Association of Traffic Engineers and Traffic Experts SVI now recommends to use of newer SQV instead (Bundesamt für Raumentwicklung ARE, 2020b; Schweizerische Vereinigung der Verkehrsingenieure und Verkehrsexperten SVI, 2019).

The GEH-value was created in the 1970s to have a measure which combines absolute and relative deviation of modelled and observed traffic volumes. This was necessary, as absolute deviation is only useful for low values and relative deviation only for high values. The SQV was developed by Friedrich et al. (2019) to address multiple issues with the GEH-value: Firstly, it is not unitless (it has a unit of sqrt(vehicles/hour)) and does not range between zero and one. Secondly, it is asymmetrical, giving a different result for the same absolute deviation above or below the observed value. And thirdly, it is best used for values in the range from 2’000 to 50’000 and cannot be scaled to serve other value ranges. To solve the first and third problem, the SQV uses a scaling factor f, which normalises the observed and modelled values and has the same unit as the value of interest. It should be chosen before model validation and should represent the order of magnitude the values are expected to be in (Bundesamt für Raumentwicklung ARE, 2020b; Friedrich, Pestel, Schiller, & Simon, 2019).

$$GEH = \sqrt{\frac{2 * (m - c)^2}{m + c}} \tag{5}$$

$$SQV = \frac{1}{1 + \sqrt{\frac{(m - c)^2}{f * c}}} \tag{6}$$

| | |
|---|---|
| m | modelled value |
| c | observed value |
| f | scaling factor |

Both GEH-value and SQV have value ranges which indicate the quality of a range of measure values. Even though they are both using three ranges for evaluation, the GEH-values and SQV cannot be directly translated. Furthermore, for the GEH-value they were created for hourly car traffic volumes and the SQV is too new to know what values are attainable in practice. Those ranges can nevertheless serve as an orientation for analysis and are shown in Table 3 and Table 4. To show these value ranges on a plot, such as in Figure 31 and Figure 32, the equations ( 5 ) and ( 6 ) need to be solved for modelled counts. Friedrich et al. (2019) did this transformation for the GEH-value (see equation ( 7 )), the transformation for SQV is shown in appendix 1, resulting in equation ( 8 ) (Friedrich, Pestel, Schiller, & Simon, 2019; Schweizerische Vereinigung der Verkehrsingenieure und Verkehrsexperten SVI, 2019).

*Table 3: Evaluation of GEH-value (Bundesamt für Strassen ASTRA, 2018).*

| GEH-value | Evaluation |
|---|---|
| < 5 | Very good match |
| < 10 | Good match |
| < 15 | Acceptable match |

*Table 4: Evaluation of SQV (Friedrich, Pestel, Schiller, & Simon, 2019).*

| **SQV** | **Evaluation** |
|---|---|
| ≥ 0.9 | Very good match |
| ≥ 0.85 | Good match |
| ≥ 0.8 | Acceptable match |

$$m = \pm \frac{\sqrt{16 * c * GEH^2 + GEH^4} + 4 * c + GEH^2}{4} \tag{7}$$

$$m = c \pm \sqrt{\frac{f * c * (1 - SQV)^2}{SQV^2}} \tag{8}$$

## 2.10) Research Gaps

During the review of the literature multiple research gaps were found, which this thesis will try to fill:

1. While a bicycle traffic route choice was done for the NPVM, they did so with only one connector node for each traffic zone. Furthermore, the road network is based on a network developed for car traffic, which does not include all ways usable by bicycles.
2. The bicycle traffic route choice model in the NPVM requires special software, which is not free to use. This hinders the creation of traffic assignment maps with modifications to the infrastructure.
3. The results of the jittering approach have, to the knowledge of the author, not been compared to bicycle count data.

The bicycle traffic assignment model developed in this paper has the advantage of relying completely on freely available data and software, making it easier to assess the impact of planned infrastructures. With the use of jittering the model has many connector points in each traffic zone, distributing it more evenly and improving local traffic patterns.

# 3) Data

## 3.1) Road Network

The road network used for this thesis is OpenStreetMap OSM from January 2017. The OSM-data for Switzerland was downloaded from the website geofabric.de (Geofabrik, 2017). OSM is an online map of the world that was founded in 2004 and is created by volunteers. As it is available with an open database license the map data can be accessed freely and used for analysis or other projects (OpenStreetMap, 2024h). As anyone, including people without geographic education or local knowledge to the area they map, can contribute to the map, OSM is an example of volunteered geographic information. A problem with such information is that its accuracy and completeness are not as reliable as that of proprietary or government maps. Traditional map makers have control over the contributors and can implement quality control systems, whereas volunteered geographic information has to deal with antisocial behaviour creating wrong data (Goodchild, 2007).

Features in OSM are stored as elements (nodes, ways and relations) with associated tags to describe their attributes. A node represents a point in space and is assigned coordinates in the coordinate reference system WGS84. (OpenStreetMap, 2024f). An ordered collection of nodes form a way, which can represent both linear and area features. Ways where the first and last node are different are called open ways, they always represent a linear feature. In closed ways the first and last node are the same, they can represent linear features (e.g. a roundabout) or area features (e.g. a house) (OpenStreetMap, 2024j). When ways cross at the same level, they need to share a node in this location (e.g. roads at an intersection). If they cross on different levels, they may not share a node (e.g. a road on a bridge passing over another road). In this case the ways should be tagged to indicate a non-level crossing (OpenStreetMap, 2024g). Multiple nodes, ways and relations can together form a relation, which defines a relationship between these elements (OpenStreetMap, 2024f). All elements can be assigned any number of tags, which give a description of the feature. Tags consist of a key and a value, where the key notes the topic/category/type and the value provides the detail. Tags are usually written with the syntax key=value. A key can only be assigned once to an element. The OpenStreetMap Wiki provides conventions on how to use tags and what meaning they have (OpenStreetMap, 2024c).

Multiple studies have been conducted to assess the quality of OSM in terms of positional accuracy, attribute accuracy, completeness and other qualities. Using the decrease in map edits as it gets more complete and a visual assessment of completeness, it was estimated that the world map was about 83% complete in 2016. The completeness varies by region and reaches above 95% for most European and North American countries, including Switzerland. It also varies with population density, being highest in areas with high and low density and less complete in areas of medium density (Barrington-Leigh & Millard-Ball, 2017). In a comparison with proprietary road maps different studies for Canada (in 2015) and Germany (in 2009) found for positional accuracy that 78 percent and 73 percent, respectively, of OSM-roads are within five meters of the reference map. In Germany all roads were within 30 meters of the reference, while 92 percent were in Canada. For both countries the completeness of OSM was lower than that of the proprietary map. Both studies showed a higher positional accuracy and completeness in urban areas than in rural areas (Ludwig, Voss, & Krause-Traudes, 2011; Zhang & Malczewski, 2018). However, a similar study for Germany in 2011 estimated that the OSM road network was 27% longer than that of a proprietary mapping agency due to a larger pedestrian network. While the road network of OSM was 9% shorter in 2011, it was estimated to be comparable to the proprietary map in terms of completeness by the end of 2012 and in topology and street name information by 2017 (Neis, Zielstra, & Zipf, 2012). Another study in Canada for 2017 focused on bicycle infrastructure in large and mid-sized cities. They found that the length of infrastructure in OSM was comparable to the map by the city, while OSM included more small paths. However, the categorisation of bicycle infrastructure was inconsistent in OSM (Ferster, Fischer, Manaugh, Nelson, & Winters, 2020). Different studies, with some focusing on bicycle tracks and lanes, have found that the completeness and accuracy of attributes in OSM varies strongly by region, even within countries (Hochmair, Zielstra, & Neis, 2015; Vierø, Vybornova, & Szell, 2024).

## 3.2) National Model for Passenger Traffic

The bicycle distribution for 2017 (Eidgenössisches Departement für Umwelt, Verkehr, Energie und Kommunikation UVEK, 2019) and for the base scenario of 2050 (Eidgenössisches Departement für Umwelt, Verkehr, Energie und Kommunikation UVEK) from the Swiss national model for passenger traffic NPVM are used in this thesis. They include a list with all pairs of traffic zones and the number of bicycle trips between them (separately for both directions). The private car assignment model for 2017 (Bundesamt für Raumentwicklung ARE, 2022a) was additionally used for visualisations, as the model for bicycle traffic is unfortunately not available. An explanation of the NPVM model is in chapter 2.1.

## 3.3) Traffic Zones

The geometry of traffic zones within Switzerland (including Liechtenstein and enclaves) (Bundesamt für Raumentwicklung ARE, 2019a) and their centroids (Bundesamt für Raumentwicklung ARE, 2020a) was used for this thesis. For visualisations the geometry of traffic zone outside of Switzerland (Bundesamt für Raumentwicklung ARE, 2019b) was also used. All traffic zone data is for the year 2017. An explanation of traffic zones is in chapter 2.1.1.2.

## 3.4) Bicycle Counting Stations

Automatic bicycle counting stations measure how many bikes pass by them and at what time. Most stations use induction coils in the ground, but radar and pressure sensors are also used. Like the more established counting stations for car traffic, they are a basis for analysing, modelling, and planning traffic. The foundation SwitzerlandMobility has started installing such stations along their bike route network in 2004 with multiple cantons and cities following. While there were only 52 counting stations along those routes in 2017, there were already 85 in 2022 (Stiftung SchweizMobil, 2018; Stiftung SchweizMobil, Bundesamt für Strassen ASTRA, 2023). Manual counts of bikes are another option to determine the number of bicyclists on a road, however they are only conducted over a limited timeframe of a few days or weeks, while automatic counters can operate year-round. Manual counts are therefore not able to capture seasonal variation in bicycle traffic and need extrapolation to get a measure of yearly bike traffic. Automatic bicycle counts are the more common type in Switzerland and will be the only method included in this thesis (Baehler, Marincek, & Rérat, 2018). To match the data from the national traffic model, annual average weekday traffic AAWT will be used instead of annual average daily traffic AADT. AADT is calculated as the total number of cyclists over the year, divided by the number of days. For AAWT only weekdays (Monday to Friday) are used in the calculation. Using only AAWT results in a focus on commuter traffic, as leisure travel is more prevalent on weekends (Stiftung SchweizMobil, 2018).

Figure 10 shows a map with the locations of all counting stations used for this thesis. The data on counting stations comes from many different sources, mainly cantons and municipalities. Appendix 4 lists the different sources and appendix 5 all stations. The next section gives an overview over the bicycle count data sources and their data:

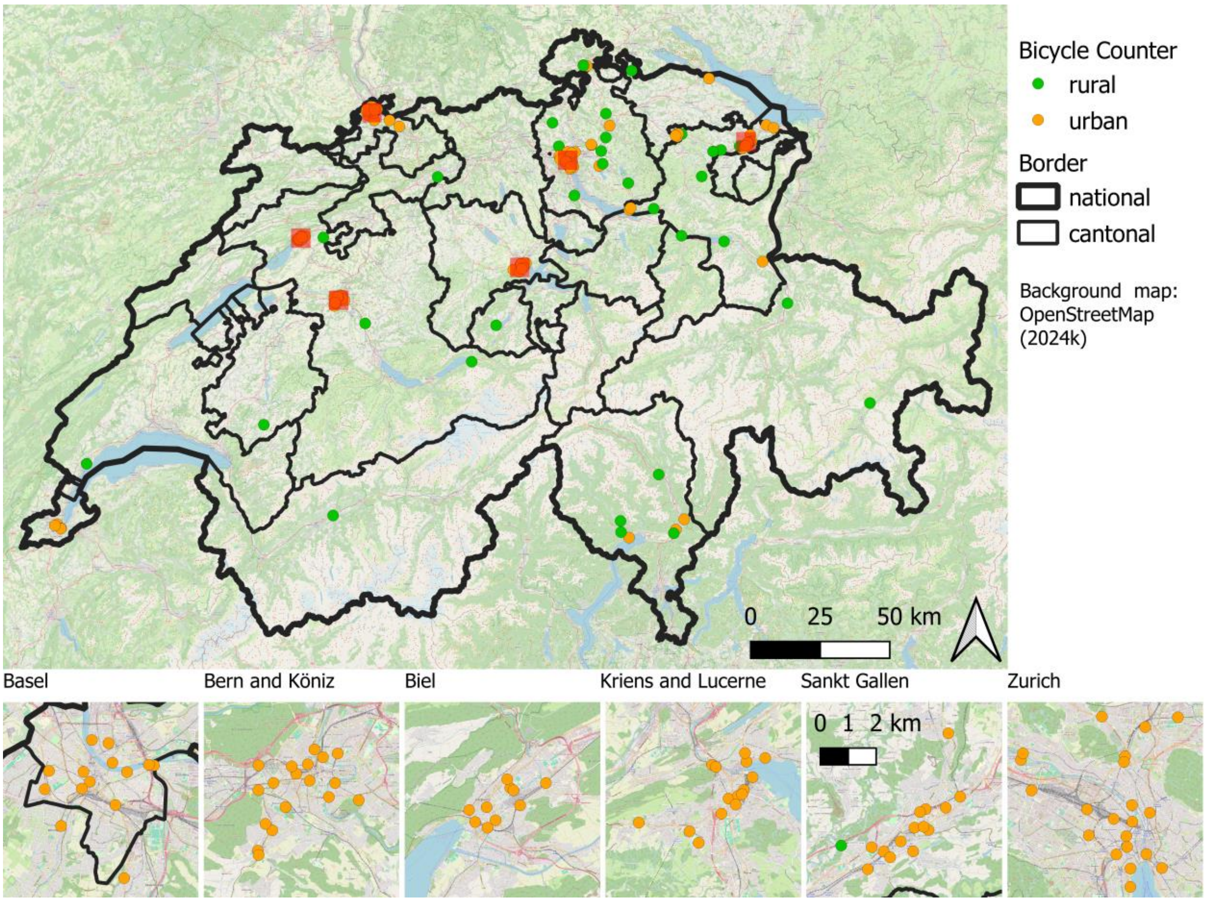


*Figure 10: Locations of all bicycle counting stations used in the analysis.*

### Canton Basel-Landschaft

AAWT is available for five stations on a monthly basis (Kanton Basel-Landschaft, 2018). Coordinates were approximated using the cantonal GIS-browser (Kanton Basel-Landschaft, n.d.).

### Canton Basel-Stadt

Hourly counts for 25 stations and coordinates are available. Two stations collect data in only one direction (Kanton Basel-Stadt, 2024). The coordinates for one station had to be obtained from a different source (Kanton Basel-Stadt, 2013).

### Canton Geneva

Hourly counts for five stations and a map with their locations were provided on request through email from Yves Steiner of the cantonal office of transport (Steiner, 2024). The coordinates were approximated using the basemap in the swisstopo GIS-Browser (Bundesamt für Landestopografie swisstopo, 2024).

### Canton Schaffhausen

Average weekday traffic for each hour of the day for three stations was provided on request through email from Martin Baggenstoss of the cantonal office of traffic and infrastructure (Baggenstoss, 2024). The coordinates are available on the cantonal GIS-Browser (Kanton Schaffhausen, 2023).

### Canton St. Gallen

AAWT for 14 stations and their coordinates were provided on request through email from Ina Stenzel of the cantonal office for building and the environment (Stenzel, 2024).

### Canton Ticino

Monthly counts and the yearly ratio of weekday to daily traffic are available for seven stations (Repubblica e Cantone Ticino, n.d. a). The ratio of weekday to daily traffic was used to calculate the monthly weekday traffic under the assumption that the ratio does not change significantly over the year using equation ( 9 ). The coordinates are available separately (Repubblica e Cantone Ticino, n.d. b).

$$MAWT_{my} = MADT_{my} * \frac{AAWT_y}{AADT_y} \tag{9}$$

| | |
|---|---|
| $MAWT_{my}$ | monthly average weekday traffic for month i in year y |
| $MADT_{my}$ | monthly average daily traffic for month i in year y |
| $AAWT_y$, $AADT_y$ | AAWT and AADT in year y |

### Canton Zürich

AADT and AAWT for 2022 and AADT for 2017 are available for ten stations on the cantonal GIS-browser, with one station only collecting data in a single direction of traffic (Kanton Zürich, 2023). To calculate the AAWT in 2017 the ratio of weekday to daily traffic for 2022 was applied to the AADT in 2017 using equation ( 10 ), under the assumption that the ratio of weekday to daily traffic remains constant over multiple years. The coordinates of the stations were taken from the GIS-browser.

$$AAWT_i = AADT_i * \frac{AAWT_j}{AADT_j} \tag{10}$$

| | |
|---|---|
| $AAWT_i$, $AADT_i$ | AAWT and AADT in year i |
| $AAWT_j$, $AADT_j$ | AAWT and AADT in reference year j |

### Municipality Bern

AAWT is available for 14 stations (Stadt Bern, 2018). The coordinates can be viewed in the cities GIS-browser (Stadt Bern, n.d.). Two of the stations only collect data for a single direction of traffic. Two other stations had missing data, which was imputed by the municipality (Stadt Bern, 2018).

### Municipality Biel

AAWT is available for ten stations as well as a map of their locations (Stadt Biel, 2020). The coordinates were approximated using the basemap in the swisstopo GIS-Browser (Bundesamt für Landestopografie swisstopo, 2024).

### Municipality Köniz

AAWT and coordinates for four stations were provided on request through email from Judith Albers of the municipal department of planning and traffic (Albers, 2024).

### Municipality Kriens

Daily counts for four stations and a map with their locations are available (Eco-Counter, 2024b). The coordinates were approximated using the basemap in the swisstopo GIS-Browser (Bundesamt für Landestopografie swisstopo, 2024).

### Municipality Lucerne

Monthly AAWT for twelve stations was provided on request through email from Martin Luternauer of the municipal office for mobility (Luternauer, 2024). The municipality of Lucerne does not include holidays in AAWT. The coordinates are available from the canton of Lucerne (Kanton Luzern, 2021).

### Municipality St. Gallen

Hourly counts for 14 stations and their coordinates are available (Stadt St. Gallen, 2024).

### Municipality Wil SG

Daily counts for three stations were provided on request through email from Alessandra D'Errico of the municipal department for spatial planning (D'Errico, 2024). The coordinates are available on the cities GIS-browser (Gemeinde Wil, n.d.).

### Municipality Winterthur

Daily counts for one station and a map with its location are available (Eco-Counter, 2024a). The coordinates were approximated using the basemap in the swisstopo GIS-Browser (Bundesamt für Landestopografie swisstopo, 2024).

### Municipality Zürich

Counts for every quarter-hour and coordinates are available for 21 locations. Three of these locations have multiple counters observing the same road segment in different directions or at different times of the year and one station only observes traffic in a single direction (Stadt Zürich, 2024a). The data of different stations at the same location was combined before further data preparation. Correction factors for each station are also available to account for measurement errors and cyclists riding next to the measurement device (Stadt Zürich, 2024a; Stadt Zürich, 2024b). These factors were applied after aggregating the data.

### SwitzerlandMobility

AAWT and maps of the locations are available for 43 stations, with one station only collecting data for one direction of travel. While there are 52 stations along the SwitzerlandMobility route network, data of nine was not published due to missing data (Stiftung SchweizMobil, 2018). The coordinates were approximated using the basemap in the swisstopo GIS-Browser (Bundesamt für Landestopografie swisstopo, 2024).

## 3.5) Other Data

### 3.5.1) Typology of Municipalities

The urban-rural classification for the year 2012 is included in the data of the traffic zones (Bundesamt für Raumentwicklung ARE, 2019a) and was also used for the NPVM (Bundesamt für Raumentwicklung ARE, 2020c). To show the typology of municipalities, the original dataset was used (Bundesamt für Statistik BFS, 2017a).

### 3.5.2) Landcover

SwissTLMRegio is a landscape model showing natural and artificial objects in a highly generalised vector map with a positional accuracy of 20 to 60 meters. It covers all of Switzerland as well as some areas of the surrounding countries. The model is separated into six different thematic groups (transportation, hydrography, landcover, buildings, miscellaneous, names). Only the landcover group is needed for this thesis, it displays the primary groundcover such as settlement areas, lakes and forests (Bundesamt für Landestopografie swisstopo, 2023b). The version for 2020 will be used, as the older ones are no longer available (Bundesamt für Landestopografie swisstopo, 2020).

### 3.5.3) Resident and Business Statistics

Information on the distribution of residents and businesses across Switzerland are available in the two datasets from the federal office of statistics: STATPOP (Bundesamt für Statistik BFS, 2018a) and STATENT (Bundesamt für Statistik BFS, 2021). They include over 70 measures of residents and households and around 600 measures of businesses and employees, including the number of residents and full-time equivalents. The data are aggregated to grid cells of one hectare and available as point data, referencing the southwest corner of each cell. The data are collected from different administrative sources, such as municipal and cantonal resident registries, and are geolocated using the federal register of buildings and dwellings. Buildings are referenced using the centre of their footprint, or another point inside the footprint if the centre falls outside it. Businesses with multiple buildings are referenced to the building which receives postal deliveries.

There are three main issues with this dataset, some of which can be resolved before use. Firstly, the data is updated annually for December except those on agricultural businesses, which is updated for January. Secondly, for data protection resident data with absolute values between one and three as well as business data between one and four are grouped together and included as either three or four. And finally, all residents and businesses which cannot be located are assigned to a cell of the hectare raster, locally distorting the values. Such resident data are assigned to the central grid cell of the municipality. Businesses which were not directly locatable are georeferenced using a three-step system, first trying to use the average coordinates of all businesses locations along the same street, then the average coordinates of all locations in the same postcode and finally assigning the business to the central grid cell of the municipality. The federal office of statistics provides a dataset which enables the removal of data from residents and businesses with approximated locations (Bundesamt für Statistik BFS, 2018b; Bundesamt für Statistik BFS, 2023a).

### 3.5.4) Borders

swissBOUNDARIES3D (Bundesamt für Landestopografie swisstopo, 2023a) is a vector map by the federal department of topography, which includes the municipal, cantonal and international borders of Switzerland. To be consistent with other data sets, the version for 2017 is used in this thesis. International borders, apart from Switzerland's, were downloaded from OSM using the website osm-boundaries.com (Ground Zero Communications AB, 2024; OpenStreetMap, 2024k).

### 3.5.5) Elevation Tiles

Elevation Tiles from NASAs Shuttle Radar Topography Mission (SRTM) are used to add elevation data to the road network. The data was collected in February 2000 using an imaging radar on the Space Shuttle, covering 80% of the earth's land surface (NASA, n.d.). The data is available in 1°-tiles with a resolution of 1 arcsecond from an external website. To cover all of Switzerland 15 tiles are required between 45° to 47° north and 5° to 10° east, see Table 5 (Watkins, n.d.). At a latitude of 45° the resolution is around 31m north-south and 22m east-west (Esri, n.d.). The routing service requires this data to be in a specific format, data from swisstopo, which is higher resolution and quality, was therefore not usable.

*Table 5: SRTM-tiles required to cover all of Switzerland (Watkins, n.d.), arranged according to their geographic locations.*

| | | | | | |
|---|---|---|---|---|---|
| | N47E006 | N47E007 | N47E008 | N47E009 | N47E010 |
| N46E005 | N46E006 | N46E007 | N46E008 | N46E009 | N46E010 |
| | N45E006 | N45E007 | N45E008 | N45E009 | |

# 4) Methodology

The aim of this bicycle traffic assignment model BTAM is to estimate the daily number of cyclists on all road segments in Switzerland in the years 2017 and 2050, based on the bicycle traffic distribution from the Swiss national model for passenger traffic NPVM. Figure 11 gives an overview of the steps taken to achieve this goal. Each origin-destination (OD) pair is included twice in the traffic matrix of the bicycle traffic distribution, once for each direction of travel. Even though this doubles the number of routes, this separation was kept as elevation, one-way streets and other characteristics of the route network can lead to differing routes in opposing directions. To nevertheless reduce computational effort, OD-pairs with very few daily trips were removed (chapter 4.1). Next, route start and end points were distributed throughout the traffic zones (chapter 4.2). The jittering method with disaggregation and weighting by population statistics was used, based on the methods described by Lovelace, Félix and Carlino (2022). After preparing both the routing engine and OpenStreetMap (OSM) road network (chapters 4.3 and 4.4), routes between traffic zones were calculated using the Valhalla routing engine (chapter 4.5). Then, for each road segment the annual average weekday traffic AAWT of all routes passing through was summed up (chapter 4.6). Finally, the results were verified (chapter 4.8) and the 2017 model was validated by comparing them to data collected by automatic bicycle counting stations across Switzerland (chapters 4.7 and 5.2.2).

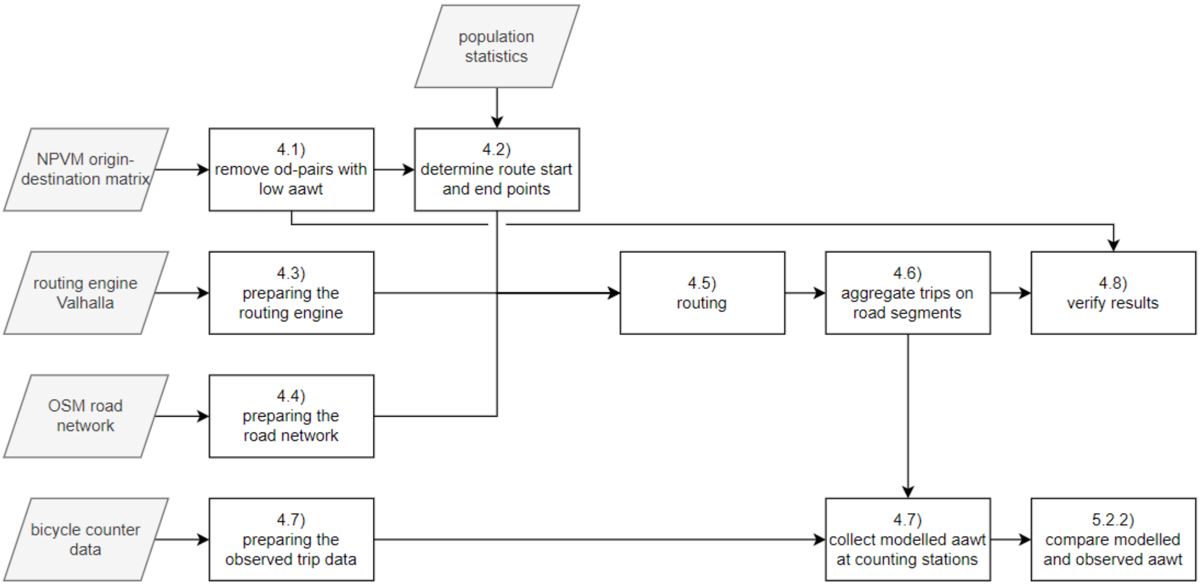


*Figure 11: Flow diagram of the methodology (only the most important datasets are shown).*

## 4.1) Exclusion of Origin-Destination Pairs with few Daily Trips

OD-pairs with few bicycle trips between them according to the NPVM traffic matrices for 2017 and 2050 were excluded from the model. Not including OD-pairs reduced the number of routes that needed to be calculated, which was the part of the model taking the longest time. By removing pairs with low AAWT the effect on the resulting model was minimised. Separate thresholds of minimum AAWT were set for traffic zones of different urban-rural typology (URT) types (urban, intermediate and rural) to account for the much higher bicycle traffic volumes in cities than in rural areas (Stiftung SchweizMobil, 2018). Pairs of traffic zones in different typologies were removed based on the lower threshold. The thresholds were also calculated separately for the years 2017 and 2050. To minimise the number of parameters needed, it was decided to remove a set percentage of trips from each URT-type and year. After experimenting with different values, 1 % was chosen.

The following steps were done separately for different URT-types and years. First, the OD-pairs were grouped according to their AAWT, but OD-pairs with zero trips between them were excluded. The bounds of the groups were set relative to the order of magnitude of the AAWT, with two digits of precision (e.g.: 0.11-0.12, 0.12-0.13, …, 0.99-1.0, 1.0-1.1, …). This allows for very fine groups at small AAWT-values and larger groups at higher AAWT-values. Then the cumulative number of trips in each of these groups and all groups with smaller individual AAWT-values was calculated. Finally, the threshold was chosen as the lowest bound, for which the cumulative trips made up at least a 1 % of the total trips. Due to the grouping of trips across a range of AAWT-values, the final thresholds are slightly larger than 1% and differ for different URT-types and years. The resulting thresholds and the percentage of trips and OD-pairs they eliminate are shown in Table 6 and Table 7.

*Table 6: Minimum number of trips per OD-pair for different URT-types in 2017.*

| **for 2017** | **threshold [AAWT]** | **OD-pairs removed [%]** (excluding OD-pairs with zero trips) | **trips removed [%]** |
|---|---|---|---|
| **rural** | 0.006 | 55 | 1.16 |
| **intermediate** | 0.01 | 69 | 1.86 |
| **urban** | 0.1 | 84 | 1.62 |
| **total** | | 71 | 1.62 |

*Table 7: Minimum number of trips per OD-pair for different URT-types in 2050.*

| **for 2050** | **threshold [AAWT]** | **OD-pairs removed [%]** (excluding OD-pairs with zero trips) | **trips removed [%]** |
|---|---|---|---|
| **rural** | 0.005 | 51 | 1.05 |
| **intermediate** | 0.01 | 63 | 1.53 |
| **urban** | 0.1 | 80 | 1.38 |
| **total** | | 65 | 1.38 |

## 4.2) Selection of the Route Start and End Points

To create a more realistic traffic pattern, the start and end points of routes were chosen using the jittering approach with disaggregation described by Lovelace, Félix, & Carlino (2022). Disaggregation allows to use multiple different routes for OD-pairs with many trips. Jittering distributes the start and end locations of routes throughout their respective traffic zones. Disaggregation was performed separately for the 2017 and 2050 data, while jittering was done together to reduce the number of routes required. The next two sections explain the process in more detail.

### 4.2.1) Disaggregation

The number of trips between traffic zones varies over multiple orders of magnitude. If there was only one route between each pair of traffic zones, the number of trips represented by that route would therefore also vary drastically. Routes associated with a high number of trips can lead to unrealistic traffic patterns at the start and end location, where a lot of traffic would suddenly appear or disappear. To reduce this issue OD-pairs with too many trips were disaggregated and assigned multiple routes with different start and end points within the same traffic zones. This way each route only carries a fraction of the trips. As with the minimum number of trips between traffic zones, this threshold is also calculated separately for 2017 and 2050. To assure disperse routing in all regions, even where bicycle traffic is low, it was calculated individually for each traffic zone and separately for incoming and outgoing trips.

First, the incoming and outgoing AAWT-values were collected for each traffic zone, with intrazonal trips being included in both groups. Next, the 90$^{th}$ percentile of these AAWT-values was selected as the maximum allowed number of trips per route. The 90th percentile was chosen after exploring different values to limit the number of additional routes created, while creating enough disaggregation. This maximum was set to two times the minimum number of trips per OD-pair, if it was below. Otherwise, the number of trips on a route would be below the minimum number of trips per route determined in the previous chapter.

Routes between OD-pairs were disaggregated, when the number of trips was higher than the lowest of these values: outgoing AAWT-threshold for the origin-traffic zone, incoming AAWT-threshold for the destination-traffic zone or AAWT of ten. The upper limit of ten on the number of trips per route was added, as the threshold for some pairs would otherwise be very high. When disaggregation was needed, the number of routes was determined using equation ( 11 ). The number of trips per route was then calculated using equation ( 12 ). The resulting AAWT for each route is lower than the threshold to allow all routes to have the same number of trips, while retaining the total number of trips between each pair of traffic zones.

$$n_r = ceil\left(\frac{AAWT}{\max{(AAWT)}}\right) \tag{11}$$

$$AAWT_r = \frac{AAWT}{n_r} \tag{12}$$

| | |
|---|---|
| $n_r$ | number of routes |
| max(AAWT) | threshold AAWT |
| $AAWT_r$ | AAWT for each route |

### 4.2.2) Jittering

The start and end points for each route were chosen from the centre points of the Swiss hectare raster within the traffic zone. They were selected randomly, weighted by the sum of population and full-time equivalents (population statistics) in the respective raster cell. This data was also used during the creation of the traffic zones (Bundesamt für Raumentwicklung ARE, 2017).

#### *4.2.2.1) Preparation of the Resident and Business Statistics*

The federal office of statistics uses the coordinates in the southwestern corner of each hectare raster cell as identifier and locator (Bundesamt für Statistik BFS, 2018b). To better represent the location of population and workplaces in the cell, the centre point was used instead for this thesis. Grid cells for which the centre point was outside of Switzerland are not able to have a traffic zone assigned and are therefore removed.

As described in chapter 3.5.3, the location of residents and workplaces was not always known and therefore had to be estimated by the federal office of statistics when creating the hectare raster datasets (Bundesamt für Statistik BFS, 2018b; Bundesamt für Statistik BFS, 2023a). As this changes the spatial distribution of the population statistics, some of these estimates were removed for the thesis using a dataset provided by the federal office of statistics together with the main data: residents and full-time equivalents which were assigned to the central coordinate of their municipality or based on their postal code were removed. The businesses with locations determined based on their street were kept, as this amount of distortion is smaller and should not be an issue for the use in this thesis.

The data on residents and businesses were combined to act as weights in the jittering process. The sum of residents and full-time equivalents was chosen as population statistics, as they best represent the number of people departing and arriving in an area. It also avoids having routes start or end outside of populated areas. Other information such as the number of students or customers is however not included, as data was not available.

#### *4.2.2.2) Jittering*

Jittering was used to select the start and end points of routes. Multiple routes can have the same start and end points, as this distributes the traffic more closely in line with the population statistics. Routes within a traffic zone must have a different start and end point. For trafficzones with only one hectarraster point, as well as special cases explained in the next chapter, the intrazonal routes were removed. 59 OD-pairs (0.003 % of OD-pairs for 2017, 0.002% for 2050) with 3308.245 trips (0.12 %) in 2017 and 4726.007 trips (0.10 %) in 2050 were skipped due to this. To reduce the number of routes being calculated, the same ones were used for both 2017 and 2050. When one year required fewer routes than the other year, the additional routes were assigned zero trips.

### 4.2.3) Special Cases

#### *4.2.3.1) Too Many Routes between Traffic Zones*

Due to disaggregation some OD-pairs required more routes than there are unique routes between the traffic zones. This limit exists, as there are only a limited number of hectare raster points within each traffic zone. It was calculated as the product of the number of hectare raster points in the origin traffic zone with those in the destination traffic zone. For all OD-pairs where the required number of routes was larger or equal to the number of possible unique routes a different approach than described above was chosen.

Instead of selecting routes based on a maximum number of trips per route, all unique routes were used. The number of trips for each route were assigned according to the fraction of population statistics at the start and end points, as illustrated in Figure 12. This approach had to be used for 517 OD-pairs (0.03 % of OD-pairs for 2017, 0.02 % for 2050).

**trips from zone A to zone B**

| | | | | | |
|---|---|---|---|---|---|
| trips: | 500 | | **zones** | A | B |
| possible routes: | 6 | | population statistics P | 100 | 200 |
| | | | start/end points | 3 | 2 |

| | | | | **A1** | **A2** | **A3** |
|---|---|---|---|---|---|---|
| | | | **P** | 20 | 30 | 50 |
| | | | **fraction(P)** | 0.2 | 0.3 | 0.5 |
| | | | **fraction(trips)** | | | |
| | **P** | **fraction(P)** | **trips** | | | |
| **B1** | 150 | 0.75 | | 0.2*0.75 | 0.3*0.75 | 0.5*0.75 |
| | | | | 75 | 112.5 | 187.5 |
| **B2** | 50 | 0.25 | | 0.2*0.25 | 0.3*0.25 | 0.5*0.25 |
| | | | | 25 | 37.5 | 62.5 |

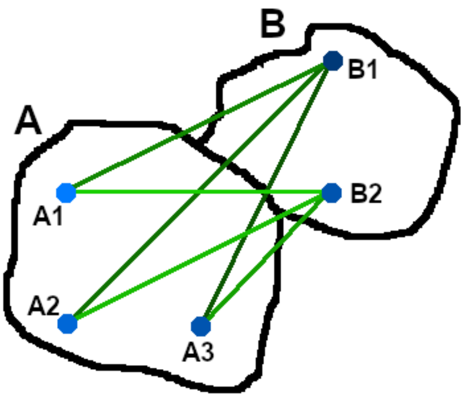


*Figure 12: Illustration for the assignment of trips to all unique routes.*

In case of intrazonal traffic the calculation of trips per route was more complicated, as routes must start and end in at different points. The fraction (from all trips for the OD-pair) of trips belonging to a route was first calculated as described above and then adjusted using a correction factor (equation ( 13 )). The correction factor was calculated using equation ( 14 ). It represents the fraction of routes that would be assigned to all routes with the same start and end point.

$$fraction(trips)_{intrazonal} = \frac{fraction(trips)_{interzonal}}{1-c} \qquad (13)$$

$$c = \sum_{i=0}^{n} \left(\frac{P_i}{P_{zone}}\right)^2 \qquad (14)$$

| | |
|---|---|
| $fraction(trips)_{intrazonal}$ | fraction of trips used for routes within a traffic zone |
| $fraction(trips)_{interzonal}$ | fraction of trips used for routes between different traffic zones (calculated as described above) |
| c | correction factor |
| n | number of hectare raster points in the traffic zone |
| $P_i$ | population statistic for hectare raster point i |
| $P_{zone}$ | population statistic for the traffic zone |

#### *4.2.3.2) Traffic Zones with Manually Assigned Coordinates*

In two cases, which are described below, the automatic assignment of route start and end points based on the hectare raster of the population statistics did not work. The route start or end coordinates for these traffic zones were assigned manually and are shown in Table 8. During jittering these manually placed points were treated the same as the automatically selected points from the hectare raster.

The traffic zone at the Papiliorama near Kerzers, FR does not contain any hectare raster points, due to the zone having a small area. To allow for the automatic assignment of routes to and from the traffic zone, a point near the entrance to the park was selected and used.

The road network in village of Zermatt, VS was mapped in OSM as mostly consisting of footways and pedestrian zones, which cannot be used by bicyclists. This resulted in the routing engine not being able to calculate many routes and other routes using hiking paths around the village. While the municipality does not allow private cars, bicycles are allowed (Zermatt Tourismus, n.d.), indicating a mapping error in OSM. As many road segments would need to be changed, it was decided against editing the erroneous road attributes. Instead, all traffic zones of Zermatt were assigned a single, common route start and end point (see Table 8) at the entrance of the village. This does however result in the model not including any traffic within the village. Fortunately, the village's only road connection is to the north resulting in an absence of through-traffic and confining the problem to the village itself.

*Table 8: Traffic zones with manually assigned coordinates as route start and end points.*

| Location | Traffic zone ids | Assigned coordinates [EPSG:4326] |
|---|---|---|
| Papiliorama, Kerzers, FR | 226503005 | 46.988675 N, 7.199911 E |
| Zermatt, VS | 630001001, 630001002, 630001003, 630001004, 630001005, 630001006, 630001007 | 46.029327 N, 7.754288 E |

## 4.3) Routing Engine Parameters

The routing engine Valhalla is used to create the paths along the OSM-network based on the route start and end points created in the previous chapter. It allows to adjust several parameters that influence the routing behaviour for bicycles. The default values and the values used in this thesis are shown in Table 9, as well as a description of their effect. As described in chapter 2.4.1.2, the routing engine searches for the path with the lowest generalized cost, which combines multiple factors influencing bicyclist route choice. Parameters are used to adjust the weighting or size of the different costs to reflect different cyclist preferences. Three different types of parameters are used in the routing engine: Cost parameters give an amount of seconds that is added to the path cost and the path time. Penalty parameters give an amount of seconds that is only added to the path cost. Factor parameters multiply the cost on a road segment to avoid or favour certain attributes (Valhalla, 2023).

*Table 9: Parameters for bicycles in the Valhalla Routing Engine (Valhalla, 2023). Changes to the default value are highlighted in blue.*

| **Parameter** | **Description** | **Default value** | **Value used** |
|---|---|---|---|
| avoid_bad_surfaces | Factor to avoid bad road surfaces, based on the bicycle type. (0: does not avoid bad surfaces, 1: avoids bad surfaces strongly) | 0.25 | 0.25 |
| bicycle_type | Type of bicycle, has an affect on the cycling speed and avoidance of bad surfaces. (Road bicycle, Hybrid/City bicycle, Cross bicycle, Mountain bicycle) | Hybrid/City | Hybrid/City |
| country_crossing_cost | Cost for crossing international borders. | 600 s | 0 s |
| country_crossing_penalty | Penalty for crossing international borders. | 0 s | 0 s |
| cycling_speed | Cycling speed on smooth roads without elevation change. Is different based on the bicycle type. The speed used in routing modifies this value based on the road surface and grade. | 18 km/h | 13.6 km/h |
| gate_cost | Cost for crossing a gate with undefined or private access. | 30 s | 10 s |
| gate_penalty | Penalty for crossing a gate with undefined access. | 300 s | 0 s |
| maneuver_penalty | Penalty, when the name of the road changes along the route. Avoids turning. | 5 s | 9.4 s |
| service_penalty | Penalty for accessing a service road (local road for access to a destination (OpenStreetMap, 2024a)). | 15 s | 0 s |
| use_ferry | Factor to avoid ferries. (0: avoids ferries strongly, 1: does not avoid ferries) | 0.5 | 0 |
| use_hills | Factor to avoid steep road sections. (0: avoids steep grades strongly, 1: does not avoid steep grades) | 0.5 | 0.0 |
| use_living_streets | Factor to avoid living streets (shared space for different modes of traffic (OpenStreetMap, 2024i)). (0: avoids living streets strongly, 1: does not avoid living streets) | 0.5 | 1 |
| use_roads | Factor to avoid roads with high speeds and certain classifications and favour cycleways and paths. (0: avoids roads strongly, 1: does not avoid roads) | 0.5 | 0.0 |

As Valhalla allows to change the routing parameters for each route, it is possible to represent different types of cyclists. Using multiple population groups and trip purposes is not as common during routing as in the other steps of traffic demand modelling (Bundesamt für Strassen ASTRA, 2018). However, cyclists route choices are strongly influenced by trip purpose and their personal preferences. These differences can be captured using cyclist typologies, of which many exist in the literature (Dill & McNeil, 2013). It would therefore be advantageous to use different parameter sets to represent these cyclist types. As the creation of suitable groups with their different characteristics is difficult and would require a lot of additional data, it was decided to not include it in this thesis.

### 4.3.1) Selecting Parameter Values

The hybrid bicycle type was chosen as it reflects both cycling for transport and recreational cycling, while the other cycling types are tailored to cycling for sports (Valhalla, 2023). The cycling speed was adjusted to match the values observed by the Swiss micro census for mobility and traffic MZMV 2015 for bikes and e-bikes, weighted by their respective daily average trip numbers. 0.24 daily trips were made by regular bicycles at an average speed of 13.3 km/h and 0.02 trips by e-bike at a speed of 17 km/h (Bundesamt für Statistik BFS, 2017d), giving a weighted average of 13.6 km/h. The cost and penalty for crossing gates and international borders were reduced, as they pose no large barrier to cycling within the Schengen area. The use of ferries is to be avoided strongly, as the OD-pairs from the NPVM represent only trips by bicycle. Even so some routes were using ferries during testing. To avoid this issue all ferry paths were removed from the OSM-network (see chapter 4.4). Living streets (shared space for different modes of traffic (OpenStreetMap, 2024i)) and service roads (local road for access to a destination (OpenStreetMap, 2024a)) are preferable for cyclists, as they have less motorised traffic.

Literature was used to identify suitable values for the parameters which have a less direct impact on routing: maneuver_penalty, use_hills and use_roads. The parameter avoid_bad_surfaces was left at its default value, because no suitable literature was found. Different papers have found that cyclists prefer smooth surfaces such as asphalt over irregular surfaces such as cobblestone or gravel, but none have analysed the implications on route choice (Hardinghaus & Weschke, 2022; Toljic, Brezina, & Emberger, 2021).

#### *4.3.1.1) Valhalla Parameter: maneuver_penalty*

The penalty parameter maneuver_penalty adds a cost in seconds to the trip cost (but not the trip time) when the road name changes along the trip. It is meant to reduce the number of turning maneuvers along a route (Valhalla, 2023). For cyclists turning adds a time delay to the route and is connected with an additional mental cost of having to remember where to turn (Broach, Dill, & Gliebe, 2012).

In a paper by Meister et al. revealed preference data from GPS sensors was used to model the effect of different attributes on cyclists' route choices in the greater Zurich area. The value of distance was used to describe how much longer/shorter a route the cyclist is willing to take is, based on the road attribute. A road section with a grade of 2-6 % for example is valued the same as a flat road section that is 55% longer. They also looked at the effect of bike infrastructure and traffic volumes, however these results are not as the authors expected and might be influenced by factors other than the cyclists route choices (Meister, Felder, Schmid, & Axhausen, 2023). Broach et al. (2012) did a similar study for commuters and non-commuters in the city of Portland, USA and have more reliable results for road types as well as turning maneuvers.

Broach et al. (2012) found that one turn per kilometre has the same effect on the route choice as an increased distance of 4.6 % for non-commuters and 2.6 % for commuters. Using a weighted average, the combined distance value for turning is therefore 3.56 %. For this thesis, the distance values for commuters and non-commuters were combined, weighted by the proportion of trip distance related to commuting, which is reported in the MZMV for 2015. Across all transport modes 52 % of the daily distance travelled on weekdays was for commuting (trips to/for work and education). This value is unfortunately not disaggregated for the different travel modes. While the proportion of bicycle trips related to commuting is also reported, it is not disaggregated into weekday and weekday, resulting in potentially larger inaccuracies (Bundesamt für Statistik BFS, 2017d).

The parameter value for maneuver_penalty has the unit of seconds and can be calculated using equation ( 15 ). The average cyclist speed (13.6 km/h, see chapter 4.3.1 and Table 9) was used in conjunction with the distance value for a kilometre (3.56 %). The result is a penalty of 9.4 seconds for every turn along the route.

$$penalty = \frac{dv}{v * 100} * 3600 \qquad (15)$$

| | |
|---|---|
| penalty | maneuver penalty in seconds |
| dv | distance value in percent per kilometre |
| v | cycling velocity in km/h |

#### *4.3.1.2) Valhalla Parameter: use_hills and use_roads*

The parameters use_hills and use_roads are factors applied during routing, making it impossible to convert their effects into value of distance and directly compare them to the literature. Instead, some routes were calculated with a variety of parameter values (ranging from 0 to 1 with a step size of 0.1). The resulting distances in each slope/road class (see Table 10 and Table 11) for each route were then weighted by the values of distance from the literature and the best parameter value was chosen: First, the route start and end points were selected from the traffic zone OD-pairs of the NPVM. As the literature evaluates bicycle trips within a city, only urban traffic zones were used. Then, a route was created from each of the traffic zones to one other, randomly chosen, traffic zone with at least one trip per day. This ensured that all urban areas across Switzerland were considered. The routes were calculated between the centroids of the traffic zones, which were weighted by population statistics (Bundesamt für Raumentwicklung ARE, 2017). The other parameter values were set to the values used in the final model (see Table 9). Next, the weighted length of the route was calculated by applying the values of distance for different slope/road classes (explained in more detail below). As a change in one parameter might lead to a change in another, use_roads and use_hills were first set to their default values. The parameter value resulting in the lowest weighted distance for the largest number of routes was selected for use in the final model. The process was repeated with the calculated values until the parameter values (rounded to 0.1) no longer changed. A weighting by population and full-time equivalents is implied by this method, as all traffic zones are of similar size in that regard (Bundesamt für Raumentwicklung ARE, 2017). In contrast, a weighting by the number of trips was not chosen, as the large cities with many trips likely would have dominated over the effects of the smaller cities with fewer trips.

**use_hills**

To calculate the weighted length of each route, the elevation every 30m along the route was taken from the routing engine. The slope between each set of neighbouring points was calculated and the distance weighted according to the slope classes from Meister et al. (2023), see Table 10. Downward slopes were unfortunately not included in the literature and had to be grouped with slopes between 0 and 2 %, which served as reference in the paper.

*Table 10: Slope classes and values of distance for 1 km of road (Meister, Felder, Schmid, & Axhausen, 2023).*

| Slope | Value of distance of 1 km |
|---|---|
| <2 % | 1 km |
| 2-6 % | 1.55 km |
| 6-10 % | 4.11 km |
| >10 % | 5.33 km |

**use_roads**

According to Broach et al. (2012), roads with a traffic volume of 10-20 thousand vehicles a day and no bike lane have an increased value of distance by 22.3% and 36.8% for non-commuters and commuters respectively. Cyclists are willing to travel longer distances when they are able to use separated bicycle infrastructure such as bike paths, which therefore have a value of distanced decreased by around 22% for non-commuters and 13.4% for commuters. While the paper makes a distinction between bike paths (off-street, regional) and bike boulevards (residential road with traffic calming and enhanced right of way), this is not possible with the OSM-data. Therefore, the average of both categories was used (Broach, Dill, & Gliebe, 2012). The aggregation of distance values for commuters and non-commuters was performed in the same way as for the parameter maneuver_penalty, resulting in a distance value increased by 30 % for busy roads and decreased by 18 % for bike paths (Table 11).

OSM-ways were classified according to their highway and cycleway tags (see appendix 3) and assigned the distance values according to Broach et al. (2012) (Table 11). The classification tries to translate the categories used in the paper into OSM tags with help of the OSM-wiki (OpenStreetMap, 2024b). The road class was determined for each route segment, allowing to weight its length by the distance values in Table 11. To be able to access the highway type along the route, a separate OSM-file had to be created where the highway type was added to the road name. This change was not applied to the OSM-file used for the model itself, as the maneuver_penalty parameter uses a change in road name as an indicator for turning maneuvers.

*Table 11: Road classes and values of distance for 1 km of road (Broach, Dill, & Gliebe, 2012).*

| Road description | Category in Broach et al. (2012) | Value of distance of 1 km |
|---|---|---|
| Bicycle friendly road | Bike boulevard and bike path | 0.82 km |
| Bicycle neutral road | Reference category | 1 km |
| Bicycle unfriendly road | AADT 10-20k without bike lane | 1.3 km |

## 4.4) OSM Tags

As discussed in chapter 3.1, the completeness and accuracy of OSM-attributes, or tags, is sometimes lacking (Ferster, Fischer, Manaugh, Nelson, & Winters, 2020; Hochmair, Zielstra, & Neis, 2015; Vierø, Vybornova, & Szell, 2024). This was confirmed when exploring the OSM-data and during the test runs of the BTAM. It was therefore decided to correct some of the attributes of nodes and ways that can influence routing. Most of the changes were applied to the entire OSM-network for Switzerland. Additionally, ways near counting stations were examined after test runs of the model to detect and manually change incorrect attributes. This way the evaluation of the model is less influenced by errors in the road network.

Summary and order of the changes made to the OSM-network:

- Ways without the tag “highway” were removed. Otherwise, Valhalla would in a few cases include ferry sections in the routes.

- Manual correction of errors near bicycle counters: To aid in the detection of errors in the road network the results of the test runs were analysed visually to detect unexpected traffic volumes in the areas around counting stations. The modelled counts were also compared to the observed bicycle counts at the bicycle counters. A comparison of the 2017 OSM-network with the 2024 OSM-network (OpenStreetMap, 2024k) and swisstopos aerial images from around 2017 (Bundesamt für Landestopografie swisstopo, 2024) was used to correct attributes and add missing ways. Additional sources on construction sites or roadway restrictions were used when necessary. Due to missing familiarity with the areas, not all errors will have been caught and the corrections may be erroneous themselves. One example is Strandweg between Oberseestrasse and Seedamm in Rapperswil (see Figure 13), near counting station C_SG_06. This road section was tagged as "footway", suggesting that cycling is prohibited and not allowing routing for bicycles. The road section is however part of the national cycle route 9 by SwitzerlandMobility, which was established along with the other national cycling routes in the 1990s, showing that cycling is allowed there (Stiftung SchweizMobil, 2009; Stiftung SchweizMobil, n.d.). To solve the issue the tags are changed to reflect the tags currently used by OSM: highway=footway is replaced with highway=path and bicycle=designated is added (OpenStreetMap, 2024k).


*Figure 13: Overview of Strandweg between Oberseestrasse and Seedamm in Rapperswil. SwitzerlandMobility cycle routes are marked in blue (source: (Bundesamt für Landestopografie swisstopo, 2024)).*

- The surface-tag was added to ways where it was missing or had an untypical value (values not in Table 12). This tag is used for the Valhalla parameter avoid_bad_surfaces but is missing from 87% of the ways available for cyclists (based on the highway tag (see appendix 3)). Due to the variety of surface types, only the general values of paved or unpaved were assigned depending on the surface types of the other ways with the same highway tag. Table 12 gives an overview over which surface types were considered as paved and which as unpaved, this categorisation is based on the OpenStreetMap Wiki (OpenStreetMap, 2024e). While this approach is simplistic and most of the ways had no surface type, all surface types are either predominantly paved or unpaved.

*Table 12: Categorisation of surface types into paved and unpaved (based on (OpenStreetMap, 2024e)).*

| **paved** | | **unpaved** | |
|---|---|---|---|
| asphalt | concrete:plates | compacted | ground |
| bricks | paved | dirt | pebblestone |
| chipseal | paving_stones | earth | rock |
| cobblestone | sett | fine_gravel | sand |
| cobblestone:flattened | unhewn_cobblestone | grass | unpaved |
| concrete | wood | grass_paver | woodchips |
| concrete:lanes | | gravel | |

- The tag bicycle=no was removed from nodes with the tag highway=crossing. These nodes indicate where pedestrians can cross the road. However, bicycle traffic following the road is also prohibited by the tag, which is not intended.
- The tags carriage, motor_vehicle, motorcar and motorcycle (based on (OpenStreetMap, 2024d)) were removed from all ways, as they have no impact on bicycle traffic, but seemed to influence routing during testing.
- The tags access and vehicle were removed from ways which had either the bicycle or cycleway tag. These tags represent access restrictions to ways. As the bicycle and cycleway tags are more specific for bicycle traffic, only they should be considered when they are available.

## 4.5) Routing

The routes were calculated by the routing engine Valhalla with the parameters described in chapter 4.3. Route start and end points from chapter 4.2 and the road network from chapter 4.4 were used. The engine returns whether routing was successful, as well as the route's length and an encoded polyline of the route path. The polyline was converted into a sorted list of points and stored. The first and last points are the closest points to the hectare raster centroids selected as route start and end points. The points in between are nodes of the OSM road segments.

The routing program was not able to find a valid route between some of the start and end points. The reason was either a lack of bicycle-accessible roads near one point or the road network around one point being disconnected. The affected point was replaced by another start or end point (selected randomly as described in chapter 4.2) and the route recalculated. The locations and number of routes affected are summarised in Table 13.

*Table 13: Inaccessible locations which caused routes to fail.*

| **Location** | **Number of routes affected** |
|---|---|
| Chüngeliinsel, Bielersee, BE | 29 |
| Engstligenalp, Adelboden, BE | 38 |
| St. Martin, Pfäfers, SG | 2 |
| **Total** | **69** |

## 4.6) Aggregation of Trips

The trips of the routes were aggregated onto the route start and end points as well as the road segments the route passes through. The number of trips starting or ending in a route start or end point was computed for both 2017 and 2050, using the first and last node returned by the routing engine.

The method to calculate trips for each route segment is based on the paper from Morgan & Lovelace (2021), which is described in chapter 2.6. Each neighbouring pair of points in the sorted list of route points represents one segment. Segments visited by at least one route were stored with the number of trips and routes passing through in 2017 and 2050. Trips were collected separately for both directions of travel. The first and last segment of each route were excluded, as the first and last point of the route do not correspond to OSM-nodes. Including them would lead to two overlapping segments (one for the routes ending and one for the routes passing through).

## 4.7) Preparation of Counting Station Data

As the data on counting stations were from many different sources, they required extensive preparation and included duplicate entries of the same station. In the case of duplicates, the data source with more information was used. This was only the case for stations from SwitzerlandMobility, which were removed as most other data sources provided coordinates, while SwitzerlandMobility only had a map for the station's location. While some counting stations can detect the direction of bicyclists, this information was not used for this study as it was only available for few of them. Some operators correct or filter the counts before publishing. This editing ranges from deleting invalid data, to interpolation of small data gaps, and accounting for weather or site-specific conditions (Baehler, Marincek, & Rérat, 2018; Stiftung SchweizMobil, 2018). While this reduces the comparability, the modifications are minor and should not change the counts so much as to make them unusable for this analysis.

As the national traffic model only considers traffic within Switzerland for bicycles, travel across the border could not be included in this thesis. The modelled traffic near the border is therefore lower than the measured traffic, which does include international trips. To remove this effect from the validation, all counting stations within 1.65 km of the border were not included. This distance was chosen, as it is half of the average trip length by bicycle in 2015. Furthermore, about 50% of trips are shorter than 1.65 km (Bundesamt für Statistik BFS, 2017d). The distance was calculated using the OpenStreetMap road network and the routing service Valhalla, using the same network and parameters as for the traffic assignment model in chapter 4.5.

For data analysis it was necessary to classify the counters into urban and rural, which is described in chapter 4.7.1. For cycling stations with count data of days or months available, the AAWT was calculated using equation ( 1 ). Missing data was imputed using the method described in chapter 4.7.2, which is based on the methods introduced in chapter 2.8.1. After all unusable stations were removed, the OSM-road segments to which the counters belong were manually identified.

Appendix 5 shows the counting stations along with their annual average weekday traffic, coordinates and data source, while Appendix 4 shows their data sources and the number of used and unused counting stations.

### 4.7.1) Classification into Urban and Rural Counting Stations

The classification of bicycle counting stations was adapted from the method used by SwitzerlandMobility, as introduced in chapter 2.7.2 (Stiftung SchweizMobil, 2018). Changes were made to allow the usage of the newer municipality classification (urban-rural-typology 2012 using municipality geometries of 2017 (Bundesamt für Statistik BFS, 2017a)) and the landcover data of swissTLMRegio (Bundesamt für Landestopografie swisstopo, 2020). The municipalities geometry was from the swissBOUNDARIES3D dataset for 2017 (Bundesamt für Landestopografie swisstopo, 2023a).

Bicycle counting stations were classified as urban when there is more urbanised than non-urbanised area in a radius of 500m around them. Within Switzerland only settlement areas in urban and intermediary municipalities were considered as urbanised. As the swissTLMRegio covers areas closely outside Switzerland, but the urban-rural typology does not, all settlement area outside of Switzerland were counted towards the urbanised area. Non-urbanised areas were made up of everything except settlement areas (regardless of their typology), lakes and reservoirs. This means they also included areas not classified by swissTLMRegio (mostly agricultural land). Lakes and reservoirs were excluded from the evaluation, as they would distort the results due to their size and oftentimes close proximity to settlements. After the automatic assignment, the classification of all counting stations was manually verified. If an obvious misclassification was detected, the stations classification was changed. Three such locations were found, see Figure 14:

- C_GE_05: changed from rural to urban (on a bridge connecting settlement areas)
- C_SG_04: changed from urban to rural (separated from much of the settlement area by a railway)
- C_TI_01: changed from rural to urban (mostly surrounded by settlement area, which was not included in swissTLMRegio)

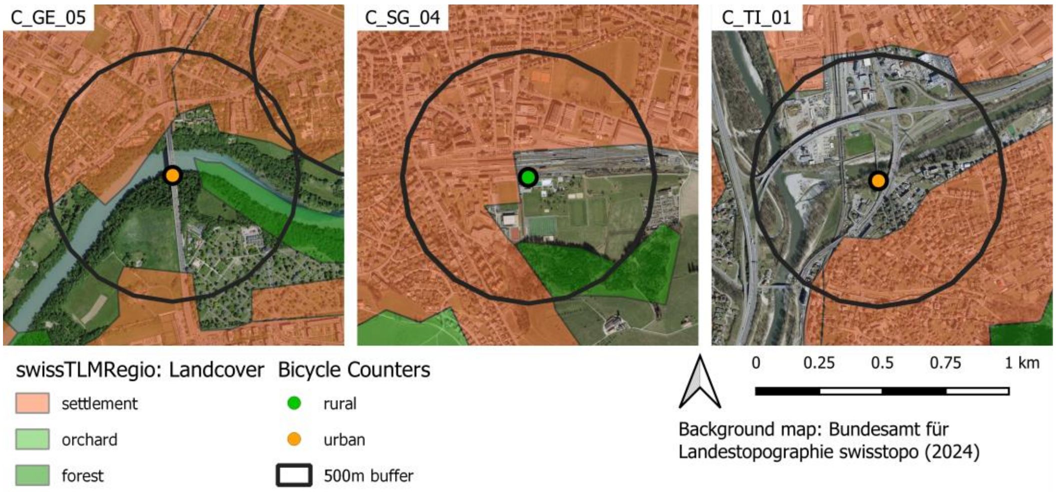


*Figure 14: Land use around the bicycle counting stations which were reclassified manually.*

### 4.7.2) Imputation of Missing Days and Months

The imputation of missing days and months for the long-term counting stations was based on the disaggregate factor method DFM and some of the additions described in chapter 2.8.1. This method was chosen as it provides good results, while only requiring count data of a single year for multiple stations. While the method was developed to calculate the annual average daily traffic AADT for short-term counting stations, it can be adapted to work for long-term counting stations and AAWT data. To select reference stations for stations with missing data, the approach by Beitel et al. (2018) was chosen, as it requires no additional data. Another advantage is that it does not assume that all stations can be grouped together, unlike the method by El Esawey (2022). During the process, counts and AAWT were always rounded to the nearest integer.

Data with subdaily frequency was aggregated to daily traffic counts. After applying the DFM to the daily data, it was aggregated to monthly counts to be used as additional reference stations for the DFM with the monthly counts. Counters with more than half a year (130 weekdays or 6 months) of missing data were removed from the analysis. The DFM-procedure is the same for days and months, for better readability it will only be presented for daily data.

#### *4.7.2.1) Calculating Correlation between Counting Stations*

First, the AAWT was calculated for each station using equation ( 1 ). Next, the correlation between each pair of bicycle counters was determined using equation ( 4 ) from Beitel et al. (2018). This method uses daily factors for each day and station (equation ( 2 )), which are expansion factors for an individual day of the year. By using the daily factors, the counts of the stations are normalised by the AAWT of the station. The daily factor therefore only describes the variation of bicycle traffic over the year and not the amount of traffic, which allows to correlate stations with different magnitudes of bicycle traffic.

Beitel et al. (2018) removed anomalous data after calculating the correlation, which results in missing data influencing the correlation between stations. For this reason, they recommend to only use stations with at most 15 days of missing data. To avoid this issue and be able to use stations with more missing data, days without data (for one of the two stations for which correlation is being calculated) were excluded for the computation of correlation in this thesis.

The resulting correlation values range from 0 and 1, with 1 indicating perfect correlation of the daily factors. A correlation of 0.75 was considered sufficient, as suggested by Beitel et al. (2018). Stations which had a sufficient correlation for fewer than two other stations were assessed manually. If the temporal pattern seemed uncharacteristic and hinted towards measurement errors the station was removed from the analysis.

#### *4.7.2.2) Imputation of Missing Data*

In the next step, the corrected AAWT was iteratively computed for each station by imputing the traffic counts of the missing days. This process was performed for each station separately. The identification of reference stations was additionally done separately for different missing days of the same station.

The selection of reference stations was adjusted from Beitel et al. (2018). The three (or two if not enough stations were available) stations with the highest correlation were selected as potential reference stations. The correlation had to be at least 0.75 and data needed to available on the day being imputed. To avoid outliers influencing the imputation, the two potential reference stations whose daily factors for the day were closer together were selected as reference stations.

The daily factors from the reference stations were then used to impute the missing count using equation ( 16 ). The equation is based on equation ( 2 ), which was introduced by Nosal (2014). It uses the mean of the daily factors of the reference stations and applies it to the previously calculated AAWT to get the traffic count on the specific day. After the counts for all missing days of a station were imputed in this way, the new AAWT was calculated using equation ( 1 ) and both imputed and measured traffic counts. If the new and old AAWT differed (when rounded to a whole number) the process of estimating traffic counts and calculating AAWT was repeated.

$$\widehat{c_{id}} = AAWT_{i,old} * \frac{1}{n_j} * \sum_j df_{jd} \qquad (16)$$

| | |
|---|---|
| $\widehat{c_{id}}$ | estimated bicycle count for station i on day d |
| $AAWT_{i,old}$ | AAWT for station i, before the current iteration of imputation |
| $n_j$ | number of reference stations j |
| $df_{jd}$ | daily factor of reference station j on day d |

#### *4.7.2.3) Skipping Identification of Anomalous Data*

The identification and replacement of anomalous data as described in Beitel et al. (2018) or El Esawey (2023) was skipped. The method from El Esawey (2023) was not usable, as it assumes all data to be correlated, which is not necessarily the case when evaluating counting stations across all of Switzerland.

The method from Beitel et al. (2018) was tested, but many of the values identified as anomalous showed no sign of irregularity upon manual inspection. When imputing the AAWT from short-term counter data of a few days or weeks it is important to remove anomalous days from the long-term counts, as their impact on the AAWT of the short-term counter is large. For this thesis however, at least half a year of data was available for the bicycle counters, reducing the impact of erroneous data. Furthermore, days with data identified as anomalous would require imputation. Together with days falsely identified as anomalous, this would introduce uncertainty into the result and undo the benefits of replacing actual outliers.

Instead, three counting stations were identified as potential references and the two of them with more similar daily factors used for imputation. This way outliers were not removed from the dataset, which comes with the uncertainty of imputation, but the effect of the outlier was not passed on to imputed counts.

### 4.7.3) Matching Modelled and Observed Traffic

To compare the model to the counting stations data the modelled trip count for 2017 at each of the counting stations was manually collected. The AAWT from the closest road segment to the counting station on the same road was chosen (see Figure 15). As the coordinates provided by the stations operators did not always line up with the OSM-roads a manual approach was deemed more reliable than an automatic process. In some cases, a road is included in OSM with multiple parallel lines to represent different lanes. Here the trips from the entire cross-section were collected (see Figure 15). For counting stations observing only one direction of traffic, the modelled trips for only that direction were used.

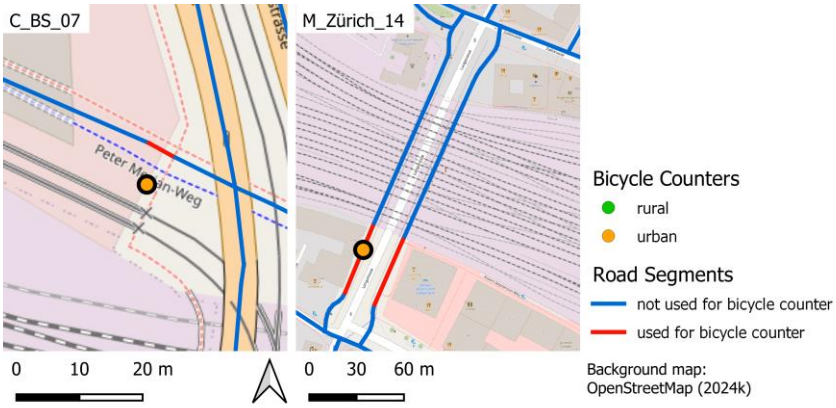


*Figure 15: Examples of matching bicycle counters with road segments.*

## 4.8) Verification

### 4.8.1) Comparing Routes

As routing took a lot of time it was performed over several days with pauses in between. Additionally, some routes needing to be replaced due to a lack of roads for bicycles or a disconnected road network. To ensure that no routes were missing or included twice, the completed routes after chapter 4.5 were compared against the planned routes from chapter 4.2. Fortunately, no routes were found to be missing or included multiple times.

### 4.8.2) Comparing Trips

The number of trips for each road segment is the main result of the model. It is therefore important to ensure that all trips are accounted for during the entire modelling process. To verify this, the number of trips before and after modelling was compared in total and for all traffic zones, for both 2017 and 2050. The OD-matrix after the removal of pairs with too few trips (chapter 4.1) was chosen as the baseline, as it is very early in the model and the number of trips does not change much afterwards. It was compared to the number of trips starting at the different route start and end points (chapter 4.6). Ideally the number of trips on road segments would have been used, as it is the main result. This was not possible, as routes traverse multiple segments, which would have resulted in all trips being counted multiple times.

To determine the total number of trips at the beginning of the model, the trips across all OD-pairs were summed up. The number of trips at the end of the model consists of multiple parts: The number of trips originating from each route start point were summed up and combined with the number of trips removed due to being within a traffic zone with only one route start and end point. As shown in Table 14, the number of trips before and after the model has remained the same.

*Table 14: Comparing the total number of trips at the beginning and end of the model.*

| | | 2017 | 2050 |
|---|---|---|---|
| **Beginning of the model** | Trips after ch. 4.1 | 2767967.379 | 4936894.222 |
| **End of the model** | Trips removed in ch. 4.2.3.2 | 3308.245 | 4726.007 |
| | Trips after ch. 4.6 | 2764659.134 | 4932168.215 |
| | Total | 2767967.379 | 4936894.222 |
| **Difference** | | **0** | **0** |

Next, the number of trips starting in each individual traffic zone before and after routing was compared. For the baseline, this was again computed using the OD-matrix, but this time summed for each traffic zone instead of across all traffic zones. To collect the trips after routing, each traffic zone was assigned the route start points (collected in chapter 4.6) which were inside its borders. The number or trips originating in a traffic zone was then calculated as the sum of all trips starting at points assigned to that traffic zone. This method has the disadvantage that the location on the road network where the path starts (and for which the number of trips was being collected) may not be in the same traffic zone as the hectare raster point the trips were assigned to in chapter 4.2. The number of trips before and after routing can therefore be different. Even so, the number of trips before and after routing is similar for most traffic zones, as shown in Figure 16. The results are very similar for both 2017 and 2050. As expected, the number of trips before and after routing is slightly different for most traffic zones, but overall following the ideal 1:1 relationship. The linear regression and R-squared also confirm the result. The traffic zones with zero trips after routing are those in Zermatt and other traffic zones where all route start points on the road network were outside the traffic zone.

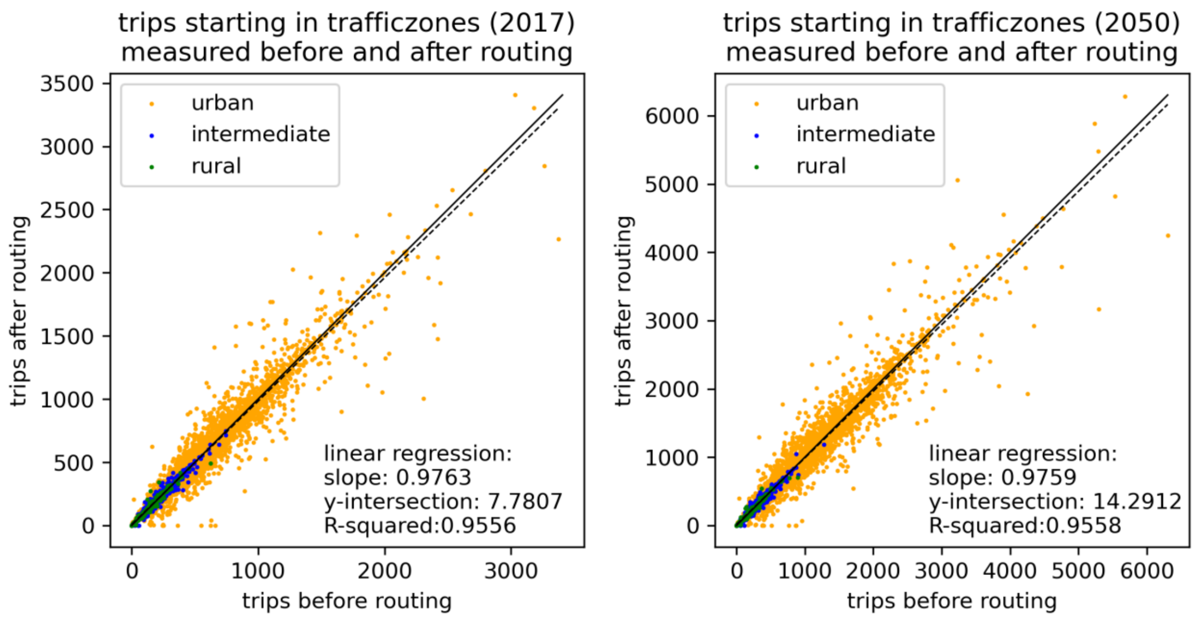


*Figure 16: Plot with the number of trips starting in each traffic zone before and after routing, for 2017 and 2050.*

# 5) Results

## 5.1) Exploratory Analysis

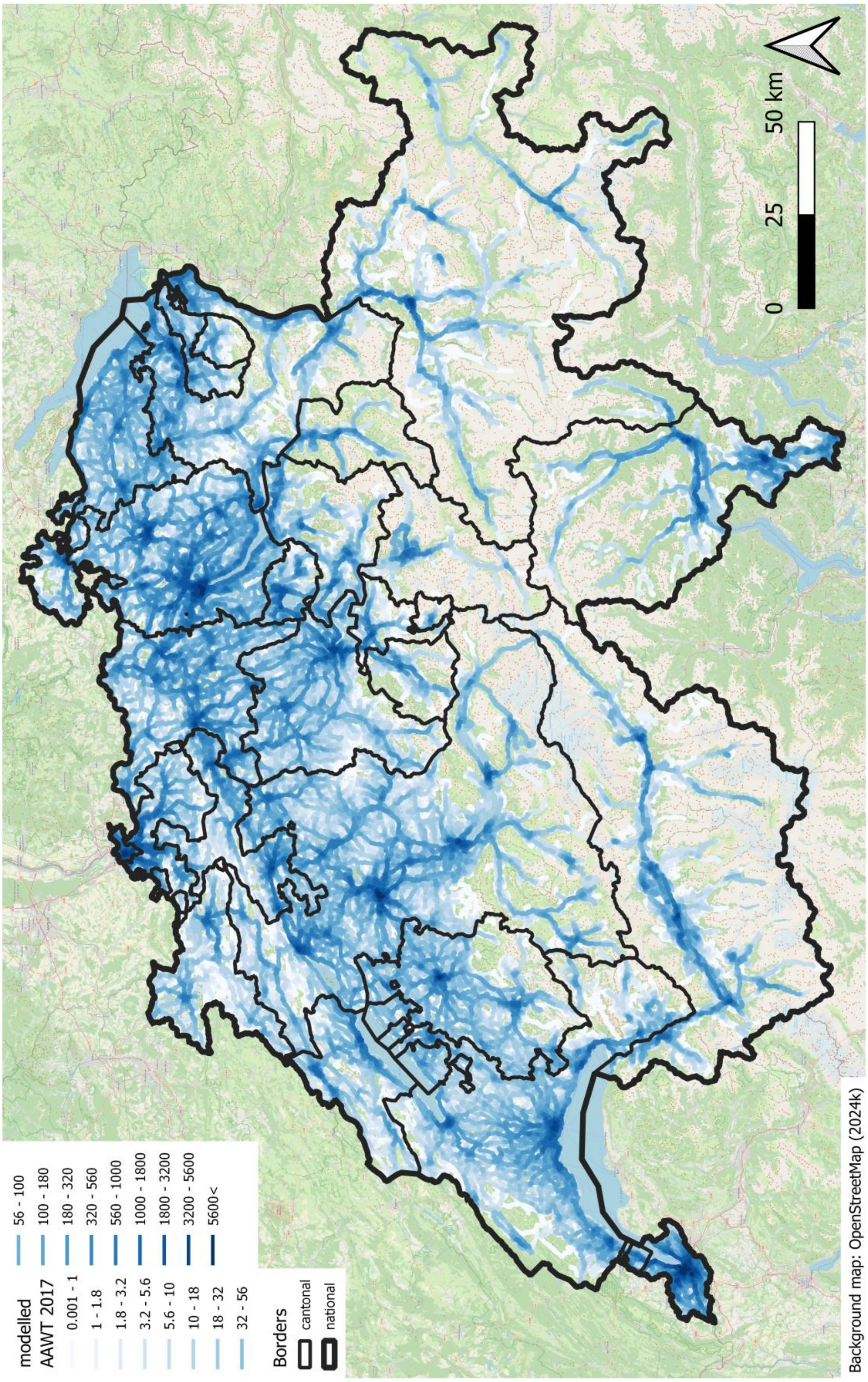


*Figure 17: Modelled bicycle traffic for Switzerland in 2017.*

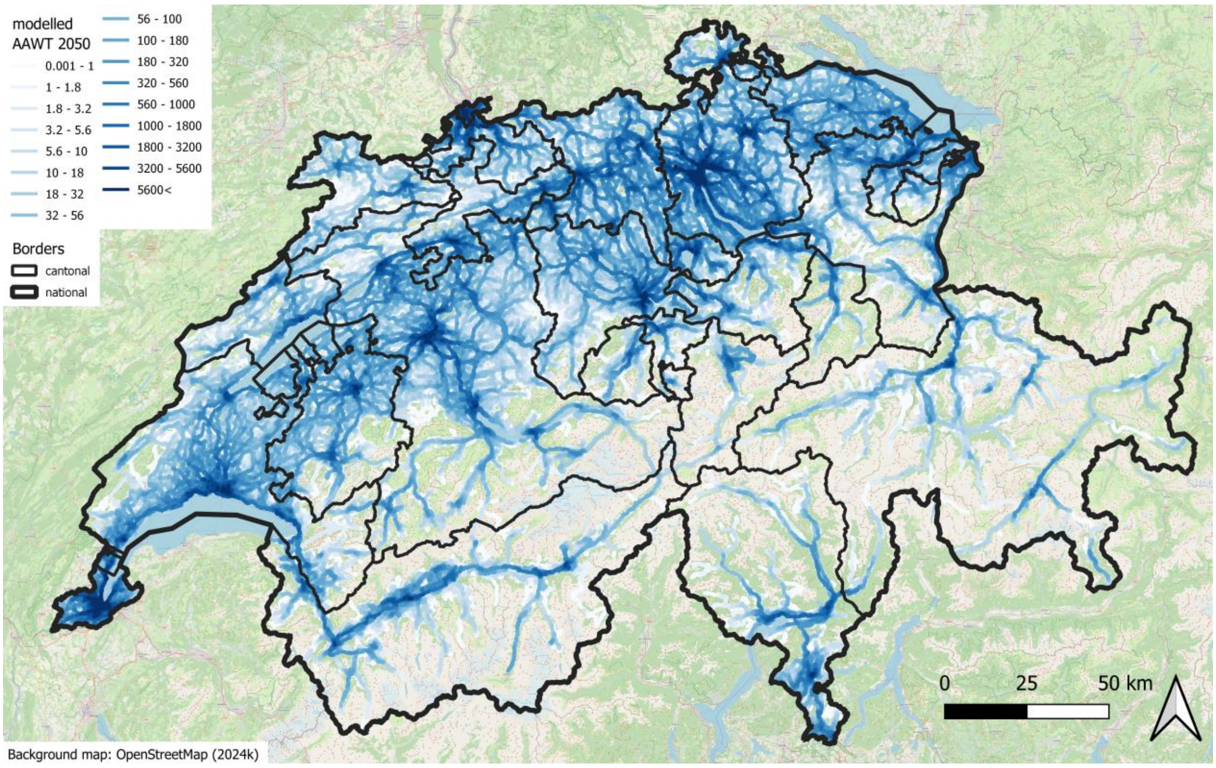


*Figure 18: Modelled bicycle traffic for Switzerland in 2050.*

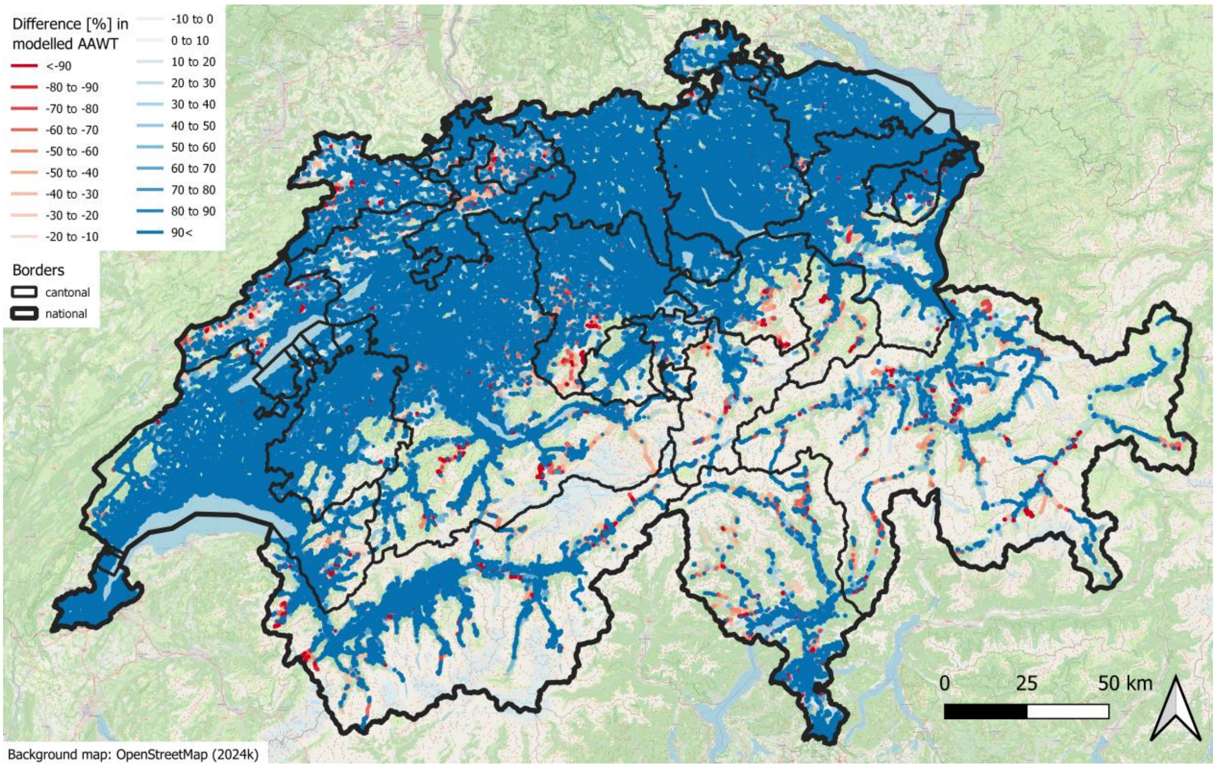


*Figure 19: Difference [%] in modelled AAWT from 2017 to 2050 across all of Switzerland.*

Figure 17: Modelled bicycle traffic for Switzerland in 2017. shows the results of the bicycle traffic assignment model BTAM for all of Switzerland in 2017. Bicycle traffic is higher in more populated areas. The difference between the alps and the Swiss plateau is especially strong. While bicycle traffic covers a dense network with relatively high traffic throughout in the plateau, in the alps bicycles are only used in the valleys. The Jura mountains are also identifiable, however the difference to the plateau is only marked by a slight decrease in traffic. Cities and their agglomerations are also easily identifiable due to their much higher bicycle traffic. Especially Geneva, Basel and Zurich appear to have very high annual average weekday traffic AAWT, but smaller cities like Chur or Yverdon do also stand out against the lower traffic in the surrounding area. While traffic in the alps is confined to the valleys and separated by mountain ranges, some mountain passes are modelled to have a significant amount of traffic. This is especially the case for the Grimselpass with over 30 cyclists a day in 2017, even though it reaches an elevation of 2165 m above sea level (myswitzerland, n.d.).

The bicycle dispersion map for 2050 (see Figure 18) looks very similar to that of 2017, with slightly higher traffic but no changes in large scale patterns visible. Figure 19 shows how the modelled AAWT has changed from 2017 to 2050. In most of Switzerland a strong increase in bicycle traffic can be seen. This increase is not limited to bigger cities where bicycle traffic is already strong in 2017, but it also extends to some of the more rural areas, especially in the Swiss plateau. Decreases in bicycle traffic are also visible, but they are mostly confined to very rural areas. In the alps many areas at the end of valleys are modelled to experience a decrease in cyclists. Additionally, some areas in the Jura mountains and the border region of the cantons of Bern and Lucerne are affected.

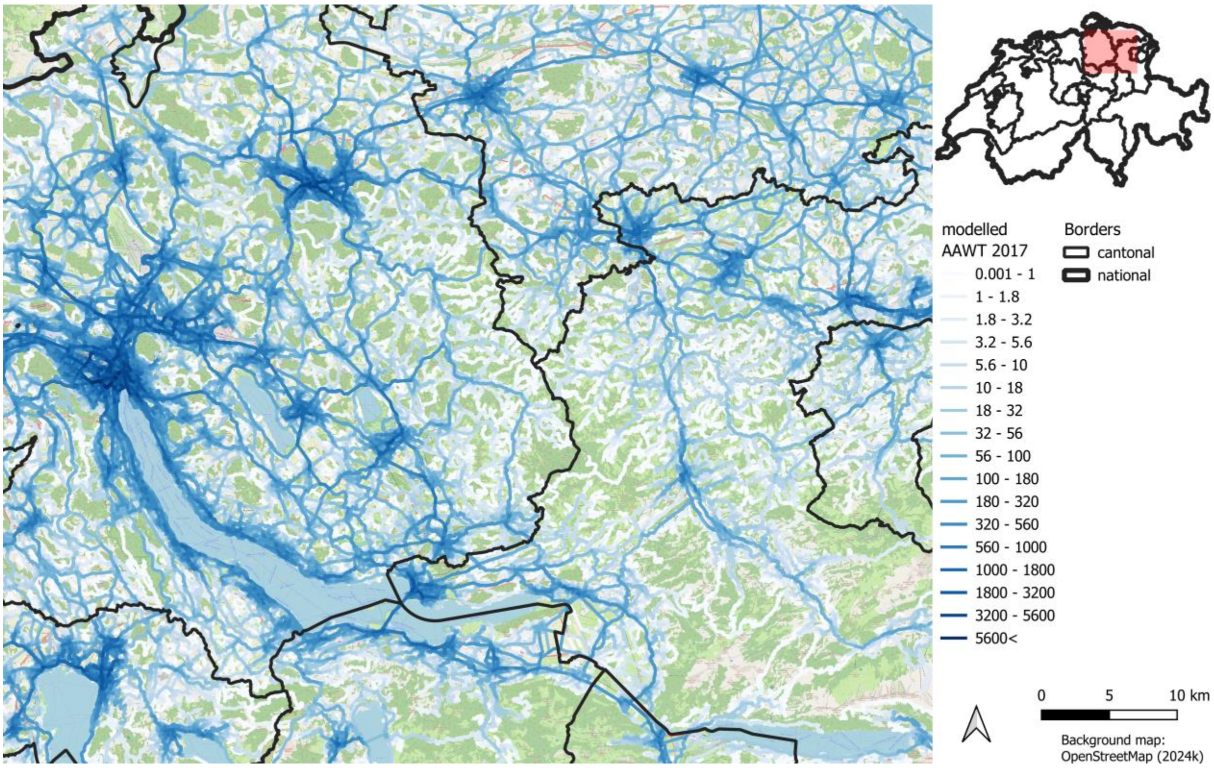


*Figure 20: Modelled bicycle traffic for 2017 in northeastern Switzerland.*

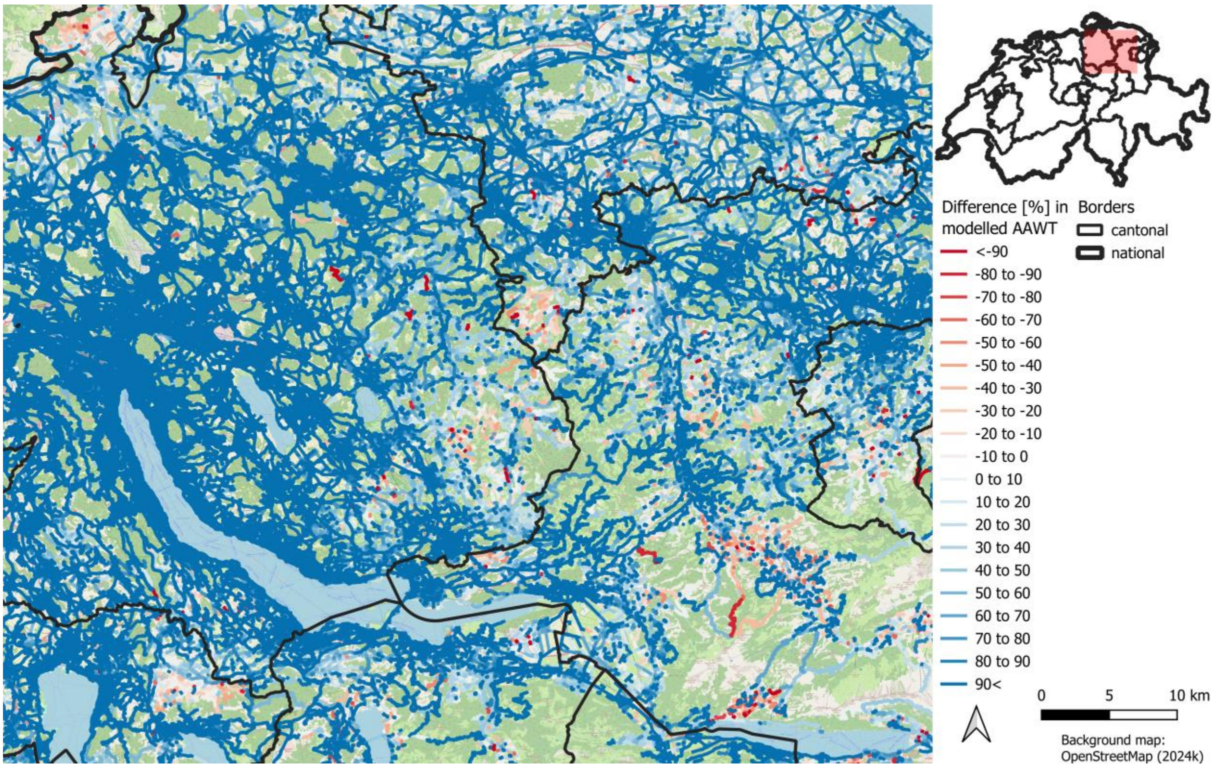


*Figure 21: Change [%] in bicycle traffic in northeastern Switzerland between 2017 and 2050.*

A closer look at northeastern Switzerland in 2017 (Figure 20), reveals a network of cities connected by roads. Cities are visible as areas with very high bicycle traffic. In bigger cities a network of major roads with more traffic is visible, especially in Zurich and Winterthur, while in smaller cities only the centre has more cyclists. Between cities there is a network of major roads, carrying a relatively high volume of traffic. The density of this network varies across the area: in the northeast a very dense network is visible, while the network in the east of the canton of Zurich is much sparser. In the southeast the connectedness of these roads is reduced even more as they only follow the valleys. Between and around the major roads a fine network of roads with little traffic is visible.

Looking at the change in bicycle traffic from 2017 to 2050 in northeastern Switzerland (Figure 21), the patterns found in the map for all of Switzerland (Figure 19) are confirmed. Bicycle traffic is expected to increase in most areas, with larger increases in urban areas. Rural areas also generally gain cyclists, but not everywhere.

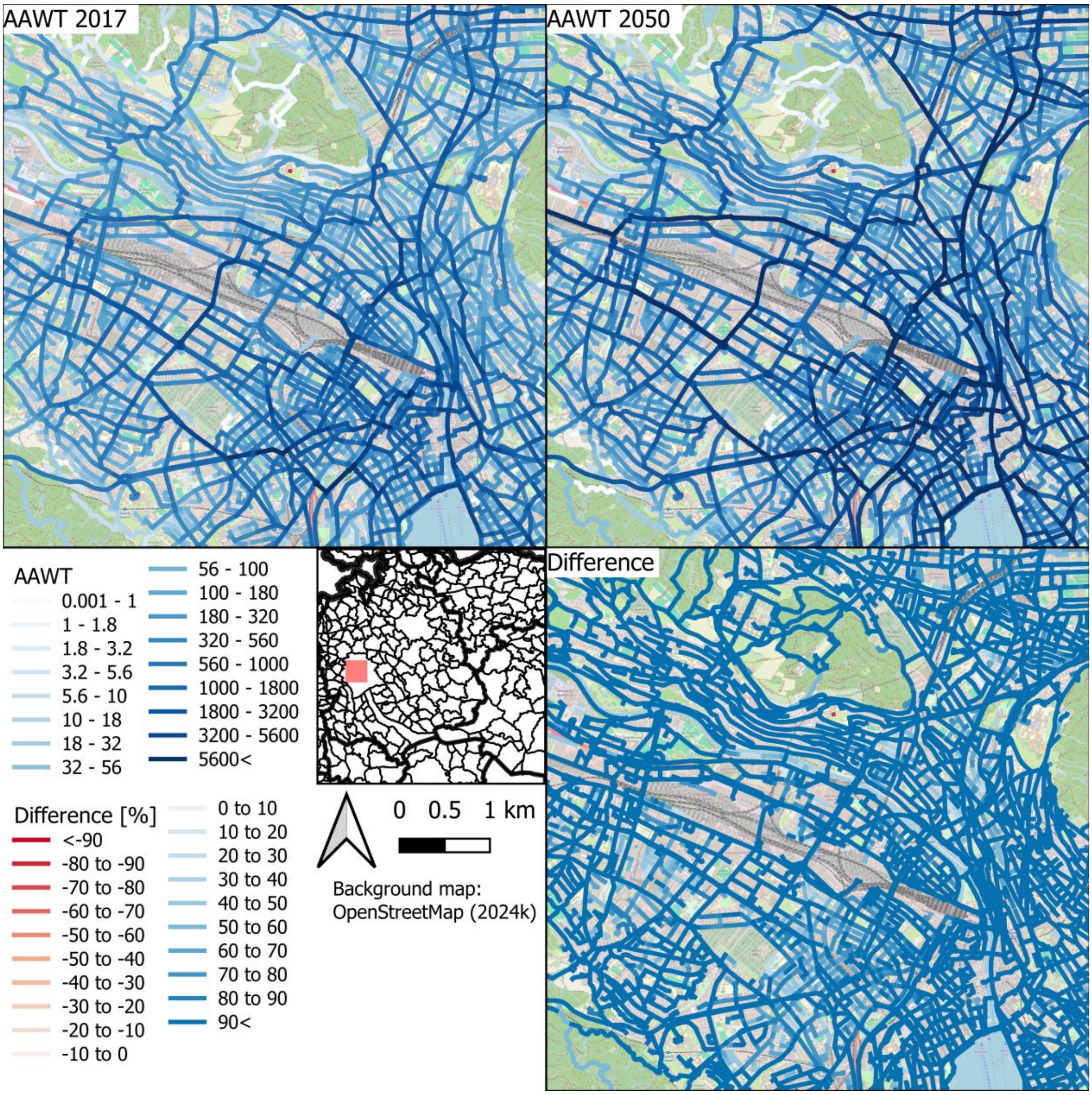


*Figure 22: Modelled bicycle traffic for the city of Zurich.*

Zurich is the largest city in Switzerland with a population of almost 400’000 in 2017 (Bundesamt für Landestopografie swisstopo, 2023a). It also belongs to the areas with the most modelled cyclists. Figure 22 shows that an increase until 2050 is nevertheless expected, with no roads in the city seeing a decrease in the number of cyclists. The largest counts are on major roads and on roads around the city centre, with over 5’600 daily cyclists. The area west of the Altstadt is expected to see a smaller increase in cyclists than the rest of the city, where a growth of over 90% is expected on almost all roads. A lack of cyclists, especially in 2017, can be seen along the south bank of the river Limmat (in the west of the city), which is part of a SwitzerlandMobility bicycle route (Bundesamt für Landestopografie swisstopo, 2024). Bicycle counter M_Zürich_11 is also located there and observed 367 bicycles, whereas only two have been modelled.

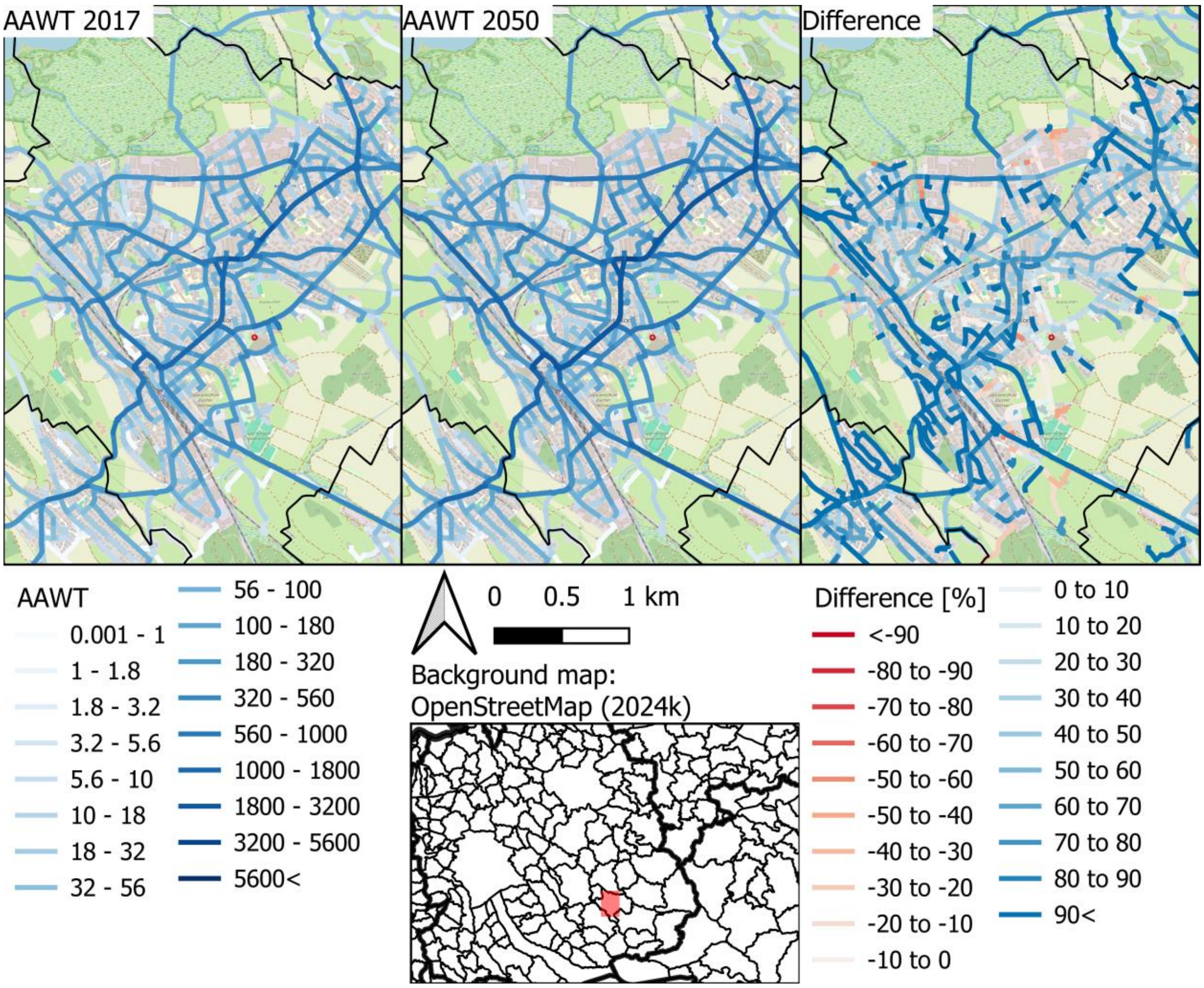


*Figure 23: Modelled bicycle traffic for the town of Wetzikon in the canton of Zurich.*

Even in the smaller town of Wetzikon, which had a population of almost 25'000 in 2017 (Bundesamt für Landestopografie swisstopo, 2023a), there are only few small roads with a decrease in traffic. These roads are very short and the decrease may be due to the random assignment of trips. In 2017 the road going southwest to northeast carries the most bicycle traffic, with almost 2'000 daily cyclists in some sections. By 2050 two other roads going perpendicular to that road carry a similar amount of traffic, which has increased to well over 2'000. This is due to the traffic increase being mostly along and near these roads, while the growth is smaller in the bulk of the town. In general, the increase in bicycle traffic is much lower than in the city of Zurich.

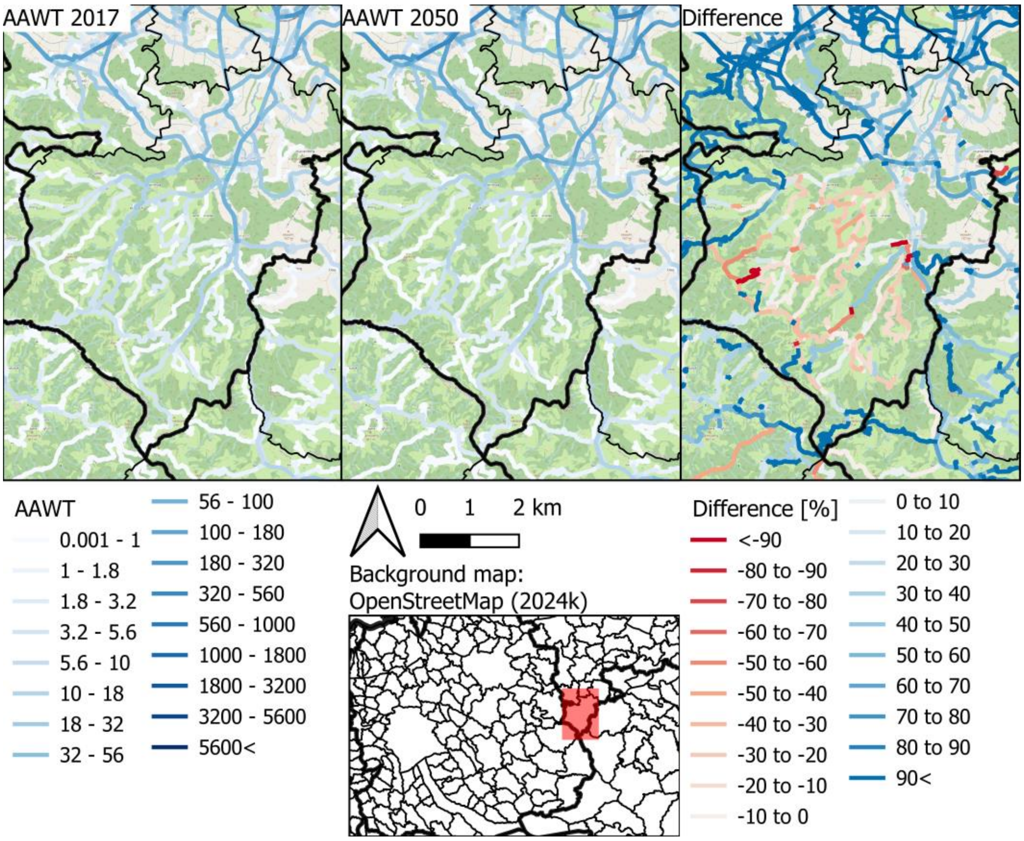


*Figure 24: Modelled bicycle traffic for rural municipality of Fischingen in the canton of Thurgau.*

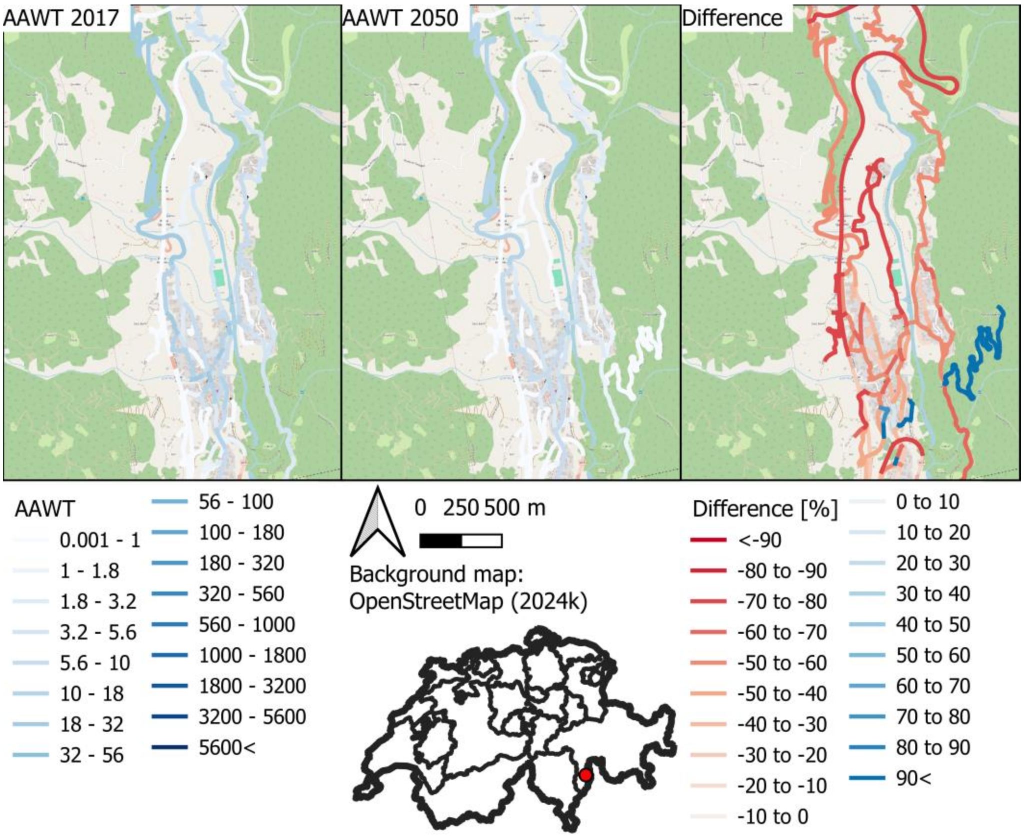


*Figure 25: Modelled bicycle traffic for village of Mesocco in the canton of Grisons.*

The rural areas of Fischingen in Figure 24 and Mesocco in Figure 25 show a different pattern than the urban areas shown before. Fischingen had a population of 2'600 in 2017 and is located in the Swiss plateau. Mesocco had a population of only 1'300 and is towards the end of a valley in the southern alps (Bundesamt für Landestopografie swisstopo, 2023a). Overall, there are way fewer cyclists, the largest number of cyclists is in the town of Balterswil to the northwest of Fischingen. The villages within the municipalities of Fischingen and Mesocco have barely more cyclists than the roads between settlements: up to 90 AAWT in Fischingen and 20 in Mesocco (for 2017). The largest difference to the urban municipalities however is the change from 2017 to 2050. While the urban municipalities had almost no road segments with decreasing bicycle traffic, in these rural areas it is very common. In Fischingen the villages in the north of the municipality see a small increase in cyclists, but in the area to the south, where there are only a few hamlets, a decrease can be seen. In Mesocco the decrease is much stronger than in Fischingen and encompasses almost all roads in the municipality. The difference in traffic development between these two rural municipalities and to the urban municipalities is expected: Under the base future scenario, the population increase in Switzerland is modelled to be mainly in cities and their agglomerations. Rural areas on the other hand, especially in poorly accessible regions, will see small growth or even population loss (Bundesamt für Raumentwicklung ARE, 2022b). Another observation is in the 2050 BTAM for Mesocco: A winding road in the forest has traffic up to a certain point and no traffic afterwards, which indicates that there is a route start or end point there. Such unexpected route start or end points are also visible in other locations, where remote homes or mountain huts have access to the road network.

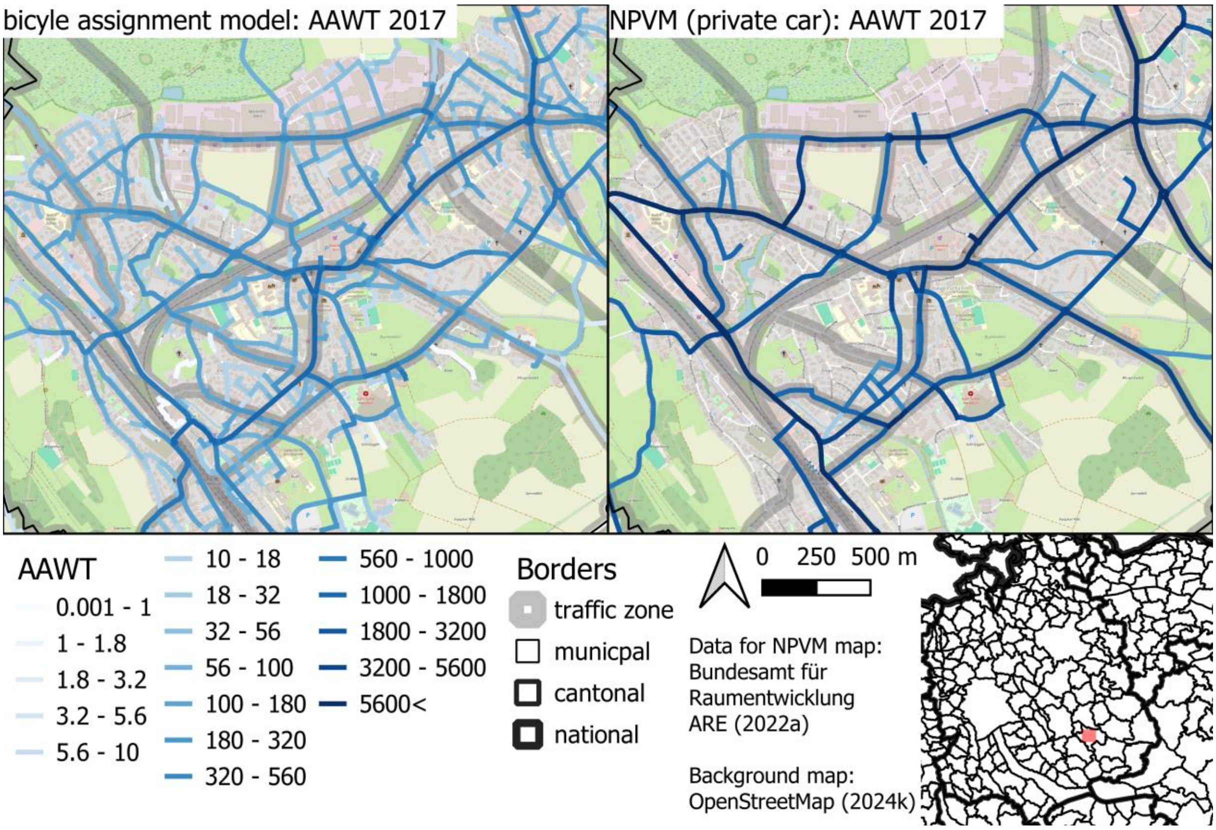


*Figure 26: Results of the BTAM (left) compared to the private car assignment performed during the NPVM (right) for Wetzikon.*

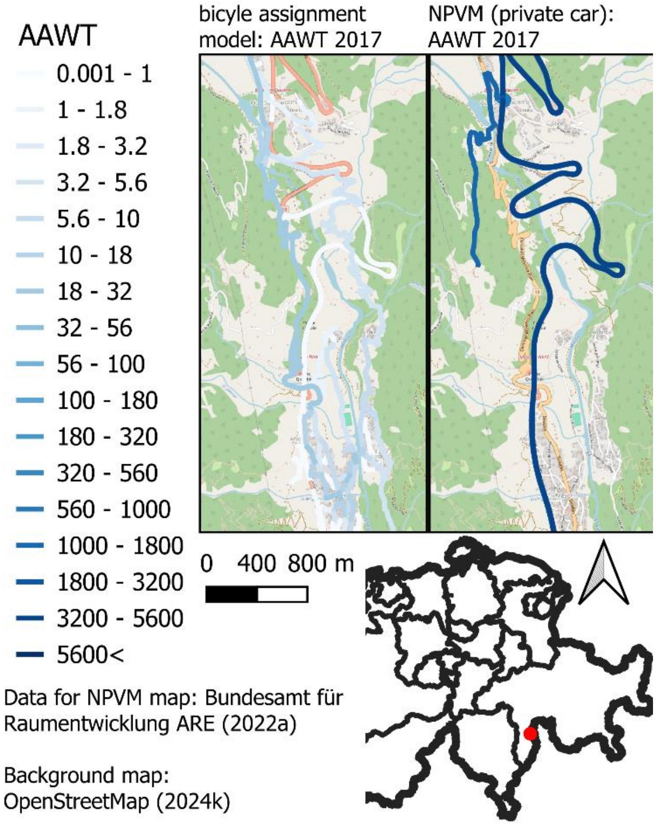


*Figure 27: Results of the BTAM (left) compared to the private car traffic assignment performed during the NPVM (right) for Mesocco, Grisons.*

Figure 26 and Figure 27 show a comparison of the BTAM with jittering and disaggregation to the car assignment model from the NPVM, which did not use these methods. Instead, the NPVM selected only one point in most traffic zones to assign traffic onto the road network, as was explained in chapter 2.1.1.5 (Bundesamt für Raumentwicklung ARE, 2020b). While the BTAM shows traffic on almost all roads within the settlement, the NPVM assignment model leaves many roads empty. This difference is striking, even when taking into account that bicycles are able to use some paths that cars cannot. In Wetzikon a network of roads in the settlement areas is used by NPVM, which includes all major roads. This contrasts with Mesocco, where traffic is only on the highway, and even the cantonal road (in orange) sees no traffic. The only exception is one road leading into the forest. The end of this road is likely where routes to and from this traffic zone start and end. Such traffic on smaller roads which suddenly ends is also visible in the NPVM model in Wetzikon, one in each traffic zone. However, they are shorter and always end within the settlement area. Traffic dead ends like these are also present in the BTAM, but mainly occur at the edge of the settlement or in dead end roads. Within the settlement it is not easily possible to detect points where routes start or end, unlike in the NPVM. In some rare cases, such as visible in the BTAM for 2050 in Mesocco (see Figure 25), traffic leads to remote houses and ends there, similar to the NPVM in Mesocco (see Figure 27).

## 5.2) Validation

### 5.2.1) Analysis of Route Lengths

The length of calculated routes was returned by the routing engine Valhalla. It includes all segments of the routed path, but not the distance from the selected coordinates of the hectare raster to the nearest road segment. This means that only the distance covered by bicycle is included and not the access to the road system (Valhalla, 2023).

#### *5.2.1.1) Comparison to Shortest Path*

The Valhalla parameters influence how much longer than the shortest path the calculated routes are, by prioritising path attributes other than distance. Comparing the amount of detour to values from literature can give an idea of whether the parameter set is reasonable. The routing engine does provide an option to calculate the shortest path between two points. When enabled, only distance is used to evaluate route options and other parameters, such as use_hills, are ignored (Valhalla, 2023). Using the same urban OD pairs as for the evaluation of the use_hills and use_roads parameters (chapter 4.3.1.2), it was observed that around 75 % of routes were less than 10% shorter than the shortest possible path. Around 2.6 % of routes were more than 50 % longer than the shortest path. The result does not change much, when including traffic zones of all municipality types. Broach et al. (2012) observed that the routes chosen by cyclists in Portland, USA were less than 10 % longer than the shortest path in half of the cases and 5 % of routes were more than 50 % longer (see Table 15), which is considerably lower than with the routing from Valhalla. The higher percentage of routes with small detours indicates that the routes are shorter than what was observed by Broach et al. One explanation could be that the Valhalla parameter set overvalues the route distance and undervalues other effects influencing a cyclist's route choice. Differences in the road networks of Portland and Switzerland may also lead to differences in the amounts of detour. As most of the parameters, especially use_roads and use_hills, are already chosen in a way resulting in longer detours, changes in the parameter set are unlikely improve the model in this regard.

*Table 15: Route length compared to the shortest possible path.*

| | **Broach et al. (2012)** | **Urban traffic zones** | **All traffic zones** |
|---|---|---|---|
| <10 % longer than shortest path | 50 % | 75.4 % | 74.5 % |
| <50 % longer than shortest path | 95 % | 98.6 % | 98.4 % |

### *5.2.1.2) Trip Length Distribution*

Figure 28 shows the distribution of route lengths across the trips in both 2017 and 2050. The cumulative distributions in the left plot for 2017 and 2050 are very similar. They have the same shape with many short routes below four kilometres and almost no routes above ten kilometres. The histogram on the right also shows a strong increase in the number of bicycle trips in the 2050 basic scenario compared to the 2017 model. The mean shows that trips in 2050 are slightly longer than those in 2017: It grows from 2.23 km to 2.6 km (see Table 16). In both years more than half of trips are shorter than two kilometres, the median trip length in 2017 was modelled to be 1.45 km and 1.59 km in 2050. The histogram shows that most trips are between 0.5 and 3 kilometres long with almost no trips longer than six kilometres. There are however few trips in both years which are zero kilometres long and some which are up to 294 km. Routes can have a length of zero kilometres even though they do not have the same start and end coordinates (see chapter 4.2.2.2), as the closest point on the road network may be the same.

*Table 16: Characteristics of the trip length distribution for the BTAM and MZMV 2015. Source for MZMV data: (Bundesamt für Statistik BFS, 2017b).*

| | **BTAM 2017** | **BTAM 2050** | **MZMV 2015 (AAWT)** | **MZMV 2015 (AADT)** |
|---|---|---|---|---|
| **Mean [km]** | 2.23 | 2.60 | 2.9 | 3.3 |
| **Median [km]** | 1.45 | 1.59 | -- | -- |
| **Minimum [km]** | 0 | 0 | -- | -- |
| **Maximum [km]** | 294.31 | 294.65 | -- | -- |

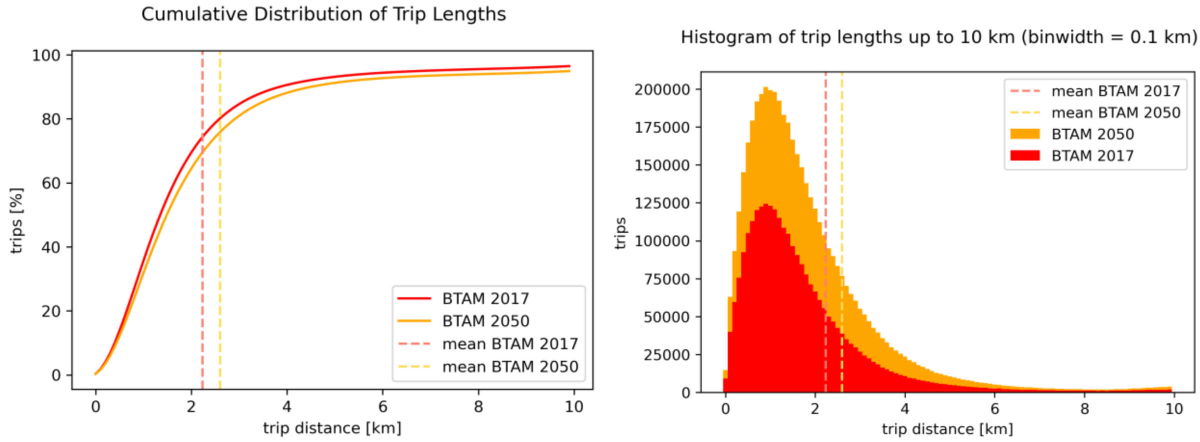


*Figure 28: Distribution of trip lengths for the BTAM.*

To validate the results, the modelled distribution of trip lengths was compared to that observed by the Swiss micro census for mobility and traffic MZMV in 2015. The distribution of trip lengths was unfortunately only available for annual average daily traffic AADT, while the model was created using annual average weekday traffic AAWT. While weekday and weekly traffic are different, they are similar enough to draw a useful comparison. Figure 29 shows the percentage of trips in different distance classes. While the general shape of all curves is very similar, the MZMV shows fewer trips between one and three kilometres and more between five and ten. This difference is also present in the mean trip distance, which is 2.9 km for AAWT according to the MZMV and only 2.23 in the BAM (see Table 16). The MZMV mean trip distance for AADT with 3.3 km is larger than that for AAWT, indicating that the difference in the distributions is at least in part due to using a comparison of weekday with weekly traffic.

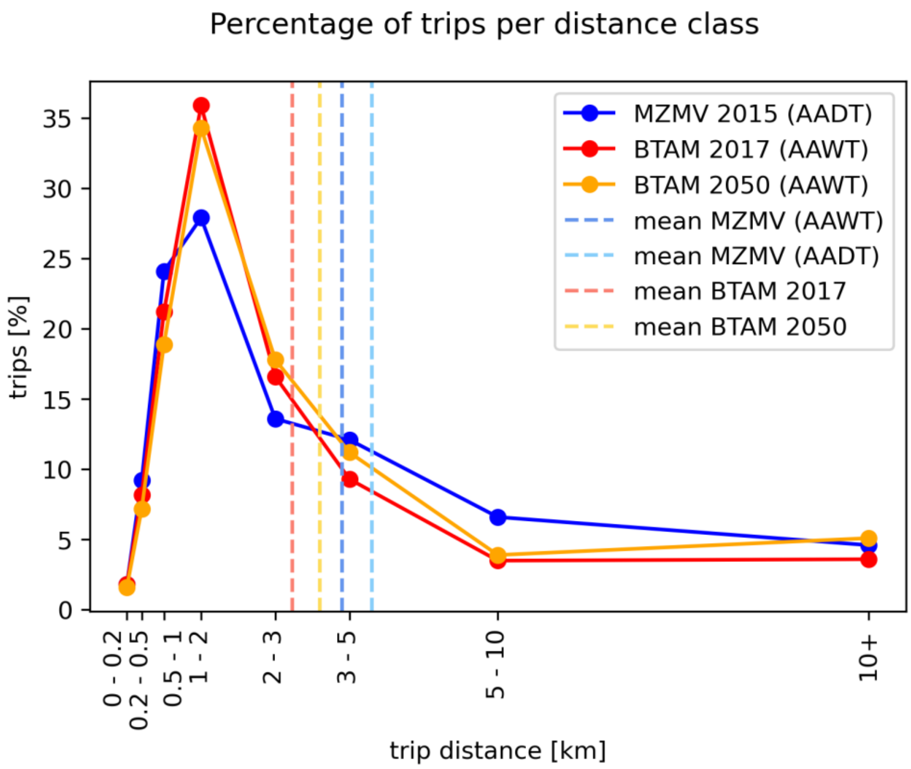


*Figure 29: Distribution of trip lengths in the BTAM compared to observations from MZMV 2015. Data from MZMV is for the entire week (AADT), data from the assignment model only on weekdays (AAWT) (MZMV data: (Bundesamt für Statistik BFS, 2017d)).*

## 5.2.2) Comparison with Bicycle Counters

In this chapter the bicycle traffic modelled with the BTAM on individual street segments will be compared to bicycle counts observed by counting stations across Switzerland, using the data set prepared in chapter 4.7.

### *5.2.2.1) Linear Regression*

Figure 30 shows plots of observed AAWT against modelled AAWT at counting stations for the BTAM of this thesis. Ideally all points would fall onto the solid line which shows the 1:1-relationship, where observed and modelled values are equal. Upon a visual comparison of the different plots, urban counting stations, especially those with high counts, fall closest to this line and rural counting are very spread out. While urban stations have observed and modelled counts up to around 8'000 with the bulk around 1'000, the rural stations only reach 500 for the observed and 1'200 for the modelled values. Three counting stations have a modelled count of zero, meaning that no bicycles were modelled to use the road section for 2017, even though bicycles were observed there.

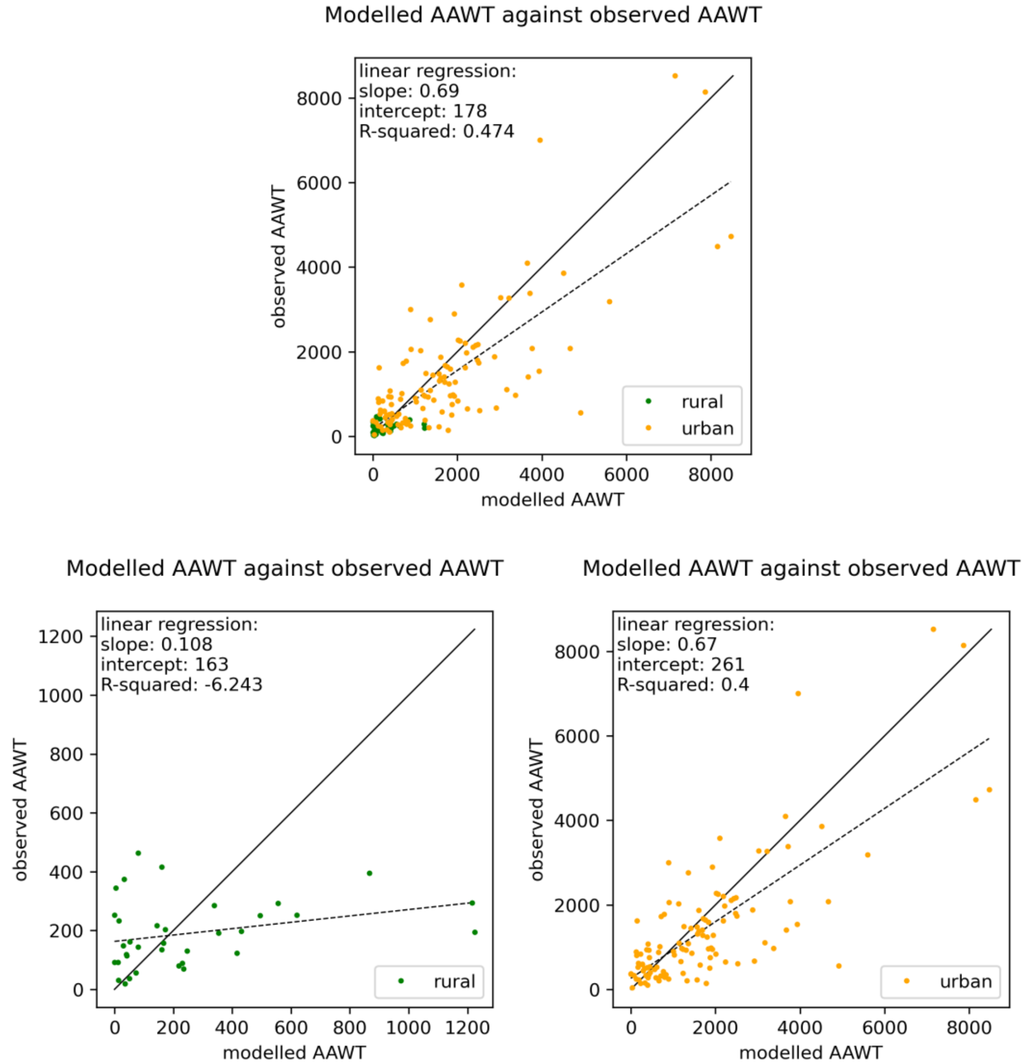


*Figure 30: Plot of observed AAWT against modelled AAWT at counting stations. The dotted line is a linear regression and the solid line shows the ideal 1:1-relationship.*
*Top: all counting stations*
*Bottom left: rural counting stations*
*Bottom right: urban counting stations*

The linear regression characteristics support the observations that the BTAM for urban stations has the best results: The intersection with the y-axis is similar for all three plots, ranging from 163 to 261. The slopes of the different plots are all positive and below one, indicating an underestimation of the modelled values. This is especially the case for rural counting stations, where the slope is only 0.11, which is almost horizontal. The urban counters have a significantly higher slope with 0.67 and across all counters it is even a bit better with 0.69. The coefficient of determination R-squared supports the analysis of the slope, also indicating that urban counters perform best, and the rural counters worst. The highest R-squared is for of all counters, which is however still quite low with 0.47. The value for urban counters is slightly lower with 0.4. The R-squared for rural counters is -6.2; a negative R-squared indicates that the regression line is a worse fit than a horizontal line through the mean of the modelled values (Chicco, Warrens, & Jurman, 2021), showing that the BTAM performed very poorly for rural counters.

##### *5.2.2.2) GEH-Value and SQV Evaluation*

The share of bicycle counting stations in the different GEH-classes for the BTAM is similar to the NPVM (see Table 17), with the NPVM having slightly better results. Around half the stations have a GEH-value smaller than 15, which is considered acceptable. Rural counters performed better, with almost 70 % being acceptable, higher than the 60 % of the NPVM. The GEH-value is however best suited for counts above 2’000 and overestimates the quality of lower values (Bundesamt für Raumentwicklung ARE, 2020b). The urban bicycle counting stations having the highest counts and the rural ones the lowest counts may be the reason for this difference rather than the quality of the models. When looking at the Scalable Quality Value SQV (Table 18) only 35 % of counters are considered acceptable with a SQV above 0.8. Rural counters are again performing better than urban ones. The SQV was scaled with a scaling factor f of 1’000, as the mean of the observed counts is 1130 and the median is 636. With rural counting stations having counts of around 200, the same effect may apply as for the GEH-values where low counts get better results.

*Table 17: Distribution of GEH-values at bicycle counting stations in the BTAM and the NPVM (Bundesamt für Raumentwicklung ARE, 2020b).*

| GEH | Cumulative fraction [%] | | | |
|---|---|---|---|---|
| | BTAM | | | NPVM |
| | All counters | Urban counters | Rural counters | |
| <= 5 | 18 | 16.5 | 22.9 | 24 |
| 5-10 | 38.7 | 38.3 | 40 | 43 |
| 10-15 | 51.3 | 46.1 | 68.6 | 58 |
| 15-20 | 66 | 60.9 | 82.9 | 68 |
| 20-25 | 74 | 68.7 | 91.4 | 74 |
| >25 | 100 | 100 | 100 | 100 |

*Table 18: Distribution of SQV at bicycle counting stations in the BTAM.*

| SQV (f=1000) | Cumulative fraction [%] | | |
|---|---|---|---|
| | All counters | Urban counters | Rural counters |
| >= 0.9 | 13.3 | 11.3 | 20 |
| 0.85-0.9 | 21.3 | 19.1 | 28.6 |
| 0.8-0.85 | 35.3 | 35.6 | 34.3 |
| 0.75-0.8 | 40.6 | 38.2 | 48.6 |
| 0.7-0.75 | 45.3 | 42.5 | 54.3 |
| < 0.7 | 100 | 100 | 100 |

Figure 31 and Figure 32 show the plots of observed against modelled AAWT again, coloured by GEH-value and SQV. They confirm the observations made about the tables, with most rural counters being within the dotted line of acceptable GEH and SQV. It also confirms that the low counts from the rural stations are responsible for the better GEH and SQV, as the range of acceptable values is very wide for low counts. The worse results for SQV compared to GEH are explained by the narrower acceptable range of SQV.

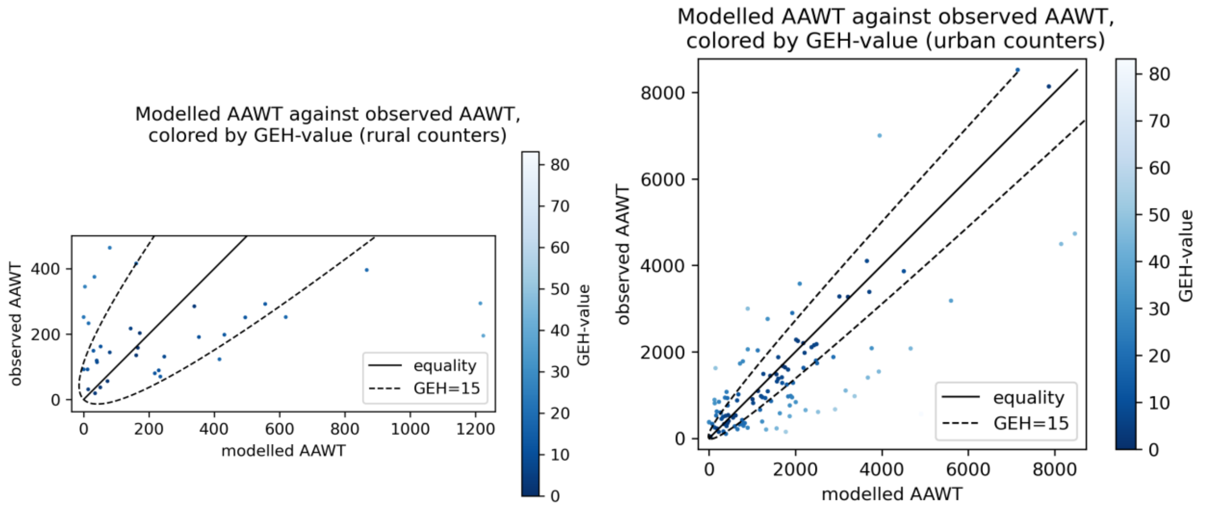


*Figure 31: Plot of observed AAWT against modelled AAWT for bicycle counters. Coloured by GEH. The solid line shows the ideal 1:1-relationship, values inside the dotted line are considered acceptable.*

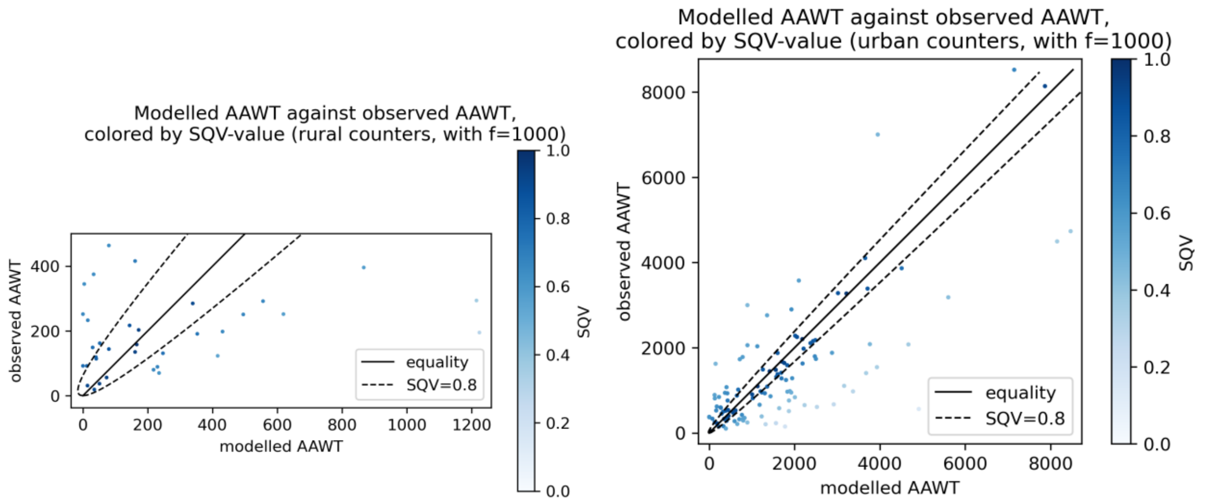


*Figure 32: Plot of observed AAWT against modelled AAWT for bicycle counters. Coloured by SQV, with f=1000. The solid line shows the ideal 1:1-relationship, values inside the dotted line are considered acceptable.*

The results from the linear regression and GEH/SQV are contradictory, with former indicating better performance of the BTAM for urban stations and latter a better performance of rural stations. This is likely due to lower counts being given better evaluations by SQV and GEH-value (Friedrich, Pestel, Schiller, & Simon, 2019) and urban stations generally observing more traffic. To address this issue the SQV was recalculated using separate scaling factors f for urban and rural counting stations. With a mean of 190 and a median of 162 for the observed traffic, rural counting stations get a scaling factor of 100. Urban counting stations have a mean of 1416 and a median of 950 and therefore remain with a scaling factor of 1’000. Table 19 and Figure 33 show the new results: only 14.3 % of rural counters are now considered acceptable, compared to 34.3 % with a scaling factor of 1’000. The acceptable range in the plot is now also much narrower, showing most points far outside it. These results with different scaling factors do match up with the observations from the linear regression: The BTAM performs relatively well for urban counters and badly for rural ones.

*Table 19: Distribution of SQV at bicycle counting stations in the BTAM, using different scaling factors for urban and rural counters.*

| SQV | Cumulative fraction [%] | |
|---|---|---|
| | Urban counters (f = 1'000) | Rural counters (f = 100) |
| >= 0.9 | 11.3 | 2.9 |
| 0.85-0.9 | 19.1 | 2.9 |
| 0.8-0.85 | 35.6 | 14.3 |
| 0.75-0.8 | 38.2 | 20 |
| 0.7-0.75 | 42.5 | 22.9 |
| < 0.7 | 100 | 100 |

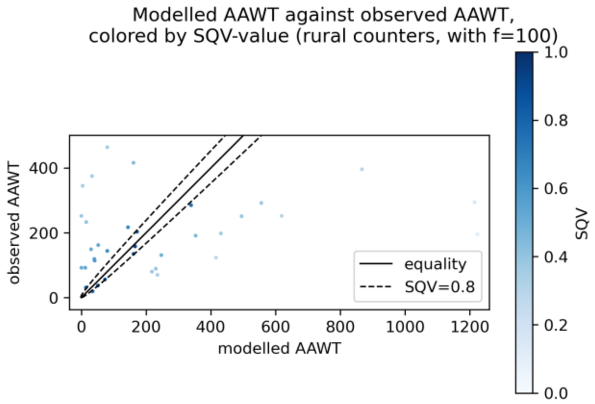


*Figure 33: Plot of observed AAWT against modelled AAWT for rural bicycle counters. Coloured by SQV, with f=100. The solid line shows the ideal 1:1-relationship, values inside the dotted line are considered acceptable.*

# 6) Discussion

The aim of this thesis was to create a bicycle traffic distribution model BTAM based on the bicycle distribution model from the Swiss national model for passenger traffic NPVM. By using the disaggregation and jittering approaches described by Lovelace et al. (2022), the model was supposed to distribute route start- and endpoints across traffic zones and allow for realistic traffic patterns even on a local level. In this chapter the research questions introduced in chapter 1.2 will be addressed and limitations of the approach will be discussed.

## 6.1) Discussion of Research Questions

### 6.1.1) Research Question 1: How can the jittering method developed by Lovelace et al. be applied to Switzerland?

The jittering and disaggregation method was developed by Lovelace et al. (2022) in order to distribute the route start and end points in traffic assignment throughout a traffic zone. The purpose of this was to create more diffuse traffic, which is important for local traffic analysis and short routes such as from bicycles. The jittering approach achieves this goal by having different route start and end points for all routes. These locations can be chosen randomly from the entire traffic zone, only a certain subzone or weighted by a geographic variable. Additionally, disaggregation can be applied to create multiple routes for one origin-destination (OD) pair (Lovelace, Félix, & Carlino, 2022; Schnabel & Lohse, 2011).

In this thesis both jittering and disaggregation were used, with route start and end points being distributed using a weighting method. Geographically referenced data on population and companies in Switzerland is available aggregated for raster cells with an area of one hectare (Bundesamt für Statistik BFS, 2018b; Bundesamt für Statistik BFS, 2018b). For the BTAM the centre points of these hectare raster cells were used as potential route start and end points for the jittering algorithm. They were selected randomly, weighted by the sum of population and full-time equivalents (see chapter 4.2.2), a method also used for the NPVM (Bundesamt für Raumentwicklung ARE, 2020b). Using these weights not only assigns more routes to areas with more people, but also avoids route start and end points in areas without buildings.

In the paper by Lovelace et al. (2022) it is suggested to sample these points in a way that reflects traffic demand, for example using the density of the transport network, city centres or workplaces. While the data used for the BTAM is well suited to reflect trips to and from work, it does not include other trip attractors such as shopping centres, public transport stations or leisure facilities. With 78 % of trips starting or ending at home and 28 % of trips being conducted for commute this methodology includes the most important route start and end points (Bundesamt für Raumentwicklung ARE, 2020c). While including additional data would have improved the model, collecting and combining it would have been challenging. Another issue with the selection of route start and end locations is that the distance between these points was not directly included. Especially for trips within a traffic zone or between neighbouring ones this can result in very short trips, which are not common according to the Swiss micro census for mobility and traffic MZMV (Bundesamt für Statistik BFS, 2017d). Other issues resulting from this omission are routes which start and end in the same location or involve too few segments to be included in the trip aggregation. The first issue occurs when one location on the road network is the closest road to two separate hectare raster points. When a route is assigned to start and end at such hectare raster points, it has a length of zero metres. The second issue is a result of removing the first and last segment of each route. This is necessary to allow for trip aggregation as explained in chapter 4.6, but results in routes with fewer than three segments being completely ignored for aggregation. Preventing either of these issues would be complicated and likely not worth it for the few cases where the problem occurs.

When applying the disaggregation approach, the maximum number of trips for routes before they get disaggregated must be set. Due to the recent publication of these methods, the optimal value is not yet known or even well analysed. (Lovelace, Félix, & Carlino, 2022). For the BTAM this threshold was set differently for each traffic zone, using the 90$^{th}$ percentile of all OD-pairs involving this traffic zone. This was done to account for the wide range of values across the country with the aim of, on one hand, creating a diffuse network, even in rural areas with very few trips. And on the other hand, avoid creating extremely many routes in cities with many trips. The same idea was also applied to the removal of OD-pairs with very few trips, where the removal threshold was set separately for urban, intermediate and rural municipalities. Figure 24 and Figure 25 show the results of the BTAM for the rural municipalities of Fischingen and Mesocco. They show a diffuse traffic pattern, even though the traffic volume is small. While this shows that the idea of using separate thresholds for different areas works, a comparison to a model without this modification would show if it is necessary.

Figure 26 and Figure 27 show a comparison of the BTAM of 2017 with the car assignment model from the NPVM. The BTAM used the jittering and disaggregation approach based on Lovelace et al. (2022), which created many route start and end points throughout the traffic zone, even in the rural municipality of Mesocco. This contrasts with the NPVM, which only used one connector point for these traffic zones. The result shows a much less diffuse traffic pattern with obvious route start and end points. This is not much of an issue for regional car traffic, which has a hierarchical road network and long distances. Bicycle traffic however has shorter routes without a clear road hierarchy, which means that all roads need to be included at any level of road traffic analysis (Schnabel & Lohse, 2011). In Mesocco (Figure 27) the connector point of the NPVM is even in the forest, creating a locally very unrealistic traffic pattern. While the BTAM also has some route start and end locations in seemingly unpopulated areas, the use of the hectare raster ensures that there always is someone working or living in the area. The use of the traffic zone centroid, as done for the NPVM, does not guarantee this.

The use of the jittering and disaggregation method with the Swiss hectare raster worked well and resulted in a dense traffic pattern without obvious route start and end points. Weighting hectare raster cells by their population and full-time equivalents includes the two most important types of origins and destinations (home and workplace), but leaves out many others.

### 6.1.2) Research Question 2: How can a nationwide bicycle traffic distribution model be created, which is usable on a local level?

As discussed in the previous section, the jittering and disaggregation method from Lovelace et al. (2022) were used in this thesis, which helped to distribute the modelled bicycle traffic across all roads, even minor ones. The comparison to the NPVM, where this was not done, showed that an approach such as this is necessary to model traffic on minor roads and therefore necessary for use of the model at a scale smaller than regional. Nevertheless, there are issues with the distribution of traffic in the model, as was mentioned in chapter 5.1: Roads outside of settlements which do not directly connect any settlements are often modelled to have no traffic, as for example along the south bank of the Limmat in Figure 22. Especially leisure cyclist do often not follow a direct route and instead prefer attractive scenery (Bernardi, La Paix Puello, & Geurs, 2018), which cannot be modelled using the routing service used for this thesis (Valhalla, 2023). Especially in rural areas this can lead to bad modelling results, which is also supported by the linear regression performed in chapter 5.2.2.1.

The linear regression for the BTAM (chapter 5.2.2.1, Figure 30) and NPVM (chapter 2.1.3, Figure 4) for bicycles show similar spreads when looking at counts below 4000, which is around the maximum for the NPVM. However, the BTAM shows a cluster of points following the 1:1-line, while the NPVM is spread out more evenly. Furthermore, the NPVM has a lot of counting stations with a modelled AAWT of zero, where the observed AAWT is up to 1500 cyclists a day. The BTAM does also have such values, however there are only three of them and all have an observed AAWT of less than 400. Both are however much worse than the results for the NPVM model for car traffic (Bundesamt für Raumentwicklung ARE, 2020b).

Table 20 summarises the characteristic values for the linear regressions for NPVM and BTAM from Figure 4 and Figure 30. While the intercept for rural BTAM counters is best among the bicycle models, this is only by a small amount and they perform by far the worst when considering slope and R-squared. The slope shows slightly better results for urban counters from BTAM (0.67) than for NPVM bicycle counters (0.541). A larger difference exists with R-squared, where the urban counters from BTAM (0.474) perform significantly better than NPVM (0.192). Even so, less than half of the variation is explained by the model. The NPVM model for car traffic was plotted with the axis of modelled and observed values switched, which changes the values for slope and intercept (Piñeiro, Perelman, Guerschman, & Paruelo, 2008). It is nevertheless possible to observe that it performs much better in all metrics than the four bicycle models (Bundesamt für Raumentwicklung ARE, 2020b).

*Table 20: Characteristic values for the linear regression of BTAM and NPVM (Bundesamt für Raumentwicklung ARE, 2020b).*

| | BTAM | | | NPVM | |
|---|---|---|---|---|---|
| | **All counters** | **Rural** | **Urban** | **Bicycle** | **Car *** |
| **Slope** | 0.69 | 0.108 | 0.67 | 0.541 | 1.00 |
| **Intercept** | 178 | 163 | 261 | 383 | -7.38 |
| **R-squared** | 0.474 | -6.243 | 0.4 | 0.192 | 1.00 |
| * The linear regression for the NPVM with car traffic was performed with observed values on the x-axis instead of the y-axis. This means the values for slope and intercept are not directly comparable to the other regressions (Piñeiro, Perelman, Guerschman, & Paruelo, 2008). | | | | | |

The analysis shows that the method presented in this thesis can be used to create a bicycle traffic assignment model which creates a dense enough network for local bicycle traffic analysis. Furthermore, the use of freely available data and software makes it possible to modify the model itself or its inputs. The accuracy of the BTAM however is not great. While the results in urban areas are acceptable, the model performed very poorly in rural areas.

## 6.2) Methodology and Limitations

### 6.2.1) Route Preparation

In chapter 4.1, the first part of the methodology, origin-destination OD pairs from the NPVM bicycle distribution model were excluded for the BTAM. The removal was based on the number of trips between the traffic zones and their municipality type (urban, intermediate or rural). The aim was to remove many OD-pairs to reduce the number of routes needed to be calculated, while keeping as many trips as possible. The results are shown in Table 6 and Table 7, with 71 % of OD-pairs and only 1.62 % of trips being removed for 2017 and similar results for 2050. While the aim of reducing the number of OD-pairs was achieved, the thresholds of annual average weekday traffic AAWT between traffic zones of different municipality types vary a lot: In 2017 the threshold for rural traffic zones was only 0.006, while it was 0.1 for urban ones. One the one hand, with only around two trips per year the threshold for rural traffic zones is very low and even multiple such routes using the same road will not result in a significant amount of traffic. But on the other hand, the threshold for urban traffic zones is quite high with one trip every two weeks. This could have been corrected for by using different percentages of trip removal for the different municipality types, however that would have increased the number of parameters to be set manually. Using a different method may have resulted in better thresholds, but for the purpose of this thesis the method nevertheless seems sufficient.

In the second step of the methodology (chapter 4.2.1) the number of routes between each pair of traffic zones was determined using the method of disaggregation introduced by Lovelace et al. (2022). Similarly to the removal of OD-pairs, disaggregation needs to be balanced with the number of routes requiring calculation. This does again require the use of a manually determined parameter, in this case the 90th percentile of routes from a traffic zone was used as a maximum number of trips for each route, with a ceiling of ten trips per route. While a few values were tested for these parameters, no rigorous analysis was performed. The lack of obvious route start and end points in Figure 26 does however suggest that the choice of parameters was sufficiently good.

The jittering approach (chapter 4.2.2) was successfully used to distribute route start and end points throughout the traffic zones. However, as discussed in chapters 5.1 and 6.1.1 the method resulted in some of these points being outside of settlement areas, creating a point where there is no traffic going any further. These traffic dead ends are not always realistic, especially when they are going towards mountain huts. This issue could potentially be reduced by not using hectare raster points with a sum of population and full-time equivalents below a certain value, however this would also impact small villages and hamlets. Both the distribution of traffic across all roads (as opposed to only a few) and the general absence of obvious route start and end points indicate that the disaggregation and jittering methods worked and improved the resulting traffic assignment model.

### 6.2.2) Road Network and Routing

The road network from OpenStreetMap OSM was used for the BTAM as it is freely available and many routing engines are compatible with it. However, as it is volunteered geographic information with less quality control than traditional mapping services the quality of the road network is an issue (Goodchild, 2007). As mentioned in chapter 3.1, many studies found that the quality of OSM maps is good enough in areas where the project had time to develop, such as Switzerland. Categorisation of bicycle infrastructure however was found to be inconsistent (Ferster, Fischer, Manaugh, Nelson, & Winters, 2020). In chapter 4.4 some of these issues were addressed. While some problems were solved for the entire network, this was mostly done manually and only around bicycle counting stations. Errors in the OSM data are therefore still present in most of the network, including manually corrected areas due to a lack of local knowledge. A newer network, for example from early 2024, would likely be more reliable, as literature observed OSM to improve over time (Neis, Zielstra, & Zipf, 2012). This would however have introduced other challenges, as infrastructure changes after 2017 would change the results and would need to be reverted around bicycle counting stations.

The Valhalla routing engine was used to create the paths between route start and end point. While it does allow for the adjustment of a lot of different parameters, some aspects influencing cyclists route choice are not available. A preference for scenic routes (Prato, Halldórsdóttir, & Nielsen, 2018) for example is not reflected in any of the routing parameters in Valhalla. This results in no cyclists being modelled for roads which are more scenic but also longer. The routing service openrouteservice shows that it is possible to implement, as they have done so to preference green and quite routes, however only for pedestrian traffic (gGmbH, 2023). A major advantage of the Valhalla routing engine is the ability to change parameters for each route request. This allowed for the calibration of the use_roads and use_hills parameters and would enable the use of multiple parameter sets for different origin-destination groups with different route preferences. This was not done for this thesis as the calibration of different parameter sets would have required a lot of additional data and added a lot of complexity.

### 6.2.3) Evaluation

To validate the BTAM the modelled counts on road segments were compared to observed counts from automatic bicycle counting stations across Switzerland. The counting stations are however not distributed evenly (see Figure 10) and only 150 were available to cover all of Switzerland. With only 35 counters, rural areas are especially underrepresented. This misrepresentation can potentially have an impact on the evaluation of the model quality by skewing the results towards areas with more counters. To enable the use of more counting stations, some missing data was imputed. Additionally, the annual average weekday traffic AAWT for stations from the cantons of Ticino and Zurich had to be estimated using annual average daily traffic AADT. While these measures inherently introduce error, it is likely much smaller than those of the BTAM and therefore does not significantly influence the evaluation results. Another issue with counting stations and the model is that the model cannot represent all factors influencing cycling. Weather for example has a strong influence on cycling (Fyhri, Heinen, Fearnley, & Sundfør, 2017) but is not included in the NPVM (Bundesamt für Raumentwicklung ARE, 2020b) and therefore not in the BTAM. Finally, the use of AAWT instead of AADT results in a focus on commuter traffic, as leisure traffic is more prevalent on weekends (Stiftung SchweizMobil, 2018). This was not avoidable, as the NPVM was calculated using AAWT and not transformed to AADT for bicycles (Bundesamt für Raumentwicklung ARE, 2020b). This is likely to have improved the results of the BTAM, routing engines are better at predicting commuter traffic than leisure traffic, where scenic routes are often preferred (Prato, Halldórsdóttir, & Nielsen, 2018).

The second evaluation approach used GEH-value and SQV, which are commonly used in traffic planning and recommended by the Swiss Association of Traffic Engineers and Traffic Experts SVI (Schweizerische Vereinigung der Verkehrsingenieure und Verkehrsexperten SVI, 2019). As mentioned before, the value range of 2'000 to 50'000 from the GEH-values does not match with the observed or modelled bicycle traffic (Bundesamt für Raumentwicklung ARE, 2020b). The SQV does solve this problem by using a scaling factor. The issue of smaller counts resulting in better evaluations by these measures does however persist (Friedrich, Pestel, Schiller, & Simon, 2019). For the evaluation of the BTAM with the same scaling factor for urban and rural stations, this resulted in better results for rural counting stations than for urban counting stations, as the latter have generally higher traffic volumes. This result is contrary to the observations from plotting the data and using linear regression. Using different scaling factors for urban and rural stations gave results that matched up with the linear regression. There are however urban counting stations with traffic volumes as low as some of the rural ones. These are still benefitting from the high scaling factor and being evaluated too optimistically.

# 7) Conclusion

The aim of this thesis was to create a bicycle traffic assignment model with a high network density. To map the trips onto the road network, the bicycle distribution from the Swiss national model for passenger traffic NPVM for 2017 and 2050 was used in combination with the road network from OpenStreetMap OSM and the routing engine Valhalla. The start and end points of the routes were determined using the disaggregation and jittering approach from Lovelace et al. (2022), weighted by the population and full-time equivalents of the area. The result was a map with the estimated bicycle traffic on road segments in all of Switzerland for both 2017 and 2050. The main goal was achieved, as the model resulted in a traffic pattern utilizing almost all roads within settlements.

A comparison of the model with observations from 150 bicycle counting stations across Switzerland was performed to assess the quality of the model. This analysis consisted of both a linear regression and the calculation of GEH-values and SQV. The traffic volumes modelled in urban areas matched up with the observations to an acceptable degree. In rural areas however, the model performed badly.

The thesis provides a methodology to create traffic assignment models for bicycles that utilise the entire road network, instead of focussing on major roads only like the NPVM bicycle traffic assignment model did. Additionally, only freely available software and data were used and it is possible to modify the road network. These characteristics make the model useful in spatial and traffic planning for bicycles and enable the modelling of possible infrastructure changes.

## 7.1) Future Work

Multiple different options for future work based on this thesis exist:

Firstly, the model could be improved upon. Using a routing engine that can model routes preferred by leisure cyclists may improve the model outside of settlements. This could be combined with the use of different routing parameter sets to model route choices of different types of cyclists. To reduce the time the model requires to run, the thresholds used during jittering and disaggregation could be optimized.

Secondly, the model could be redone when the next iteration of the NPVM becomes available. This would allow the use of a newer and improved OSM road network. As the number of bicycle counting stations has increased over the past years, the analysis would also benefit from such work.

Thirdly, the idea of the methodology could be applied to other countries. However, given the data requirements this may require extensive modifications.

And finally, the model could be applied and compared to other tools available for bicycle traffic planning.

# References


Albers, J. (2024, 01 12). *personal communication*.

Baehler, D., Marincek, D., & Rérat, P. (2018). *Les comptages vélos dans les villes suisses.* Université de Lausanne, Institut de géographie et durabilité.

Baggenstoss, M. (2024, 01 31). *personal communication*.

Barrington-Leigh, C., & Millard-Ball, A. (2017). The world's user-generated road map is more than 80% complete. *PLoS ONE, 12*(8). doi:10.1371/journal.pone.0180698

Beitel, D., & Miranda-Moreno, L. F. (2016). Methods for Improving and Automating the Estimation of Average Annual Daily Bicyclists. *Transportation Research Board 95th Annual Meeting.* Washington DC, United States.

Beitel, D., McNee, S., McLaughlin, F., & Miranda-Moreno, L. F. (2018). Automated Validation and Interpolation of Long-Duration Bicycle Counting Data. *Transportation Research Record, 2672*(73), 75-86. doi:10.1177/0361198118783123

Bernardi, S., La Paix Puello, L., & Geurs, K. (2018). Modelling route choice of Dutch cyclists using smartphone data. *Journal of Transport and Land Use, 11*(1), 883-900. doi:10.5198/jtlu.2018.1143

Broach, J., Dill, J., & Gliebe, J. (2012). Where do cyclists ride? A route choice model developed with revealed preference GPS data. *Transportation Research Part A, 46*, 1730-1740. doi:10.1016/j.tra.2012.07.005

Bundesamt für Landestopografie swisstopo. (2020, 09 08). *Bundesamt für Landestopografie swisstopo.* Retrieved 02 08, 2024, from swissTLMRegio: https://www.swisstopo.admin.ch/de/landschaftsmodell-swisstlmregio#Das-kleinmassst%C3%A4bliche-digitale-Landschaftsmodell-der-Schweiz

Bundesamt für Landestopografie swisstopo. (2023a, 08 15). *Bundesamt für Landestopografie swisstopo.* Retrieved 03 20, 2024, from swissBOUNDARIES3D 2017: https://www.swisstopo.admin.ch/de/landschaftsmodell-swissboundaries3d#dokumente

Bundesamt für Landestopografie swisstopo. (2023b). *swissTLMRegio Produktinformation.*

Bundesamt für Landestopografie swisstopo. (2024). *Geoportal des Bundes*. Retrieved 2024, from Kartenviewer: map.geo.admin.ch

Bundesamt für Raumentwicklung ARE. (2017). *NPVM 2016: Zonenstruktur und Verkehrsnetze.* Bundesamt für Raumentwicklung ARE.

Bundesamt für Raumentwicklung ARE. (2019a, 08 28). *opendata.swiss.* Retrieved 10 28, 2023, from Verkehrszonen in der Schweiz: https://opendata.swiss/de/dataset/vm-uvek-zones-2017/resource/29b98f2c-42f2-4e72-b8b1-a39500ed0ad0

Bundesamt für Raumentwicklung ARE. (2019b, 12 19). *opendata.swiss.* Retrieved 08 06, 2024, from Verkehrszonen im Ausland: https://opendata.swiss/de/dataset/vm-uvek-zones-2017/resource/ccdcc222-2b77-4f65-a054-2bd622145e4e

Bundesamt für Raumentwicklung ARE. (2020a, 5 25). *opendata.swiss.* Retrieved 10 31, 2023, from Zentroide der Verkehrszonen in der Schweiz: https://opendata.swiss/de/dataset/vm-uvek-zones-2017/resource/c295b850-3e3f-4299-b06e-c6e06d56f685

Bundesamt für Raumentwicklung ARE. (2020b). *Modelletablierung Nationales Personenverkehrsmodell (NPVM) 2017.* Bundesamt für Raumentwicklung ARE.

Bundesamt für Raumentwicklung ARE. (2020c). *Nationales Personenverkehrsmodell NPVM 2017.*

Bundesamt für Raumentwicklung ARE. (2022a, 09 14). *data.geo.admin.ch.* Retrieved 09 10, 2024, from Load (vehicles) on the Swiss road network (passengers and freight): https://data.geo.admin.ch/browser/index.html#/collections/ch.are.belastung-personenverkehr-strasse

Bundesamt für Raumentwicklung ARE. (2022b). *Schweizerische Verkehrsperspektiven 2050.*

Bundesamt für Raumentwicklung ARE. (n.d.). *Bundesamt für Raumentwicklung ARE*. Retrieved 08 31, 2024, from Verkehrsperspektiven 2050: Szenarien und Methodik: https://www.are.admin.ch/are/de/home/mobilitaet/grundlagen-und-daten/verkehrsperspektiven/szenarien-methodik.html

Bundesamt für Statistik BFS. (2014). *Raum mit städtischem Charakter der Schweiz 2012.* Neuchâtel.

Bundesamt für Statistik BFS. (2017a, 05 04). *Statistischer Atlas der Schweiz.* Retrieved 01 03, 2024, from Stadt/Land-Typologie 2012: https://www.atlas.bfs.admin.ch/maps/13/de/12362_12361_3191_227/20389.html

Bundesamt für Statistik BFS. (2017b, 05 16). *Bundesamt für Statistik BFS.* Retrieved 07 12, 2024, from Tagesdistanz, Tagesunterwegszeit und Anzahl Etappen mit dem Langsamverkehr nach Wochentag, Jahreszeit und Bevölkerungsgruppen: https://www.bfs.admin.ch/bfs/de/home/statistiken/mobilitaet-verkehr/personenverkehr/verkehrsverhalten/tabellen-2015/hauptbericht.assetdetail.2503202.html

Bundesamt für Statistik BFS. (2017c). *Raumgliederungen der Schweiz - Gemeindetypologie und Stadt/Land-Typologie 2012.* Neuchâtel.

Bundesamt für Statistik BFS. (2017d). *Verkehrsverhalten der Bevölkerung - Ergebnisse des Mikrozensus Mobilität und Verkehr 2015.* Neuchâtel.

Bundesamt für Statistik BFS. (2018a, 10 04). *Bundesamt für Statistik.* Retrieved 10 28, 2023, from Statistik der Bevölkerung und Haushalte (STATPOP), Geodaten 2017: https://www.bfs.admin.ch/bfs/de/home/dienstleistungen/geostat/geodaten-bundesstatistik/gebaeude-wohnungen-haushalte-personen/bevoelkerung-haushalte-ab-2010.assetdetail.6248347.html

Bundesamt für Statistik BFS. (2018b). *Statistik der Bevölkerung und der Haushalte (STATPOP) ab 2010.*

Bundesamt für Statistik BFS. (2021, 11 25). *Bundesamt für Statistik.* Retrieved 10 28, 2023, from Statistik der Unternehmensstruktur (STATENT), Beschäftigte und Arbeitsstätten: Geodaten 2017: https://www.bfs.admin.ch/bfs/de/home/dienstleistungen/geostat/geodaten-bundesstatistik/arbeitsstaetten-beschaeftigung/statistik-unternehmensstruktur-statent-ab-2011.assetdetail.20124095.html

Bundesamt für Statistik BFS. (2023a). *Geodaten in Hektarauflösung zur Statistik der Unternehmensstruktur (STATENT).* Neuchâtel.

Bundesamt für Statistik BFS. (2023b). *Mobilitätsverhalten der Bevölkerung - Ergebnisse des Mikrozensus Mobilität und Verkehr 2021.* Neuchâtel.

Bundesamt für Statistik BFS. (2024, 03 21). *Bundesamt für Statistik*. Retrieved 04 27, 2024, from Räumliche Typologien: https://www.bfs.admin.ch/bfs/de/home/statistiken/querschnittsthemen/raeumliche-analysen/raeumliche-gliederungen/raeumliche-typologien.html

Bundesamt für Strassen ASTRA. (2018). *Qualitätssicherung von Verkehrsmodellberechnungen.*

Cairns, S., Behrendt, F., Raffo, D., Beaumont, C., & Kiefer, C. (2017). Electrically-assisted bikes: Potential impacts on travel behaviour. *Transportation Research Part A, 103*, 327-342. doi:10.1016/j.tra.2017.03.007

Chicco, D., Warrens, M. J., & Jurman, G. (2021). The coefficient of determination R-squared is more informative than SMAPE, MAE, MAPE, MSE and RMSE in regression analysis evaluation. *PeerJ Computer Sciense*. doi:10.7717/peerj-cs.623

de Hartog, J. J., Boogaard, H., Nijland, H., & Hoek, G. (2010). Do the Health Benefits of Cycling Outweigh the Risks? *Environmental Health Perspectives, 118*(8), 1109-1116. doi:10.1289/ehp.0901747

D'Errico, A. (2024, 01 30). *personal communication*.

Dill, J., & McNeil, N. (2013). Four Types of Cyclists? Examination of Typology for Better Understanding of Bicycling Behavior and Potential. *Transportation Research Record: Journal of the Transportation Research Board, 2387*, 129-138. doi:10.3141/2387-15

docker. (n.d. a). *docker*. Retrieved 03 09, 2024, from Docker Desktop: https://www.docker.com/products/docker-desktop/

docker. (n.d. b). *docker*. Retrieved 06 27, 2024, from What is a container?: https://www.docker.com/resources/what-container/

Eco-Counter. (2024a). *Eco-Counter*. Retrieved 01 03, 2024, from Automatische Velozählstellen in Winterthur – Frohbergstrasse: http://winterthur.eco-counter.com/

Eco-Counter. (2024b). *Eco-Counter*. Retrieved 01 05, 2024, from Gemeinde Kriens: https://data.eco-counter.com/ParcPublic/?id=4951#

Eidgenössisches Departement für Umwelt, Verkehr, Energie und Kommunikation UVEK. (2019, 08 28). *zenodo.* Retrieved 10 27, 2023, from Verkehrsmodellierung im UVEK; Daten Zustand 2017: https://zenodo.org/records/7777651

Eidgenössisches Departement für Umwelt, Verkehr, Energie und Kommunikation UVEK. (n.d.). Velo Nachfragematrizen BASIS 2050 DWV. *personal communication with Raphaël Ancel*. Retrieved 01 09, 2024

El Esawey, M. (2017). Estimation of Daily Bicycle Traffic Volumes Using Spatiotemporal Relationships. *Journal of Transportation Engineering, Part A: Systems, 143*(11). doi: 10.1061/JTEPBS.0000089

El Esawey, M. (2018a). Daily Bicycle Traffic Volume Estimation: Comparison of Historical Average and Count Models. *Journal of Urban Planning and Development, 144*(2). doi: 10.1061/(ASCE)UP.1943-5444.0000443

El Esawey, M. (2018b). Impact of data gaps on the accuracy of annual and monthly average daily bicycle volume calculation at permanent count stations. *Computers, Environment and Urban Systems, 70*, 125-137. doi:10.1016/j.compenvurbsys.2018.03.002

El Esawey, M. (2023). An Approach for Detecting Data Anomalies at Permanent Cycling Count Stations. *Journal of Transportation Engineering, Part A: Systems, 149*(1). doi:10.1061/JTEPBS.TEENG-6985

Esri. (n.d.). *ArcUser Online*. Retrieved 06 27, 2024, from Measuring in Arc-Seconds: https://www.esri.com/news/arcuser/0400/wdside.html

Ferster, C., Fischer, J., Manaugh, K., Nelson, T., & Winters, M. (2020). Using OpenStreetMap to inventory bicycle infrastructure: A comparison with open data from cities. *International Journal of Sustainable Transportation, 14*(1), 64-73. doi:10.1080/15568318.2018.1519746

FOSSGIS e.V. (2024, 06 26). *OpenStreetMap*. Retrieved 06 27, 2024, from Valhalla FOSSGIS Server Demo App: https://valhalla.openstreetmap.de/

Friedrich, M., & Galster, M. (2009). Methods for Generating Connectors in Transport Planning Models. *Journal of the Transportation Research Board, 2132*, 133-142. doi:10.3141/2132-15

Friedrich, M., Pestel, E., Schiller, C., & Simon, R. (2019). Scalable GEH: A Quality Measure for Comparing Observed and Modeled Single Values in a Travel Demand Model Validation. *Transport Research Record, 2673*(4), 722-732. doi:10.1177/0361198119838849

Fyhri, A., Heinen, E., Fearnley, N., & Sundfør, H. B. (2017). A push to cycling—exploring the e-bike's role in overcoming barriers to bicycle use with a survey and an intervention study. *International Journal of Sustainable Transportation, 11*(9), 681-695. doi:10.1080/15568318.2017.1302526

Gemeinde Wil. (n.d.). *Geoportal Wil*. Retrieved 01 30, 2024, from Strategie Velo Gde Wil: https://www.geoportal.ch/wil/map/2314?y=2721268.05&x=1258227.84&scale=10000&rotation=0

Geofabrik. (2017, 01 02). *Switzerland.* Retrieved 01 02, 2024, from Geofabrik downloads: switzerland-170101.osm.pbf: https://download.geofabrik.de/europe/switzerland.html

gGmbH, H. (2023, 11 20). *Github*. Retrieved 01 05, 2023, from Openrouteservice: https://giscience.github.io/openrouteservice/documentation/Documentation

GIS-OPS. (2021). *GIS-OPS*. Retrieved 06 27, 2024, from https://gis-ops.com/

GIS-OPS. (2024, 03 07). *Github*. Retrieved 03 09, 2024, from gis-ops/docker-valhalla: https://github.com/gis-ops/docker-valhalla

Goodchild, M. F. (2007). Citizens as sensors: the world of volunteered geography. *GeoJournal, 69*, 211-221. doi:10.1007/s10708-007-9111-y

Goodman, A. (2019, 07 27). *PCT Blog*. Retrieved 06 25, 2024, from New PCT Schools layer scenario: Go Cambridge: https://blog.pct.bike/2019/07/27/go-cambridge-a-new-scenario-in-the-schools-layer/

Goodman, A., Fridman Rojas, I., Woodcock, J., Aldred, R., Berkoff, N., Morgan, M., . . . Lovelace, R. (2019). Scenarios of cycling to school in England, and associated health and carbon impacts: Application of the 'Propensity to Cycle Tool'. *Journal of Transport & Health, 12*, 263-278. doi:10.1016/j.jth.2019.01.008

Google. (2024, 06 20). *Google Maps Platform*. Retrieved 06 26, 2024, from Encoded Polyline Algorithm Format: https://developers.google.com/maps/documentation/utilities/polylinealgorithm

Google. (n.d.). *Google Maps*. Retrieved 01 07, 2024, from Google Maps: www.google.com/maps

Gössling, S., & Choi, A. S. (2015). Transport transitions in Copenhagen: Comparing the cost of cars and bicycles. *Ecological Economics, 113*, 106-113. doi:10.1016/j.ecolecon.2015.03.006

Gössling, S., & McRae, S. (2022). Subjectively safe cycling infrastructure: New insights for urban designs. *Journal of Transport Geography*. doi:10.1016/j.jtrangeo.2022.103340

Ground Zero Communications AB. (2024). *OSM-Boundaries*. Retrieved 08 27, 2024, from Map: https://osm-boundaries.com/map

Hardinghaus, M., & Weschke, J. (2022). Attractive infrastructure for everyone? Different preferences for route characteristics among cyclists. *Transportation Research Part D, 111*. doi:10.1016/j.trd.2022.103465

Hart, P. E., Nilsson, N. J., & Raphael, B. (1968). A Formal Basis for the Heuristic Determination of Minimum Cost Paths. *IEEE Transactions of Systems Science and Cybernetics, 4*(2), 100-107.

Hochmair, H. H., Zielstra, D., & Neis, P. (2015). Assessing the Completeness of Bicycle Trail and Lane Features in OpenStreetMap for the United States. *Transactions in GIS, 19*(1), 63-81. doi:10.1111/tgis.12081

IDE, S. (2023). *spyder (version 5.4.3)*. Retrieved from https://www.spyder-ide.org/

Jafari, E., Gemar, M. D., Ruiz Juri, N., & Duthie, J. (2015). Investigation of Centroid Connector Placement for Advanced Traffic Assignment Models with Added Network Detail. *Journal of the Transportation Research Board, 2498*, 19-26. doi:10.3141/2498-03

Jansen, F., & Custódio, B. M. (2024). *PyPi.* Retrieved from polyline (version 2.0.2): https://pypi.org/project/polyline/

Johansson, C., Lövenheim, B., Schantz, P., Wahlgren, L., Almström, P., Markstedt, A., . . . Sommar, J. N. (2017). Impacts on air pollution and health by changing commuting from car to bicycle. *Science of the Total Environment, 584-585*, 55-63. doi:10.1016/j.scitotenv.2017.01.145

Kanton Basel-Landschaft. (2018, 01 10). *Basel Landschaft.* Retrieved 01 05, 2024, from Verkehrsstatistik 2017: https://www.baselland.ch/politik-und-behorden/direktionen/bau-und-umweltschutzdirektion/tiefbauamt/kennzahlen/verkehrserhebungen/

Kanton Basel-Landschaft. (n.d.). *GeoView BL*. Retrieved 01 05, 2024, from Zählstellen Velo: https://geoview.bl.ch/?map_x=2615775&map_y=1255190.1523252&map_zoom=2&baselayer_opacity=100&baselayer_ref=grundkarte_sw&tree_group_layers_Verkehr=verkehrszaehlstellen_velo%2Cverkehrszaehlstellen_miv&tree_groups=Verkehr

Kanton Basel-Stadt. (2013). *Übersichtsplan A3: Dauerzählstellen Velo.* Bau- und Verkehrsdepartement.

Kanton Basel-Stadt. (2024, 01). *Open BS*. Retrieved 01 03, 2024, from Verkehrszähldaten Velos und Fussgänger: https://data.bs.ch/explore/dataset/100013/information/?sort=datetimefrom&calendarview=month

Kanton Luzern. (2021). *Resultate der automatischen Velozählungen 2019 - 2020.*

Kanton Schaffhausen. (2023). *Geoportal Schaffhausen*. Retrieved from Verkehrszählstellen Velo: https://map.geo.sh.ch/geoportal/legend?project=Geoportal%20Schaffhausen&legend=Legende&rotation=0.00&scale=152993&center=2683620,1281486

Kanton Zürich. (2023). *GIS-ZH*. Retrieved 01 08, 2024, from Verkehrsmessstellen: https://maps.zh.ch/

Lee, R. J., Sener, I. N., & Jones, S. N. (2017). Understanding the role of equity in active transportation planning in the United States. *Transport Reviews, 37*(2), 211-226. doi:10.1080/01441647.2016.1239660

Lindsay, G., Macmillan, A., & Woodward, A. (2011). Moving urban trips from cars to bicycles: impact on health and emissions. *Australian and New Zealand Journal of Public Health, 35*(1), 54-60. doi:10.1111/j.1753-6405.2010.00621.x

Lovelace, R., & Morgan, M. (2023a, 12 21). *NPT Scotland*. Retrieved 06 25, 2024, from Network Planning Tool: https://www.npt.scot/#13.25/55.94857/-3.17858

Lovelace, R., & Morgan, M. (2023b, 12 21). *NPT Scotland*. Retrieved 06 24, 2024, from NPT Manual: www.npt.scot/manual

Lovelace, R., Félix, R., & Carlino, D. (2022). Jittering: A Computationally Efficient Method for Generating Realistic Route Networks from Origin-Destination Data. *Transport Findings*. doi:10.32866/001c.33873

Lovelace, R., Goodman, A., Aldred, R., Berkoff, N., Abbas, A., & Woodcock, J. (2017). The Propensity to Cycle Tool: An open source online system for sustainable transport planning. *The Journal of Transport and Land Use, 10*(1), 505-528. doi:10.5198/jtlu.2016.862

Ludwig, I., Voss, A., & Krause-Traudes, M. (2011). A Comparison of the Street Networks of Navteq and OSM in Germany. In S. Geertman, W. Reinhardt, & F. Toppen (Eds.), *Advancing Geoinformation Science for a Changing World* (pp. 65-84). Springer-Verlag. doi:10.1007/978-3-642-19789-5_4

Luternauer, M. (2024, 01 15). *personal communication*.

Macmillan, A., Connor, J., Witten, K., Kearns, R., Rees, D., & Woodward, A. (2014). The Societal Costs and Benefits of Commuter Bicycling: Simulating the Effects of Specific Policies Using System Dynamics Modeling. *Environmental Health Perspectives, 122*(4), 335-344. doi:10.1289/ehp.1307250

Mapzen. (2019, 01 29). *Mapzen*. Retrieved 06 27, 2024, from Mapzen is now a Linux Foundation project!: https://www.mapzen.com/blog/mapzen-is-now-a-linux-foundation-project/

Meister, A., Felder, M., Schmid, B., & Axhausen, K. W. (2023). Route choice modeling for cyclists on urban networks. *Transportation Research Part A, 173*. doi:10.1016/j.tra.2023.103723

Morgan, M., & Lovelace, R. (2021). Travel flow aggregation: Nationally scalable methods for interactive and online visualisation of transport behaviour at the road network level. *Urban Analytics and City Science, 48*(6), 1684-1696. doi:10.1177/2399808320942779

Mueller, N., Rojas-Rueda, D., Cole-Hunter, T., de Nazelle, A., Dons, E., Gerike, R., . . . Nieuwenhuijsen, M. (2015). Health impact assessment of active transportation: A systematic review. *Preventive Medicine, 76*, 103-114. doi:10.1016/j.ypmed.2015.04.010

myswitzerland. (n.d.). *switzerland*. Retrieved 09 01, 2024, from Grimselpass: https://www.myswitzerland.com/de-de/erlebnisse/grimsel-pass/

NASA. (n.d.). *Earthdata*. Retrieved 06 27, 2024, from Shuttle Radar Topography Mission (SRTM): https://www.earthdata.nasa.gov/sensors/srtm

Neis, P., Zielstra, D., & Zipf, A. (2012). The Street Network Evolution of Crowdsourced Maps: OpenStreetMap in Germany 2007–2011. *Future Internet, 4*, 1-21. doi:10.3390/fi4010001

Nosal, T. (2014). *Improving the accuracy of bicycle AADT estimation: temporal patterns, weather and bicycle AADT estimation methods.* Master's Thesis, McGill University, Department of Civil Engineering and Applied Mechanics, Montreal.

Nosal, T., Miranda-Moreno, L. F., & Krstulic, Z. (2014). Incorporating weather: a comparative analysis of Average Annual Daily Bicyclist estimation methods. *Transportation Research Board Annual Meeting.*

NumFOCUS. (2023). *pandas (version 2.0.3).* Retrieved from https://pandas.pydata.org/

NumPy team. (2023). *NumPy (version 1.24.3).* Retrieved from https://numpy.org/

Nuttall, S., & Lucas-Smith, M. (n.d.). *CycleStreets.net*. Retrieved 01 05, 2024, from https://www.cyclestreets.net/

Oja, P., Titze, S., Bauman, A., de Geus, B., Krenn, P., Reger-Nash, B., & Kohlberger, T. (2011). Health benefits of cycling: a systematic review. *Scandinavian Journal of Medicine and Science in Sports, 21*, 496-509. doi:10.1111/j.1600-0838.2011.01299.x

OpenStreetMap. (2023, 12 25). *OpenStreetMap Wiki*. Retrieved 01 05, 2024, from List of OSM-based services: https://wiki.openstreetmap.org/wiki/List_of_OSM-based_services#Routing

OpenStreetMap. (2024a, 02 17). *OpenStreetMap Wiki*. Retrieved 05 16, 2024, from Tag:highway=service: https://wiki.openstreetmap.org/wiki/Tag:highway%3Dservice

OpenStreetMap. (2024b, 02 18). *OpenStreetMap Wiki*. Retrieved 04 19, 2024, from Key:highway: https://wiki.openstreetmap.org/wiki/Key:highway

OpenStreetMap. (2024c, 02 25). *OpenStreetMap Wiki*. Retrieved 06 15, 2024, from Tags: https://wiki.openstreetmap.org/wiki/Tags

OpenStreetMap. (2024d, 03 09). *OpenStreetMap Wiki*. Retrieved 04 19, 2024, from Key:vehicle: https://wiki.openstreetmap.org/wiki/Key:vehicle

OpenStreetMap. (2024e, 03 11). *OpenStreetMap Wiki*. Retrieved 03 16, 2024, from Key:surface: https://wiki.openstreetmap.org/wiki/Key:surface

OpenStreetMap. (2024f, 03 20). *OpenStreetMap Wiki*. Retrieved 06 15, 2024, from Elements: https://wiki.openstreetmap.org/wiki/Elements

OpenStreetMap. (2024g, 03 25). *OpenStreetMap Wiki*. Retrieved 06 15, 2024, from Node: https://wiki.openstreetmap.org/wiki/Node

OpenStreetMap. (2024h, 04 01). *OpenStreetMap Wiki*. Retrieved 04 06, 2024, from About OpenStreetMap: https://wiki.openstreetmap.org/wiki/About_OpenStreetMap

OpenStreetMap. (2024i, 05 08). *OpenStreetMap Wiki*. Retrieved 05 16, 2024, from Tag:highway=living_street: https://wiki.openstreetmap.org/wiki/Tag:highway%3Dliving_street

OpenStreetMap. (2024j, 06 15). *OpenStreeetMap Wiki*. Retrieved 06 15, 2024, from Way: https://wiki.openstreetmap.org/wiki/Way

OpenStreetMap. (2024k). *OpenStreetMap*. Retrieved 2024, from Map: openstreetmap.org

Ortúzar, J. d., & Willumsen, L. G. (2011). *Modelling Transport* (4th ed.). Chichester: John Wiley & Sons, Ltd.

Osmcode. (2023). *Osmcode.* Retrieved from PyOsmium (version 3.7.0): https://osmcode.org/pyosmium/

Piñeiro, G., Perelman, S., Guerschman, J. P., & Paruelo, J. M. (2008). How to evaluate models: Observed vs. predicted or predicted vs. observed? *Ecological Modelling, 216*, 316-322. doi:10.1016/j.ecolmodel.2008.05.006

Prato, C. G., Halldórsdóttir, K., & Nielsen, O. A. (2018). Evaluation of land-use and transport network effects on cyclists' route choices in the Copenhagen Region in value-of-distance space. *International Journal of Sustainable Transportation, 12*(10), 770-781. doi:10.1080/15568318.2018.1437236

Python Software Foundation. (2023). *python (version 3.11.5)*. Retrieved from https://www.python.org/

QGIS. (2024). *QGIS (Version 3.28.15 Firenze).* Retrieved from https://qgis.org/

Rabl, A., & de Nazelle, A. (2012). Benefits of shift from car to active transport. *Transport Policy, 19*, 121-131. doi:10.1016/j.tranpol.2011.09.008

Reitz, K. (2023). *Requests (version 2.31.0).* Retrieved from https://requests.readthedocs.io/en/latest/

Repubblica e Cantone Ticino. (n.d. a). *Repubblica e Cantone Ticino*. Retrieved 01 08, 2024, from Rapporto 2017 documento di dettaglio: https://www4.ti.ch/dt/dstm/sm/temi/traffico-stradale/per-saperne-di-piu/rapporti-e-studi

Repubblica e Cantone Ticino. (n.d. b). *Repubblica e Cantone Ticino*. Retrieved 01 08, 2024, from Ubicazione e distribuzione: https://www4.ti.ch/dt/dstm/sm/temi/traffico-stradale/conteggi/mobilita-ciclabile/ubicazione-dei-posti

Rérat, P. (2021). The rise of the e-bike: Towards an extension of the practice of cycling? *Mobilities, 16*(3), 423-439. doi:10.1080/17450101.2021.1897236

Schepers, P., Helbich, M., Hagenzieker, M., de Geus, B., Dozza, M., Agerholm, N., . . . Aldred, R. (2021). The development of cycling in European countries since 1990. *European Journal of Transport and Infrastructure Research, 21*(2), 41-70. doi:10.18757/ejtir.2021.21.2.5411

Schnabel, W., & Lohse, D. (2011). *Grundlagen der Straßenverkehrstechnik und der Verkehrsplanung* (3rd ed., Vol. Band 2: Verkehrsplanung). (DIN Deutsches Institut für Normung e.V., Ed.) Berlin and Bonn: Beuth Verlag GmbH and Kirschbaum Verlag GmbH.

Schweizerische Vereinigung der Verkehrsingenieure und Verkehrsexperten SVI. (2019). *Leitfaden 2019/01: Qualitätssicherung von Verkehrsmodellen.*

scikit-learn. (2024). *scikit-learn (version 1.5.0).* Retrieved from https://scikit-learn.org/stable/index.html#

SciPy. (2023). *SciPy (version 1.11.1).* Retrieved from https://scipy.org/

Stadt Bern. (2018). *Velodaten Bern 2014 - 2017.* Direktion für Tiefbau, Verkehr und Stadtgrün, Verkehrsplanung, Bern.

Stadt Bern. (n.d.). *Stadt Bern*. Retrieved 01 03, 2024, from Verkehrsdaten: https://map.bern.ch/stadtplan/?grundplan=Stadtplan_farbig_Geoportal|Stadtplan_farbig_Extern_Region&koor=2601585,1200091&zoom=1&hl=0&layer=Verkehrsdaten

Stadt Biel. (2020). *Monitoring de la mobilite 2019.* Biel.

Stadt St. Gallen. (2024). *Open Data St. Gallen*. Retrieved 01 03, 2024, from Velozählungen Stadt St.Gallen ab 2016: https://daten.stadt.sg.ch/explore/dataset/velozahlungen-stadt-stgallen/information/?disjunctive.bezeichnung&disjunctive.arbeitstag&disjunctive.wochentag&disjunctive.tag_nr&sort=-datum&refine.datum=2017

Stadt Zürich. (2024a, 02 06). *Stadt Zürich*. Retrieved 02 23, 2024, from Standorte der automatischen Fuss- und Velozählungen: https://www.stadt-zuerich.ch/geodaten/download/Standorte_der_automatischen_Fuss__und_Velozaehlungen

Stadt Zürich. (2024b). *Stadt Zürich Open Data*. Retrieved 01 03, 2024, from Daten der automatischen Fussgänger- und Velozählung - Viertelstundenwerte: https://data.stadt-zuerich.ch/dataset/ted_taz_verkehrszaehlungen_werte_fussgaenger_velo

Stadt Zürich. (n.d.). *Stadt Zürich Tiefbau- und Entsorgungsdepartement*. Retrieved 01 07, 2024, from Online Stadtplan und Routenplaner: https://www.stadt-zuerich.ch/ted/de/index/stadtverkehr2025/downloads_bestellungen/downloads.html

Steiner, Y. (2024, 03 28). *personal communication*.

Stenzel, I. (2024, 01 15). *personal communication*.

Stiftung SchweizMobil. (2009). *Stiftung SchweizMobil*. Retrieved 07 02, 2024, from Geschichte: https://www.schweizmobil.org/schweizmobil/geschichte.html

Stiftung SchweizMobil. (2018). *Velo-Zähldatenzentrale - 2017 - Auswertung.* Bern.

Stiftung SchweizMobil. (n.d.). *SchweizMobil*. Retrieved 07 02, 2024, from Seen-Route: https://schweizmobil.ch/de/veloland/route-9

Stiftung SchweizMobil, Bundesamt für Strassen ASTRA. (2023). *Velo-Zähldatenzentrale - Auswertung 2022 - Teil 1: Zusammenfassung.* Bern.

The Matplotlib development team. (2023). *Matplotlib (version 3.7.2).* Retrieved from https://matplotlib.org/

Toljic, M., Brezina, T., & Emberger, G. (2021). Influence of surface roughness on cyclists' velocity choices. *Proceedings of the Institution of Civil Engineers – Municipal Engineer, 174*(1), 2-13. doi:10.1680/jmuen.18.00058

Tordai, D., Munkácsy, A., Andrejszki, T., & Hauger, G. (2023). The real value of cycling. *Transportation Research Procedia , 72*, 2896-2903. doi:10.1016/j.trpro.2023.11.835

Valhalla. (2023, 11 28). *Github*. Retrieved 02 05, 2024, from Valhalla Docs: https://valhalla.github.io/valhalla/

Vierø, A. R., Vybornova, A., & Szell, M. (2024). How Good Is Open Bicycle Network Data? A Countrywide Case Study of Denmark. *Geographical Analysis*. doi:10.1111/gean.12400

Watkins, D. (n.d.). *dwtkns*. Retrieved 03 10, 2024, from 30-Meter SRTM Tile Downloader: https://dwtkns.com/srtm30m/

Whitaker, J. (2023). *PyPi.* Retrieved from pyproj (version 3.6.1): https://pypi.org/project/pyproj/

Wolfram. (n.d.). *WolframAlpha*. Retrieved 07 14, 2024, from WolframAlpha: https://www.wolframalpha.com/

Woodcock, J., Goodman, A., Lovelace, R., Aldred, R., Abbas, A., Berkoff, N., & Morgan, M. (n.d. a). *Propensity to Cycle Tool*. Retrieved 06 25, 2024, from About the Propensity to Cycle Tool: https://www.pct.bike/about.html

Woodcock, J., Goodman, A., Lovelace, R., Aldred, R., Abbas, A., Berkoff, N., & Morgan, M. (n.d. b). *Propensity to Cycle Tool*. Retrieved 06 25, 2024, from Map - Oxfordshire: https://www.pct.bike/m/?r=oxfordshire

Zermatt Tourismus. (n.d.). *Zermatt*. Retrieved 07 15, 2024, from Zermatt ist autofrei: https://www.zermatt.ch/nachhaltigkeit/Elektros-Autofrei-Anreise/Zermatt-ist-autofrei

Zhang, H., & Malczewski, J. (2018). Accuracy Evaluation of the Canadian OpenStreetMap Road Networks. *International Journal of Geospatial and Environmental Research, 5*(2).

# Appendix

## 1) Solving the SQV-Equation for Modelled Counts

Process of solving the SQV-equation (equation ( 6 ), (Friedrich, Pestel, Schiller, & Simon, 2019)) for modelled counts m. The transformation was aided and verified using the WolframAlpha answer engine (Wolfram, n.d.).

$$SQV = \frac{1}{1 + \sqrt{\frac{(m-c)^2}{f * c}}} \tag{6}$$

take the reciprocal and reverse the equality:

$$1 + \sqrt{\frac{(m-c)^2}{f * c}} = \frac{1}{SQV}$$

subtract *1*:

$$\sqrt{\frac{(m-c)^2}{f * c}} = \frac{1 - SQV}{SQV}$$

raise to the power of *2*:

$$\frac{(m-c)^2}{f * c} = \frac{(1 - SQV)^2}{SQV^2}$$

multiply by *f*c*:

$$(m-c)^2 = \frac{f * c * (1 - SQV)^2}{SQV^2}$$

take the square root:

$$m - c = \pm \sqrt{\frac{f * c * (1 - SQV)^2}{SQV^2}}$$

add *c*:

$$m = c \pm \sqrt{\frac{f * c * (1 - SQV)^2}{SQV^2}} \tag{10}$$

## 2) Software Used

Geographical operations and visualisations were performed using the graphical modeller in QGIS Firenze version 3.28.15 (QGIS, 2024). Python version 3.11.5 (Python Software Foundation, 2023) was used with the development environment Spyder version 5.4.3 (IDE, 2023). Within Python many external packages were used:

- Matplotlib, version 3.7.2 (The Matplotlib development team, 2023)
- Numpy, version 1.24.3 (NumPy team, 2023)
- PyOsmium, version 3.7.0 (Osmcode, 2023)
- Pandas, version 2.0.3 (NumFOCUS, 2023)
- Polyline, version 2.0.2 (Jansen & Custódio, 2024)
- Pyproj, version 3.6.1 (Whitaker, 2023)
- Requests, version 2.31.0 (Reitz, 2023)
- Scipy, version 1.11.1 (SciPy, 2023)
- Sklearn, version 1.5.0 (scikit-learn, 2024)

## 3) Classification of OSM-Ways into Bicycle Friendly, Neutral and Unfriendly

**Bicycle friendly road** (bicycle way separated from motorised traffic or on a living street)

- highway=cycleway
- highway=footway
- highway=living_street
- highway=path
- highway=pedestrian
- highway=steps
- highway=track
- Bicycle track (separated from motorised traffic)
    - highway=* + cycleway=designated
    - highway=* + cycleway=segregated
    - highway=* + cycleway=track
    - highway=* + cycleway=opposite_track
    - highway=* + cycleway=track;opposite_track

**Bicycle neutral road** (bicycle lane or low to medium traffic volume)

- highway=residential
- highway=road
- highway=service
- highway=unclassified
- Bicycle lane (not separated from motorised traffic)
- highway=* + cycleway=* (except no, none)

**Bicycle unfriendly road** (high traffic volume)

- highway=primary
- highway=primary_link
- highway=secondary
- highway=secondary_link
- highway=tertiary
- highway=tertiary_link
- highway=trunk
- highway=trunk_link

## 4) List of Sources of Counting Stations

| name | ID | data frequency | counting stations | counting stations included | urban stations included | rural stations included |
|---|---|---|---|---|---|---|
| Canton Basel Landschaft | C_BL | monthly | 5 | 4 | 4 | 0 |
| Canton Basel Stadt | C_BS | subdaily | 25 | 12 | 12 | 0 |
| Canton Geneva | C_GE | subdaily | 5 | 4 | 4 | 0 |
| Canton Sankt Gallen | C_SG | yearly | 14 | 13 | 7 | 6 |
| Canton Schaffhausen | C_SH | yearly | 3 | 3 | 1 | 2 |
| Canton Ticino | C_TI | monthly | 7 | 7 | 3 | 4 |
| Canton Zürich | C_ZH | yearly | 10 | 10 | 1 | 9 |
| Municipality Bern | M_Bern | yearly | 14 | 14 | 14 | 0 |
| Municipality Biel | M_Biel | yearly | 10 | 10 | 10 | 0 |
| Municipality Köniz | M_Köniz | yearly | 4 | 4 | 4 | 0 |
| Municipality Kriens | M_Kriens | daily | 4 | 3 | 3 | 0 |
| Municipality Luzern | M_Luzern | monthly | 12 | 12 | 12 | 0 |
| Municipality Sankt Gallen | M_StGallen | subdaily | 14 | 14 | 13 | 1 |
| Municipality Wil | M_Wil | daily | 3 | 3 | 3 | 0 |
| Municipality Winterthur | M_Winterthur | daily | 1 | 1 | 1 | 0 |
| Municipality Zurich | M_Zürich | subdaily | 21 | 21 | 21 | 0 |
| SwitzerlandMobility | SM | yearly | 43 | 15 | 2 | 13 |
| **Total** | | | **195** | **150** | **115** | **35** |

## 5) List of all Bicycle Counting Stations

| data source | station ID (from source) | station ID | east | north | direction observed | days imputed | months imputed | classifi-cation | included in analysis | reason for exclusion | AAWT observed | AAWT modelled |
|---|---|---|---|---|---|---|---|---|---|---|---|---|
| Canton Basel Landschaft | 650 | C_BL_01 | 2610120 | 1265244 | both | 0 | 2 | urban | yes | | 1737 | 2500 |
| Canton Basel Landschaft | 1050 | C_BL_02 | 2612382 | 1263376 | both | 0 | 0 | urban | yes | | 1087 | 1359 |
| Canton Basel Landschaft | 2150 | C_BL_03 | 2621405 | 1261213 | both | 0 | 0 | urban | yes | | 224 | 186 |
| Canton Basel Landschaft | 2750 | C_BL_04 | 2617843 | 1263399 | both | 0 | 4 | urban | yes | | 837 | 2007 |
| Canton Basel Landschaft | 2751 | C_BL_05 | 2619689 | 1264675 | both | 0 | 0 | urban | no | too close to border | 333 | |
| Canton Basel Stadt | 350 | C_BS_01 | 2610808 | 1268902 | both | 0 | 0 | urban | no | too close to border | 5267 | |
| Canton Basel Stadt | 352 | C_BS_02 | 2611223 | 1268324 | west | 0 | 0 | urban | yes | | 3576 | 2100 |
| Canton Basel Stadt | 354 | C_BS_03 | 2611960 | 1267510 | both | 0 | 0 | urban | yes | | 8524 | 7148 |
| Canton Basel Stadt | 403 | C_BS_04 | 2611151 | 1266828 | both | 0 | 0 | urban | yes | | 2899 | 1927 |
| Canton Basel Stadt | 659 | C_BS_05 | 2609684 | 1269581 | both | 0 | 0 | urban | no | too close to border | 316 | |
| Canton Basel Stadt | 660 | C_BS_06 | 2609310 | 1269351 | both | 0 | 0 | urban | no | too close to border | 112 | |
| Canton Basel Stadt | 901 | C_BS_07 | 2612066 | 1265994 | both | 0 | 0 | urban | yes | | 3272 | 3216 |
| Canton Basel Stadt | 902 | C_BS_08 | 2610867 | 1266582 | both | 0 | 0 | urban | yes | | 7004 | 3950 |
| Canton Basel Stadt | 903 | C_BS_09 | 2614016 | 1269097 | both | 0 | 0 | rural | no | too close to border | 2102 | |
| Canton Basel Stadt | 904 | C_BS_10 | 2611817 | 1268208 | both | 0 | 0 | urban | yes | | 1543 | 3931 |
| Canton Basel Stadt | 905 | C_BS_11 | 2610922 | 1267185 | both | 0 | 0 | urban | yes | | 2154 | 2433 |
| Canton Basel Stadt | 906 | C_BS_12 | 2609956 | 1267796 | both | 0 | 0 | urban | no | too close to border | 2181 | |

| data source | station ID (from source) | station ID | east | north | direction observed | days imputed | months imputed | classifi-cation | included in analysis | reason for exclusion | AAWT observed | AAWT modelled |
|---|---|---|---|---|---|---|---|---|---|---|---|---|
| Canton Basel Stadt | 907 | C_BS_13 | 2609443 | 1267936 | both | 0 | 0 | urban | no | too close to border | 459 | |
| Canton Basel Stadt | 908 | C_BS_14 | 2614063 | 1267937 | both | 0 | 0 | urban | no | too close to border | 1864 | |
| Canton Basel Stadt | 909 | C_BS_15 | 2609535 | 1266556 | both | 0 | 0 | urban | yes | | 1378 | 1602 |
| Canton Basel Stadt | 910 | C_BS_16 | 2609688 | 1267215 | both | 0 | 0 | urban | yes | | 1729 | 716 |
| Canton Basel Stadt | 911 | C_BS_17 | 2613448 | 1267413 | both | 0 | 0 | urban | yes | | 2058 | 896 |
| Canton Basel Stadt | 912 | C_BS_18 | 2610056 | 1269573 | both | 0 | 0 | urban | no | too close to border | 949 | |
| Canton Basel Stadt | 913 | C_BS_19 | 2609117 | 1268773 | both | 0 | 0 | urban | no | not enough valid data | | |
| Canton Basel Stadt | 914 | C_BS_20 | 2611638 | 1270570 | both | 0 | 0 | urban | no | too close to border | 1039 | |
| Canton Basel Stadt | 916 | C_BS_21 | 2611743 | 1269878 | both | 74 | 0 | urban | no | too close to border | 470 | |
| Canton Basel Stadt | 917 | C_BS_22 | 2613267 | 1267433 | south | 0 | 0 | urban | yes | | 579 | 1639 |
| Canton Basel Stadt | 918 | C_BS_23 | 2610864 | 1269466 | both | 0 | 0 | urban | no | not enough valid data | | |
| Canton Basel Stadt | 919 | C_BS_24 | 2612483 | 1267172 | both | 22 | 0 | urban | yes | | 1315 | 1572 |
| Canton Basel Stadt | 920 | C_BS_25 | 2612113 | 1266089 | both | 0 | 0 | urban | no | not enough valid data | | |
| Canton Geneva | 9000 Aire (Furet) | C_GE_01 | 2498309 | 1118116 | both | 89 | 0 | urban | yes | | 1404 | 3677 |
| Canton Geneva | 9001 Ansermet Totem | C_GE_02 | 2499722 | 1116630 | both | 1 | 0 | urban | yes | | 1674 | 1705 |
| Canton Geneva | 9002 Acacias | C_GE_03 | 2499615 | 1116522 | both | 0 | 0 | urban | yes | | 3183 | 5603 |
| Canton Geneva | 9003 Florissant | C_GE_04 | 2502505 | 1115453 | both | 0 | 0 | urban | no | too close to border | 662 | |
| Canton Geneva | 9004 Pont Butin | C_GE_05 | 2497498 | 1117633 | both | 0 | 0 | urban | yes | | 1629 | 2187 |

| data source | station ID (from source) | station ID | east | north | direction observed | days imputed | months imputed | classifi-cation | included in analysis | reason for exclusion | AAWT observed | AAWT modelled |
|---|---|---|---|---|---|---|---|---|---|---|---|---|
| Canton Sankt Gallen | 125 | C_SG_01 | 2730171 | 1243238 | both | 0 | 0 | rural | yes | | 19 | 35 |
| Canton Sankt Gallen | 200 | C_SG_02 | 2754695 | 1225947 | both | 0 | 0 | urban | no | too close to border | 311 | |
| Canton Sankt Gallen | 202 | C_SG_03 | 2753418 | 1261689 | both | 0 | 0 | urban | yes | | 598 | 265 |
| Canton Sankt Gallen | 203 | C_SG_04 | 2737106 | 1252725 | both | 0 | 0 | rural | yes | | 345 | 4 |
| Canton Sankt Gallen | 204 | C_SG_05 | 2722963 | 1258463 | both | 0 | 0 | rural | yes | | 191 | 353 |
| Canton Sankt Gallen | 205 | C_SG_06 | 2704119 | 1231233 | both | 0 | 0 | urban | yes | | 423 | 766 |
| Canton Sankt Gallen | 206 | C_SG_07 | 2738218 | 1219832 | both | 0 | 0 | rural | yes | | 114 | 41 |
| Canton Sankt Gallen | 208 | C_SG_08 | 2704608 | 1231879 | both | 0 | 0 | urban | yes | | 948 | 1922 |
| Canton Sankt Gallen | 209 | C_SG_09 | 2721323 | 1257557 | both | 0 | 0 | urban | yes | | 102 | 390 |
| Canton Sankt Gallen | 210 | C_SG_10 | 2752057 | 1212570 | both | 0 | 0 | urban | yes | | 250 | 129 |
| Canton Sankt Gallen | 211 | C_SG_11 | 2756034 | 1260683 | both | 0 | 0 | urban | yes | | 537 | 443 |
| Canton Sankt Gallen | 212 | C_SG_12 | 2747650 | 1258126 | both | 0 | 0 | urban | yes | | 497 | 325 |
| Canton Sankt Gallen | 213 | C_SG_13 | 2734257 | 1252205 | both | 0 | 0 | rural | yes | | 203 | 172 |
| Canton Sankt Gallen | 214 | C_SG_14 | 2722915 | 1221880 | both | 0 | 0 | rural | yes | | 149 | 30 |
| Canton Schaffhausen | 9983 | C_SH_01 | 2687617 | 1283214 | both | 0 | 0 | rural | yes | | 123 | 416 |
| Canton Schaffhausen | 9984 | C_SH_02 | 2688878 | 1282973 | both | 0 | 0 | urban | yes | | 159 | 332 |
| Canton Schaffhausen | 9985 | C_SH_03 | 2687646 | 1283120 | both | 0 | 0 | rural | yes | | 144 | 80 |
| Canton Ticino | 5101 | C_TI_01 | 2723833 | 1119882 | both | 0 | 1 | urban | yes | | 244 | 894 |
| Canton Ticino | 5102 | C_TI_02 | 2720901 | 1116206 | both | 0 | 1 | urban | yes | | 315 | 774 |

| data source | station ID (from source) | station ID | east | north | direction observed | days imputed | months imputed | classifi-cation | included in analysis | reason for exclusion | AAWT observed | AAWT modelled |
|---|---|---|---|---|---|---|---|---|---|---|---|---|
| Canton Ticino | 5103 | C_TI_03 | 2720122 | 1114864 | both | 0 | 0 | rural | yes | | 396 | 867 |
| Canton Ticino | 5301 | C_TI_04 | 2714698 | 1136002 | both | 0 | 0 | rural | yes | | 162 | 52 |
| Canton Ticino | 5401 | C_TI_05 | 2704037 | 1113292 | both | 0 | 2 | urban | yes | | 1480 | 1559 |
| Canton Ticino | 5402 | C_TI_06 | 2701150 | 1115278 | both | 0 | 0 | rural | yes | | 285 | 339 |
| Canton Ticino | 5403 | C_TI_07 | 2700967 | 1119297 | both | 0 | 3 | rural | yes | | 131 | 247 |
| Canton Zürich | 217 | C_ZH_01 | 2676485 | 1262503 | both | 0 | 0 | rural | yes | | 37 | 51 |
| Canton Zürich | 316 | C_ZH_02 | 2693307 | 1246934 | both | 0 | 0 | urban | yes | | 620 | 177 |
| Canton Zürich | 317 | C_ZH_03 | 2690493 | 1254553 | both | 0 | 0 | rural | yes | | 89 | 230 |
| Canton Zürich | 416 | C_ZH_04 | 2694535 | 1247785 | both | 0 | 0 | rural | yes | | 292 | 556 |
| Canton Zürich | 516 | C_ZH_05 | 2695665 | 1257225 | south | 0 | 0 | rural | yes | | 158 | 166 |
| Canton Zürich | 517 | C_ZH_06 | 2694001 | 1252331 | both | 0 | 0 | rural | yes | | 70 | 235 |
| Canton Zürich | 616 | C_ZH_07 | 2678790 | 1254016 | both | 0 | 0 | rural | yes | | 294 | 1215 |
| Canton Zürich | 617 | C_ZH_08 | 2695707 | 1265826 | both | 0 | 0 | rural | yes | | 252 | 619 |
| Canton Zürich | 716 | C_ZH_09 | 2678747 | 1254056 | both | 0 | 0 | rural | yes | | 195 | 1224 |
| Canton Zürich | 817 | C_ZH_10 | 2703727 | 1240830 | both | 0 | 0 | rural | yes | | 198 | 431 |
| Municipality Bern | 501 | M_Bern_01 | 2600042 | 1200472 | both | 0 | 0 | urban | yes | | 1016 | 679 |
| Municipality Bern | 502 | M_Bern_02 | 2598033 | 1199013 | both | 0 | 0 | urban | yes | | 332 | 75 |
| Municipality Bern | 503 | M_Bern_03 | 2599004 | 1198406 | both | 0 | 0 | urban | yes | | 1095 | 1134 |
| Municipality Bern | 504 | M_Bern_04 | 2600876 | 1200326 | both | 0 | 0 | urban | yes | | 4103 | 3655 |
| Municipality Bern | 505 | M_Bern_05 | 2599868 | 1199351 | both | 0 | 0 | urban | yes | | 4734 | 8471 |
| Municipality Bern | 506 | M_Bern_06 | 2598575 | 1199273 | east | 0 | 0 | urban | yes | | 904 | 1006 |
| Municipality Bern | 507 | M_Bern_07 | 2599802 | 1199939 | both | 0 | 0 | urban | yes | | 3281 | 3018 |
| Municipality Bern | 508 | M_Bern_08 | 2600559 | 1198766 | both | 0 | 0 | urban | yes | | 2201 | 2182 |

| data source | station ID (from source) | station ID | east | north | direction observed | days imputed | months imputed | classifi-cation | included in analysis | reason for exclusion | AAWT observed | AAWT modelled |
|---|---|---|---|---|---|---|---|---|---|---|---|---|
| Municipality Bern | 509 | M_Bern_09 | 2598037 | 1199904 | both | 0 | 0 | urban | yes | | 1446 | 1417 |
| Municipality Bern | 510 | M_Bern_10 | 2601629 | 1198658 | both | 0 | 0 | urban | yes | | 1489 | 1257 |
| Municipality Bern | 511 | M_Bern_11 | 2600349 | 1200194 | north | 0 | 0 | urban | yes | | 2761 | 1356 |
| Municipality Bern | 512 | M_Bern_12 | 2600782 | 1199268 | both | 0 | 0 | urban | yes | | 3865 | 4510 |
| Municipality Bern | 513 | M_Bern_13 | 2599389 | 1199603 | both | 0 | 0 | urban | yes | | 2033 | 1127 |
| Municipality Bern | 514 | M_Bern_14 | 2599228 | 1199867 | both | 0 | 0 | urban | yes | | 1642 | 1758 |
| Municipality Biel | V1 | M_Biel_01 | 2584734 | 1220676 | both | 0 | 0 | urban | yes | | 450 | 289 |
| Municipality Biel | V2 | M_Biel_02 | 2586210 | 1221472 | both | 0 | 0 | urban | yes | | 890 | 126 |
| Municipality Biel | V3 | M_Biel_03 | 2584951 | 1220252 | both | 0 | 0 | urban | yes | | 860 | 1436 |
| Municipality Biel | V4 | M_Biel_04 | 2585394 | 1220046 | both | 0 | 0 | urban | yes | | 1880 | 2878 |
| Municipality Biel | V5 | M_Biel_05 | 2585685 | 1220313 | both | 0 | 0 | urban | yes | | 760 | 1869 |
| Municipality Biel | V6 | M_Biel_06 | 2586562 | 1220847 | both | 0 | 0 | urban | yes | | 660 | 1181 |
| Municipality Biel | V7 | M_Biel_07 | 2587482 | 1221647 | both | 0 | 0 | urban | yes | | 400 | 453 |
| Municipality Biel | V8 | M_Biel_08 | 2586099 | 1221782 | both | 0 | 0 | urban | yes | | 670 | 2918 |
| Municipality Biel | V9 | M_Biel_09 | 2585362 | 1220779 | both | 0 | 0 | urban | yes | | 980 | 1890 |
| Municipality Biel | V10 | M_Biel_10 | 2586325 | 1221387 | both | 0 | 0 | urban | yes | | 1280 | 1694 |
| Municipality Köniz | K5-VV | M_Köniz_01 | 2598015 | 1196845 | both | 0 | 0 | urban | yes | | 590 | 273 |
| Municipality Köniz | K6-VV | M_Köniz_02 | 2598041 | 1196689 | both | 0 | 0 | urban | yes | | 950 | 1234 |

| data source | station ID (from source) | station ID | east | north | direction observed | days imputed | months imputed | classifi-cation | included in analysis | reason for exclusion | AAWT observed | AAWT modelled |
|---|---|---|---|---|---|---|---|---|---|---|---|---|
| Municipality Köniz | L2-VV | M_Köniz_03 | 2598528 | 1197576 | both | 0 | 0 | urban | yes | | 930 | 424 |
| Municipality Köniz | L3-VV | M_Köniz_04 | 2598285 | 1197805 | both | 0 | 0 | urban | yes | | 940 | 369 |
| Municipality Kriens | Horwerstrasse | M_Kriens_01 | 2664231 | 1209343 | both | 6 | 0 | urban | yes | | 329 | 349 |
| Municipality Kriens | Langmatt | M_Kriens_02 | 2662416 | 1209657 | both | 0 | 0 | urban | yes | | 352 | 428 |
| Municipality Kriens | Nidfeldstrasse | M_Kriens_03 | 2665284 | 1209048 | both | 0 | 0 | urban | no | not enough valid data | | |
| Municipality Kriens | Schlundstrasse | M_Kriens_04 | 2664559 | 1208934 | both | 1 | 0 | urban | yes | | 876 | 649 |
| Municipality Luzern | 603 | M_Luzern_01 | 2665630 | 1210518 | both | 0 | 0 | urban | yes | | 2178 | 2488 |
| Municipality Luzern | 604 | M_Luzern_02 | 2666273 | 1211842 | both | 0 | 0 | urban | yes | | 4495 | 8154 |
| Municipality Luzern | 605 | M_Luzern_03 | 2666180 | 1210824 | both | 0 | 3 | urban | yes | | 1977 | 2212 |
| Municipality Luzern | 606 | M_Luzern_04 | 2666494 | 1211286 | both | 0 | 0 | urban | yes | | 1876 | 1602 |
| Municipality Luzern | 607 | M_Luzern_05 | 2666945 | 1211977 | both | 0 | 0 | urban | yes | | 1283 | 1944 |
| Municipality Luzern | 608 | M_Luzern_06 | 2666221 | 1212155 | both | 0 | 4 | urban | yes | | 2077 | 4668 |
| Municipality Luzern | 610 | M_Luzern_07 | 2665037 | 1211726 | both | 0 | 0 | urban | yes | | 759 | 431 |
| Municipality Luzern | 611 | M_Luzern_08 | 2665974 | 1210619 | both | 0 | 0 | urban | yes | | 1589 | 1829 |
| Municipality Luzern | 612 | M_Luzern_09 | 2666116 | 1210676 | both | 0 | 0 | urban | yes | | 2281 | 2016 |
| Municipality Luzern | 613 | M_Luzern_10 | 2665176 | 1211654 | both | 0 | 0 | urban | yes | | 810 | 131 |
| Municipality Luzern | 614 | M_Luzern_11 | 2665885 | 1210304 | both | 0 | 0 | urban | yes | | 1410 | 1686 |
| Municipality Luzern | 615 | M_Luzern_12 | 2665378 | 1209981 | both | 0 | 0 | urban | yes | | 1104 | 3162 |

| data source | station ID (from source) | station ID | east | north | direction observed | days imputed | months imputed | classifi-cation | included in analysis | reason for exclusion | AAWT observed | AAWT modelled |
|---|---|---|---|---|---|---|---|---|---|---|---|---|
| Municipality Sankt Gallen | Burgstrasse 12 | M_StGallen_01 | 2745336 | 1253891 | both | 10 | 0 | urban | yes | | 283 | 406 |
| Municipality Sankt Gallen | Lindenstrasse 134 | M_StGallen_02 | 2748073 | 1255854 | both | 8 | 0 | urban | yes | | 229 | 1564 |
| Municipality Sankt Gallen | Lindenstrasse 81 | M_StGallen_03 | 2747554 | 1255462 | both | 0 | 0 | urban | yes | | 203 | 1321 |
| Municipality Sankt Gallen | Linsebühlstrasse / Singenbergstrasse | M_StGallen_04 | 2746938 | 1254665 | both | 0 | 0 | urban | yes | | 352 | 827 |
| Municipality Sankt Gallen | Museumstrasse | M_StGallen_05 | 2746437 | 1254745 | both | 0 | 0 | urban | yes | | 347 | 806 |
| Municipality Sankt Gallen | Oberstrasse 149 | M_StGallen_06 | 2744761 | 1253254 | both | 0 | 0 | urban | yes | | 609 | 2524 |
| Municipality Sankt Gallen | Rorschacher Strasse 61 / Singenberg | M_StGallen_07 | 2746765 | 1254778 | both | 0 | 0 | urban | yes | | 561 | 4911 |
| Municipality Sankt Gallen | Rosenbergstrasse Veloweg | M_StGallen_08 | 2744901 | 1254044 | both | 0 | 0 | urban | yes | | 478 | 556 |
| Municipality Sankt Gallen | Sitterviadukt A1 / Gaiserwaldweg | M_StGallen_09 | 2743810 | 1254104 | both | 0 | 0 | rural | yes | | 135 | 161 |
| Municipality Sankt Gallen | Splügenweg / Olma | M_StGallen_10 | 2746835 | 1255406 | both | 0 | 0 | urban | yes | | 209 | 658 |
| Municipality Sankt Gallen | St.Georgen / Mühlegg | M_StGallen_11 | 2746390 | 1253897 | both | 0 | 0 | urban | yes | | 276 | 594 |
| Municipality Sankt Gallen | St.Jakob-Strasse 84 / Olma | M_StGallen_12 | 2746631 | 1255304 | both | 0 | 0 | urban | yes | | 387 | 1229 |
| Municipality Sankt Gallen | Teufener Strasse 55 | M_StGallen_13 | 2745565 | 1253682 | both | 0 | 0 | urban | yes | | 149 | 1777 |
| Municipality Sankt Gallen | Vadianstrasse 8 | M_StGallen_14 | 2745945 | 1254253 | both | 1 | 0 | urban | yes | | 931 | 1303 |
| Municipality Wil | Haldenstrasse | M_Wil_01 | 2721169 | 1258569 | both | 0 | 0 | urban | yes | | 526 | 164 |
| Municipality Wil | Klosterweg | M_Wil_02 | 2721673 | 1258548 | both | 5 | 0 | urban | yes | | 289 | 797 |
| Municipality Wil | Wilenstrasse | M_Wil_03 | 2720798 | 1257896 | both | 2 | 0 | urban | yes | | 529 | 615 |
| Municipality Winterthur | Frohbergstrasse | M_Winterthur_01 | 2697038 | 1261505 | both | 85 | 0 | urban | yes | | 1073 | 405 |

| data source | station ID (from source) | station ID | east | north | direction observed | days imputed | months imputed | classifi-cation | included in analysis | reason for exclusion | AAWT observed | AAWT modelled |
|---|---|---|---|---|---|---|---|---|---|---|---|---|
| Municipality Zurich | 5 | M_Zürich_01 | 2682933 | 1248821 | both | 1 | 0 | urban | yes | | 967 | 1832 |
| Municipality Zurich | 6 | M_Zürich_02 | 2682873 | 1245891 | both | 1 | 0 | urban | yes | | 1781 | 783 |
| Municipality Zurich | 7 | M_Zürich_03 | 2681857 | 1251991 | both | 7 | 0 | urban | yes | | 652 | 2234 |
| Municipality Zurich | 8 | M_Zürich_04 | 2683573 | 1248545 | both | 1 | 0 | urban | yes | | 1797 | 2475 |
| Municipality Zurich | 9 | M_Zürich_05 | 2684578 | 1251967 | both | 32 | 0 | urban | yes | | 511 | 1867 |
| Municipality Zurich | 10 | M_Zürich_06 | 2682375 | 1247055 | both | 0 | 0 | urban | yes | | 2083 | 3765 |
| Municipality Zurich | 12 | M_Zürich_07 | 2681385 | 1247736 | both | 1 | 0 | urban | yes | | 1623 | 149 |
| Municipality Zurich | 13 | M_Zürich_08 | 2682683 | 1250570 | south | 1 | 0 | urban | yes | | 977 | 1203 |
| Municipality Zurich | 15 | M_Zürich_09 | 2683405 | 1251617 | both | 7 | 0 | urban | yes | | 321 | 705 |
| Municipality Zurich | 16 | M_Zürich_10 | 2682647 | 1250364 | both | 25 | 0 | urban | yes | | 1242 | 1800 |
| Municipality Zurich | 52 | M_Zürich_11 | 2678956 | 1250443 | both | 21 | 0 | urban | yes | | 367 | 2 |
| Municipality Zurich | 53 | M_Zürich_12 | 2679028 | 1250674 | both | 4 | 0 | urban | yes | | 39 | 35 |
| Municipality Zurich | 54 | M_Zürich_13 | 2684006 | 1246566 | both | 0 | 0 | urban | yes | | 2107 | 2373 |
| Municipality Zurich | 55+1997+2319+ 722+2320+2637 | M_Zürich_14 | 2682278 | 1248325 | both | 0 | 0 | urban | yes | | 8140 | 7869 |
| Municipality Zurich | 56 | M_Zürich_15 | 2679337 | 1249346 | both | 17 | 0 | urban | yes | | 519 | 382 |
| Municipality Zurich | 57 | M_Zürich_16 | 2682946 | 1248225 | both | 0 | 0 | urban | yes | | 2251 | 2057 |
| Municipality Zurich | 59 | M_Zürich_17 | 2682755 | 1247323 | both | 0 | 0 | urban | yes | | 815 | 1021 |
| Municipality Zurich | 60 | M_Zürich_18 | 2682731 | 1247708 | both | 1 | 0 | urban | yes | | 974 | 3370 |

| data source | station ID (from source) | station ID | east | north | direction observed | days imputed | months imputed | classifi-cation | included in analysis | reason for exclusion | AAWT observed | AAWT modelled |
|---|---|---|---|---|---|---|---|---|---|---|---|---|
| Municipality Zurich | 61+62 | M_Zürich_19 | 2683447 | 1247063 | both | 0 | 0 | urban | yes | | 3387 | 3711 |
| Municipality Zurich | 732+1037 | M_Zürich_20 | 2681319 | 1248665 | both | 0 | 0 | urban | yes | | 2999 | 895 |
| Municipality Zurich | 1692 | M_Zürich_21 | 2682881 | 1246549 | both | 119 | 0 | urban | yes | | 377 | 0 |
| Switzerland Mobility | BE-00001 | SM_01 | 2594070 | 1221299 | both | 0 | 0 | rural | yes | | 375 | 33 |
| Switzerland Mobility | BE-00002 | SM_02 | 2609107 | 1190343 | both | 0 | 0 | rural | yes | | 464 | 80 |
| Switzerland Mobility | BE-00003 | SM_03 | 2647415 | 1176579 | both | 0 | 0 | rural | yes | | 92 | 12 |
| Switzerland Mobility | BL-00006 | SM_04 | 2610181 | 1265331 | both | 0 | 0 | urban | no | duplicate | 1711 | |
| Switzerland Mobility | BS-00354 | SM_05 | 2611959 | 1267512 | both | 0 | 0 | urban | no | duplicate | 8524 | |
| Switzerland Mobility | BS-00901 | SM_06 | 2611753 | 1266134 | both | 0 | 0 | urban | no | duplicate | 3272 | |
| Switzerland Mobility | BS-00905 | SM_07 | 2610925 | 1267191 | both | 0 | 0 | urban | no | duplicate | 2154 | |
| Switzerland Mobility | BS-00914 | SM_08 | 2611615 | 1270626 | both | 0 | 0 | urban | no | duplicate | 1039 | |
| Switzerland Mobility | FR-00001 | SM_09 | 2572663 | 1153901 | both | 0 | 0 | rural | yes | | 31 | 14 |
| Switzerland Mobility | GE-00010 | SM_10 | 2502555 | 1115428 | both | 0 | 0 | urban | no | duplicate | 625 | |
| Switzerland Mobility | GR-00001 | SM_11 | 2761027 | 1197607 | both | 0 | 0 | rural | yes | | 251 | 495 |
| Switzerland Mobility | GR-00002 | SM_12 | 2790693 | 1161708 | both | 0 | 0 | rural | yes | | 80 | 218 |
| Switzerland Mobility | OW-00001 | SM_13 | 2656207 | 1189683 | both | 0 | 0 | rural | yes | | 119 | 40 |
| Switzerland Mobility | SG-00001 | SM_14 | 2712898 | 1231630 | both | 0 | 0 | rural | yes | | 233 | 15 |
| Switzerland Mobility | SG-00202 | SM_15 | 2753420 | 1261679 | both | 0 | 0 | urban | no | duplicate | 598 | |

| data source | station ID (from source) | station ID | east | north | direction observed | days imputed | months imputed | classifi-cation | included in analysis | reason for exclusion | AAWT observed | AAWT modelled |
|---|---|---|---|---|---|---|---|---|---|---|---|---|
| Switzerland Mobility | SG-00203 | SM_16 | 2737109 | 1252726 | both | 0 | 0 | rural | no | duplicate | 345 | |
| Switzerland Mobility | SG-00205 | SM_17 | 2704127 | 1231237 | both | 0 | 0 | urban | no | duplicate | 423 | |
| Switzerland Mobility | SG-00208 | SM_18 | 2704626 | 1231873 | both | 0 | 0 | urban | no | duplicate | 948 | |
| Switzerland Mobility | SG-00210 | SM_19 | 2752091 | 1212567 | both | 0 | 0 | urban | no | duplicate | 250 | |
| Switzerland Mobility | SG-00211 | SM_20 | 2756015 | 1260687 | both | 0 | 0 | urban | no | duplicate | 537 | |
| Switzerland Mobility | SG-00213 | SM_21 | 2734253 | 1252215 | both | 0 | 0 | rural | no | duplicate | 203 | |
| Switzerland Mobility | SG-00214 | SM_22 | 2722931 | 1221876 | both | 0 | 0 | rural | no | duplicate | 149 | |
| Switzerland Mobility | SH-00001 | SM_23 | 2704940 | 1281283 | both | 0 | 0 | rural | yes | | 416 | 161 |
| Switzerland Mobility | SH-00002 | SM_24 | 2687649 | 1283114 | both | 0 | 0 | rural | no | duplicate | 144 | |
| Switzerland Mobility | SO-00001 | SM_25 | 2635175 | 1243033 | both | 0 | 0 | rural | yes | | 217 | 144 |
| Switzerland Mobility | TG-00001 | SM_26 | 2732784 | 1278451 | both | 0 | 0 | urban | yes | | 843 | 229 |
| Switzerland Mobility | TI-00001 | SM_27 | 2714697 | 1136011 | both | 0 | 0 | rural | no | duplicate | 161 | |
| Switzerland Mobility | TI-00002 | SM_28 | 2720125 | 1114863 | both | 0 | 0 | rural | no | duplicate | 379 | |
| Switzerland Mobility | TI-00010 | SM_29 | 2723831 | 1119883 | both | 0 | 0 | urban | no | duplicate | 244 | |
| Switzerland Mobility | TI-00012 | SM_30 | 2704037 | 1113292 | both | 0 | 0 | urban | no | duplicate | 1603 | |
| Switzerland Mobility | TI-00013 | SM_31 | 2701150 | 1115274 | both | 0 | 0 | rural | no | duplicate | 291 | |
| Switzerland Mobility | VD-00002 | SM_32 | 2508898 | 1139845 | both | 0 | 0 | rural | yes | | 56 | 73 |
| Switzerland Mobility | VS-00001 | SM_33 | 2597565 | 1121281 | both | 0 | 0 | rural | yes | | 252 | 0 |

| data source | station ID (from source) | station ID | east | north | direction observed | days imputed | months imputed | classifi-cation | included in analysis | reason for exclusion | AAWT observed | AAWT modelled |
|---|---|---|---|---|---|---|---|---|---|---|---|---|
| Switzerland Mobility | ZH-00001 | SM_34 | 2690433 | 1254712 | both | 0 | 0 | urban | yes | | 148 | 224 |
| Switzerland Mobility | ZH-00316 | SM_35 | 2693283 | 1246952 | both | 0 | 0 | urban | no | duplicate | 641 | |
| Switzerland Mobility | ZH-01001 | SM_36 | 2681839 | 1251995 | both | 0 | 0 | urban | no | duplicate | 640 | |
| Switzerland Mobility | ZH-01003 | SM_37 | 2682704 | 1250602 | south | 0 | 0 | urban | no | duplicate | 979 | |
| Switzerland Mobility | ZH-01004 | SM_38 | 2683455 | 1247052 | both | 0 | 0 | urban | no | duplicate | 3160 | |
| Switzerland Mobility | ZH-01006 | SM_39 | 2682922 | 1248823 | both | 0 | 0 | urban | no | duplicate | 968 | |
| Switzerland Mobility | ZH-01007 | SM_40 | 2684003 | 1246566 | both | 0 | 0 | urban | no | duplicate | 2106 | |
| Switzerland Mobility | ZH-01008 | SM_41 | 2682363 | 1247052 | both | 0 | 0 | urban | no | duplicate | 2079 | |
| Switzerland Mobility | ZH-01009 | SM_42 | 2682946 | 1248226 | both | 0 | 0 | urban | no | duplicate | 2226 | |
| Switzerland Mobility | ZH-10502 | SM_43 | 2684384 | 1236400 | both | 0 | 0 | rural | yes | | 92 | 0 |

## Personal Declaration

I hereby declare that the submitted thesis is the result of my own, independent work. All external sources are explicitly acknowledged in the thesis.

Marc Morlang

Marc Morlang, 27.09.2024